AGARD-R-580-71

AGARD-R-580-71

AGARD

ADVISORY GROUP FOR AEROSPACE RESEARCH & DEVELOPMENT

7 RUE ANCELLE 92 NEUILLY-SUR-SEINE FRANCE

AGARD REPORT No. 580

on

Frequency Response Functions and Human Pilot Modelling

NORTH ATLANTIC TREATY ORGANIZATION

DISTRIBUTION AND AVAILABILITY
ON BACK COVER

AGARD Report No.580

NORTH ATLANTIC TREATY ORGANIZATION

ADVISORY GROUP FOR AEROSPACE RESEARCH AND DEVELOPMENT

(ORGANISATION DU TRAITE DE L'ATLANTIQUE NORD)

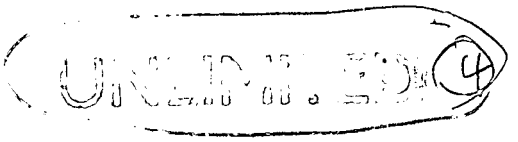

FREQUENCY RESPONSE FUNCTIONS AND HUMAN PILOT MODELLING

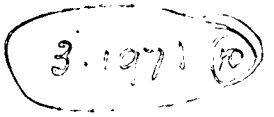

This Report was prepared at the request of the Structures and Materials Panel of AGARD.

Published March 1971

L.C.73-155460
U.D.C.629.7.072.629.7.05

Printed by Technical Editing and Reproduction Ltd
Harford House, 7-9 Charlotte St. London. W1P 1HD.

FOREWORD

The Structures and Materials Panel of the NATO Advisory Group for Aerospace Research and Development (AGARD) comprises scientists, engineers and technical administrators, from industry, government and universities throughout NATO, concerned with advancing the status of aerospace research and development and with developing technical means and data for optimizing the vehicles and equipment of interest to NATO. The Panel, therefore, provides a discussion forum, a mechanism for exchanging information, and a means for establishing and conducting cooperative studies and laboratory programs in selected technical areas.

The increasing complexity of modern aircraft arising from more stringent performance requirements – in terms of speed, range, altitude capability, maneuverability, etc. – have emphasized the critical importance of examining the inter-related facets of aircraft design and operation in a total, systems sense. The Panel, engaged through a number of cooperative projects in studying a variety of behavior phenomena and establishing as solid a basis as possible for optimization of design and minimization of flight and structural problems, has been both aware of and concerned about these inter-relationships and, in a specific instance addressed itself to the question of interactions between handling qualities, static and dynamic stability, control and structural loads.

In order to obtain a clearer picture of these interactions and their effects, it was decided that the state-of-the-art in transfer function (frequency response function) development should be assessed. This function ties together all the inter-related aspects of potential interactions between structural loads and the other sub-disciplines of aeronautics. The following reports are one such result of the Panel decision.

The Panel expresses its appreciation to the authors and to the others recognized in the Acknowledgements for this significant contribution to such an important topic.

Charles K.Grimes
Chairman, Working Group on
Interaction of Handling Qualities,
Stability, Control and Structural Loads
AGARD Structures and Materials Panel

CONTENTS

In order to obtain a clearer picture of these interactions and their effects, it was decided that the state-of-the-art in transfer function (frequency response function) development should be assessed. This function ties together all the inter-related aspects of potential interactions between structural loads and the other sub-disciplines of aeronautics. This Report was prepared at the request of the Structures and Materials Panel of AGARD.	In order to obtain a clearer picture of these interactions and their effects, it was decided that the state-of-the-art in transfer function (frequency response function) development should be assessed. This function ties together all the inter-related aspects of potential interactions between structural loads and the other sub-disciplines of aeronautics. This Report was prepared at the request of the Structures and Materials Panel of AGARD.
In order to obtain a clearer picture of these interactions and their effects, it was decided that the state-of-the-art in transfer function (frequency response function) development should be assessed. This function ties together all the inter-related aspects of potential interactions between structural loads and the other sub-disciplines of aeronautics. Papers include: list of titles on p. iv of report. 1 to 8. This Report was prepared at the request of the Structures and Materials Panel of AGARD.	In order to obtain a clearer picture of these interactions and their effects, it was decided that the state-of-the-art in transfer function (frequency response function) development should be assessed. This function ties together all the inter-related aspects of potential interactions between structural loads and the other sub-disciplines of aeronautics. This Report was prepared at the request of the Structures and Materials Panel of AGARD.

AGARD Report No.580 North Atlantic Treaty Organization, Advisory Group for Aerospace Research and Development FREQUENCY RESPONSE FUNCTIONS AND HUMAN PILOT MODELLING Published March 1971 70 pages The increasing complexity of modern aircraft arising from more stringent performance requirements – in terms of speed, range, altitude capability, maneuverability, etc. – have emphasized the critical importance of examining the inter-related facets of aircraft design and operation in a total, systems sense. P.T.O.	L.C.73-155460 U.D.C.629.7.072.629.7.05	AGARD Report No.580 North Atlantic Treaty Organization, Advisory Group for Aerospace Research and Development FREQUENCY RESPONSE FUNCTIONS AND HUMAN PILOT MODELLING Published March 1971 70 pages The increasing complexity of modern aircraft arising from more stringent performance requirements – in terms of speed, range, altitude capability, maneuverability, etc. – have emphasized the critical importance of examining the inter-related facets of aircraft design and operation in a total, systems sense. P.T.O.	L.C.73-155460 U.D.C.629.7.072.629.7.05
AGARD Report No.580 North Atlantic Treaty Organization, Advisory Group for Aerospace Research and Development FREQUENCY RESPONSE FUNCTIONS AND HUMAN PILOT MODELLING Published March 1971 70 pages The increasing complexity of modern aircraft arising from more stringent performance requirements – in terms of speed, range, altitude capability, maneuverability, etc. – have emphasized the critical importance of examining the inter-related facets of aircraft design and operation in a total, systems sense. P.T.O.	L.C.73-155460 U.D.C.629.7.072.629.7.05	AGARD Report No.580 North Atlantic Treaty Organization, Advisory Group for Aerospace Research and Development FREQUENCY RESPONSE FUNCTIONS AND HUMAN PILOT MODELLING Published March 1971 70 pages The increasing complexity of modern aircraft arising from more stringent performance requirements – ~~in terms of speed, range, altitude capability, maneuverability, etc.~~ – have emphasized the critical importance of examining the inter-related facets of aircraft design and operation in a total, systems sense. —contrary P.T.O.	L.C.73-155460 U.D.C.629.7.072.629.7.05

AGARD Report No.580 North Atlantic Treaty Organization, Advisory Group for Aerospace Research and Development FREQUENCY RESPONSE FUNCTIONS AND HUMAN PILOT MODELLING Published March 1971 70 pages The increasing complexity of modern aircraft arising from more stringent performance requirements – in terms of speed, range, altitude capability, maneuverability, etc. – have emphasized the critical importance of examining the inter-related facets of aircraft design and operation in a total, systems sense. P.T.O.	L.C.73-155460 U.D.C.629.7.072.629.7.05	AGARD Report No.580 North Atlantic Treaty Organization, Advisory Group for Aerospace Research and Development FREQUENCY RESPONSE FUNCTIONS AND HUMAN PILOT MODELLING Published March 1971 70 pages The increasing complexity of modern aircraft arising from more stringent performance requirements – in terms of speed, range, altitude capability, maneuverability, etc. – have emphasized the critical importance of examining the inter-related facets of aircraft design and operation in a total, systems sense. P.T.O.	L.C.73-155460 U.D.C.629.7.072.629.7.05
AGARD Report No.580 North Atlantic Treaty Organization, Advisory Group for Aerospace Research and Development FREQUENCY RESPONSE FUNCTIONS AND HUMAN PILOT MODELLING Published March 1971 70 pages The increasing complexity of modern aircraft arising from more stringent performance requirements – in terms of speed, range, altitude capability, maneuverability, etc. – have emphasized the critical importance of examining the inter-related facets of aircraft design and operation in a total, systems sense. P.T.O.	L.C.73-155460 U.D.C.629.7.072.629.7.05	AGARD Report No.580 North Atlantic Treaty Organization, Advisory Group for Aerospace Research and Development FREQUENCY RESPONSE FUNCTIONS AND HUMAN PILOT MODELLING Published March 1971 70 pages The increasing complexity of modern aircraft arising from more stringent performance requirements – in terms of speed, range, altitude capability, maneuverability, etc. – have emphasized the critical importance of examining the inter-related facets of aircraft design and operation in a total, systems sense. P.T.O.	L.C.73-155460 U.D.C.629.7.072.629.7.05

In order to obtain a clearer picture of these interactions and their effects, it was decided that the state-of-the-art in transfer function (frequency response function) development should be assessed. This function ties together all the inter-related aspects of potential interactions between structural loads and the other sub-disciplines of aeronautics. This Report was prepared at the request of the Structures and Materials Panel of AGARD.	In order to obtain a clearer picture of these interactions and their effects, it was decided that the state-of-the-art in transfer function (frequency response function) development should be assessed. This function ties together all the inter-related aspects of potential interactions between structural loads and the other sub-disciplines of aeronautics. This Report was prepared at the request of the Structures and Materials Panel of AGARD.
In order to obtain a clearer picture of these interactions and their effects, it was decided that the state-of-the-art in transfer function (frequency response function) development should be assessed. This function ties together all the inter-related aspects of potential interactions between structural loads and the other sub-disciplines of aeronautics. This Report was prepared at the request of the Structures and Materials Panel of AGARD.	In order to obtain a clearer picture of these interactions and their effects, it was decided that the state-of-the-art in transfer function (frequency response function) development should be assessed. This function ties together all the inter-related aspects of potential interactions between structural loads and the other sub-disciplines of aeronautics. This Report was prepared at the request of the Structures and Materials Panel of AGARD.

THE ART OF DETERMINING GUST FREQUENCY RESPONSE FUNCTIONS

by

John C.Houbolt

Aeronautical Research Associates of Princeton, Inc.
50 Washington Road,
Princeton, New Jersey 08540

SUMMARY

The art of determining the frequency response function for gust response, and of deriving the associated structural response parameters A and N_o is discussed. Measured and computed values are compared to show the degree of success obtained. It is brought out that frequency response determination is a computationally large task and that simplified procedures are needed. Emphasis is also given to the fact that there is not *a* frequency response function for the airplane, but that there are many, depending on flight conditions. A procedure is suggested for helping to establish the appropriate frequency response functions, and the A and N_o values, for use in design.

SYMBOLS

a	slope of the lift curve
A	structural response quantity as used in $\sigma_x = A\sigma_w$
c	mean aerodynamic chord
f	frequency, cps
h	altitude
$H_x(\omega)$	frequency response function of variable x
K_ϕ	spectral gust alleviation factor
L	turbulence scale
n	number of crossings with positive slope
N	number of crossings per second of load level x with positive slope
N_o	number of zero crossings per second with positive slope
P	proportion of time spent in turbulence
S	wing area
T	flight time
V	flight velocity
w	vertical gust velocity
W	aircraft weight
x	response variable, used generally in the sense of being an increment due to gusts
x_{1-g}	load level for x due to 1−g level flight condition
μ	mass parameter
ρ	air density
σ_w	rms value of vertical gust velocity
σ_x	rms value of incremental acceleration x
$\phi_w(\ )$	power spectrum of vertical gust velocities
$\phi_x(\ )$	power spectrum of response x
ω	circular frequency

THE ART OF DETERMINING GUST FREQUENCY RESPONSE FUNCTIONS

John C.Houbolt

1. INTRODUCTION

In the treatment of the response of aircraft to gust by power spectral techniques, the frequency response function plays a central role. For gust encounter, the frequency response function is defined as the response (amplitude and phase) of the variable of concern, such as acceleration, bending moment, or stress, due to a unit sinusoidal gust encounter. Through means of the frequency response function and an input spectrum, two basic structural response quantities A and N_0 are derived, which are of key significance in load response studies.

The question has been raised, "What is the state of the art of calculating the frequency response functions and, in turn, the basic A and N_0 values?" The question should be rephrased, however. At present it appears that we can determine a specific frequency response function with fair accuracy. An airplane, however, has many different flight conditions, due to variations in weight, speed, and altitude and, thus, a given airplane has many different frequency response functions, even for a given response variable. The problem, therefore, is not only that of how well we can establish a specific frequency response function, but also how well we can isolate and determine the appropriate frequency response function, or more generally, how well we can combine the various frequency response functions so as to obtain a realistic overall or composite description of the response. The purpose of this paper is thus to discuss these problems.

Acknowledgment is hereby made, and appreciation given, to Messrs Wayne B.Stanley and Asim Sen for the help they gave in deriving many of the results contained in this paper.

2. ROLE OF THE FREQUENCY RESPONSE FUNCTION

Figure 1 depicts, by way of review, the basic notions of the power spectral approach to gust response. This figure, quite well known by now, is based on the basic input-output relations

$$\phi_x(\omega) = |H(\omega)|^2 \, \phi_w(\omega) \tag{1}$$

$$\phi_{wx}(\omega) = H(\omega) \, \phi_w(\omega) \tag{2}$$

where $H(\omega)$ is the frequency response function for the response quantity under consideration. From the output spectra ϕ_x the basic structural response quantities A and N_0 are found

$$A = \frac{\sigma_x}{\sigma_w} = \left[\frac{\int_0^{\omega_c} |H|^2 \, \phi_w \, d\omega}{\int_0^{\infty} \phi_w \, d\omega} \right] \tag{3}$$

$$N_0 = \frac{1}{2\pi} \left[\frac{\int_0^{\omega_c} \omega^2 \, |H|^2 \, \phi_w \, d\omega}{\int_0^{\omega_c} |H|^2 \, \phi_w \, d\omega} \right] \tag{4}$$

These quantities are noted to be associated with the area and radius of gyration of the area under the output spectrum. The upper limit ω_c in expressions (3) and (4) represents one of the problems that is encountered in evaluating A and N_0. The means for establishing ω_c, as recommended in reference 1, is shown in figure 2. In some cases the N_0 variation with ω_c is fairly flat after a certain ω_c is reached, curve a, and in this case no difficulty is encountered in establishing N_0. In other cases N_0 seems to increase monotonically with increasing ω_c, curve b; in this case N_0 is taken at the ω_c representing the top of the knee of the A curve, as suggested in reference 1.

3. ANALYTICAL DETERMINATION OF THE FREQUENCY RESPONSE FUNCTIONS

Figure 3 depicts two common ways for treating the structural dynamics of the frequency response problem, namely, a discrete grid representation using lumped masses and influence coefficients, and a modal approach in conjunction with a dynamical equation based on a Lagrangian formulation of the problem.

Figure 4 shows the basic means generally used for treating the aerodynamics of the problem. Strip theory is still used even for some of our most modern aircraft. Tail downwash is often included in a quasi-steady sense through use of the conventional type downwash factor $1 - \frac{d\epsilon}{d\alpha}$. Sometimes attempts are made to approximately take into account spanwise aerodynamic induction effects. Compressibility effects are taken into account approximately by using 2-d compressible strip theory and by using overall corrections to account for finite span and sweep effects.

Lifting surface theory involving the kernel function, reference 2, is also used. Most of the applications in the past were by the so-called pressure mode approach. More recently, however, discrete-element-type kernel function approaches have been growing in favour. They are basically of two types. In one, concentrated loads are used and the downwash is taken in terms of average values over spanwise increments, thereby eliminating singularity troubles, reference 3. In the other, spanwise line segments of pressure and considered, and downwash is taken at discrete points, references 4, 5, 6.

Essentially, the means for deriving the frequency response function is to combine the structures and aerodynamics of figures 3 and 4 and solve the response for a sinusoidal gust input.

The following assessment is believed to be representative of the general feeling that researchers and engineers have with respect to the ease or difficulty of deriving frequency response functions. With respect to the structural dynamics, quite a bit of computational effort is, of course, required to establish the modes and frequencies in the modal approach, or to derive the influence coefficients and lumped masses in the discrete mass representation. The problem is compounded by the fact that these derivations must be made for various loading conditions of the aircraft.

For the aerodynamics, the use of strip theory is relatively computationally quite efficient and, hence, the reason why the theory is still favored by some. (Plus the fact that the theory appears to yield adequate results for certain type configurations.) For the kernel function approach which makes use of pressure modes, computations are rather involved and setup time is long, but problems with matrix inversion are kept to a minimum because of the relatively low order of the matrices involved. In the past, much difficulty was encountered computationally with the singularities present, but procedures have now become somewhat more routine in this respect. For the kernel function approach using discrete loads and a gridwork system, setup time is eased considerably, but the problem of inverting large order complex matrices becomes of concern.

The accuracy of the combined result is, of course, no better than the accuracies of the structural and aerodynamic ingredients.

It must be noted that the evaluation of the frequency response function requires explicit evaluation of matrix components and a matrix inversion (when the kernel function is used) at each of a large number of frequency values. All these computations must be repeated for each different flight condition (changes in V, W, or ρ). In general, it may be said that, while in principle the determination of the frequency response function appears straight-forward, the actual determination is an involved, laborious, and time-consuming computational task, and one that is quite expensive. The process of treating the structure, and of treating the aerodynamics and then of combining these ingredients is not an easy task. Simplified means for deriving the function are very much needed.

4. COMPARISON OF CALCULATED AND MEASURED FREQUENCY RESPONSE FUNCTIONS

Figure 5 shows a comparison of the calculated frequency response function of a large swept-wing aircraft with that deduced from flight response results, references 7 and 8. Lifting surface theory was used in this instance. The comparison brings out two points of significance. One is that in this case, fairly good agreement is found between calculated and measured values, Second, it is seen that flexible body effects are quite pronounced; the importance of including the elastic modes, at least the lower modes, is thus brought out.

In figure 6, a similar comparison is made of results obtained with a large delta-type aircraft, reference 9; lifting surface theory was also used here. Reasonably good agreement is seen in certain frequency ranges, but in other ranges the agreement is not too good, particularly near the modal peaks. The reason for the discrepancies is not known, but may be due to inadequate representation of the structural damping. Thus, knowledge of structural damping may represent an area of weakness.

Another way to assess results is to compare computed and derived A and N_o values. Figure 7 presents the comparison that was found for the frequency response case shown in figure 6. The results on the whole are encouraging, but variances are evident. It should be noted, as subsequent results will bring out, that the correctness of A is much more important than the correctness of N_o.

Besides using an adequate representation of the aerodynamics and of the structure there is another parameter which has a marked effect in the determination of the structural parameter A, namely, the scale of turbulence L. Figure 8 shows, for example, how the computed value of A varies with L for a particular case. A marked variation is noted. In contrast, the parameter N_0 seems to be nearly invariant with L. The scale L has been an elusive quantity to tie down numerically; present estimates range from $L = 500$ ft to $L = 3000$, but the appropriate value for use in computations is still an unknown.

The sample results shown in figures 5-8 show in general that, with respect to evaluating a specific frequency response function for an airplane, we can do a creditable job, but that certain areas of doubt are still present. Subsequent results will show, however, that there are greater areas of weakness in selecting the frequency response functions and, in turn, the A and N_0 values that are significant for aircraft design.

5. SOME NOTIONS RELATIVE TO LOAD EXCEEDANCE CURVES

If the airplane is considered rigid and is assumed to have the single degree of freedom of vertical motion only, rather simple general results may be derived for establishing the aircraft response to gusts. Basic results, taken from reference 1, are shown in figure 9. By means of these charts, the A and N_0 for any airplane for any given condition of flight may be established rather easily. The value of $2L/c$ is recommended in reference 1 as $2L/c = 1500/c$. (The K_g curve in figure 9 applies to the discrete-gust design concept.)

The results in figure 9 are for an assumed straight-wing airplane. The question of whether the results are affected by sweep, due to the varying gust penetration effects, is answered in part by figure 10. Results in this figure are for a value of $2L/c = 100$ and are given for various values of the parameter γ which depends on the aspect ratio and the sweep. The closeness of the curves, differing by only a few percent, indicates fortunately that the results of figure 9 can be applied in general to swept, as well as straight, wings.

With figure 9, and the P and σ_w values shown in figure 11, it is possible to construct rough or preliminary load exceedance curves that apply in the range of large response levels. The basic means, as presented in reference 1, is shown in figure 12. Essentially, for a given flight condition and altitude, the A_r and N_0 values are established by figure 9. The A value for the response quantity of concern, such as the bending moment example shown in the figure, is then found from the relation.

$$A = 1.1\, A_r x_{1\text{-}g}$$

where A_r is the value found from figure 9, and $x_{1\text{-}g}$ is the 1-g load value (bending moment in this example). The factor 1.1 is included to account approximately for elastic body amplification effects; this factor may be adjusted upward or downward if some additional insight relative to the airplane response characteristics is on hand. With the A and N_0 values, the P and σ_w values of figure 11, and a chosen time T, the load exceedance curve may be established by the equation shown in figure 12.

The results of figures 9-12 are useful in bringing out a second problem associated with the determination of the frequency response functions and the A and N_0 values; namely, of all the frequency response functions, and A and N_0 values that are possible for a given airplane, which are the most significant from a design point of view? This question is touched upon in the remaining sections.

6. VARIATIONS IN A AND N_0

In its operations, an airplane experiences many different flight conditions. Many of these are depicted in figure 13. It is seen that the speed of flight may vary by a factor of 4, the weight by a factor 2, and the density by a factor 5. In addition, the weight distributions can vary widely, involving various combinations of fuel and payload, and this variation can have a marked influence on certain response quantities such as bending moment. The lift curve slope may also be a factor; it may be relatively constant, may vary with Mach number according to a form of the Prandtl-Glauert rule, or it may involve the bending-relieving effects of swept wings in conjunction with some Mach number effect. When all these variations are considered in the light of determining A_r and N_0 by means of figure 9, it can be seen that a very significant spread in the values of A and N_0 may result.

The sensitivity of load severity and of load count to variations in the flight parameters can be shown through use of the equations shown in figure 12, as follows. A combination of parameters associated with load levels near the limit load is chosen, and by means of these equations reference values of σ_x and n are established. Each of the parameters is then varied separately, holding the others constant, and from the results changes in the σ_x and n values are deduced. Results obtained by this means for a plus 10% change in each parameter are shown in the following table.

+ 10% Change in:	% Change in: σ_x	n
V	10	70
σ_w	10	55
W	-6.7	-30
ρ	7.3	64
S(constant c)	7.3	64
c(constant S)	-2.6	-19
PT	-	10

The rather pronounced sensitivity of results to the various parameters, especially aircraft speed and gust severity, σ_w , is evident. These results show that the selection of the proper flight conditions must represent a rather critical problem in aircraft design. This observation is amplified in the next section.

7. MISSION EFFECTS

The wide variations that may be found in the values of A and N_0 due to various airplane missions. Each of the chosen missions may be broken down into various segments, and the values of A and N_0 for each segment may, in turn, be found. An example study of this nature was made for a large swept-wing jet aircraft; characteristics such as speed, rates of climb and descent, weight and weight changes representative of present day aircraft were assumed. A swept wing was considered, and use was made of the lift curve slope of the elastic airplane so as to include effects of wing bending. Results for A_r and N_0 are presented in figures 14 and 15 for various assumed missions, using six segments per mission as shown. In figure 16 and 17, corresponding results for σ_x and PN_0 are given, these quantities have also been presented because they are of significance from a load exceedance point of view (see equation in figure 12). The P and σ_w values used were those given in figure 11. Also presented in figures 16 and 17 are composite values of σ_x and PN_0 , as determined from the equations suggested in reference 1, namely,

$$\sigma_x^2 = \frac{1}{PT}(P_1 T_1 A_1^2 \sigma_1^2 + P_2 T_2 A_2^2 \sigma_2^2 + \ldots) \tag{5}$$

$$PN_0 = \frac{1}{T}(P_1 T_1 N_{0_1} + P_2 T_2 N_{0_2} + \ldots) \tag{6}$$

where $T = T_1 + T_2 + \ldots$; $PT = P_1 T_1 + P_2 T_2 + \ldots$

It is seen that not only do the A , N_0 , σ_x and PN_0 values vary greatly within a given mission, but that there is also a great variation from mission to mission; so, too, is there a marked variation of the composite values. Figures 14-17 thus bring out two of the biggest problems associated with the design of aircraft for gusts, in particular, with respect to the problem of frequency response determination. First, there is the problem of being able to establish the frequency response functions and the A and N_0 values for a given flight condition; second, there is the problem of establishing the functions for many possible conditions of flight. (The allied and equally questionable problem of establishing realistic values for the environmental parameters σ_w , P , and L is not considered in this report.) The question then arises, "Of all the A and N_0 values that are possible, which are the most appropriate for use in design?" Figure 18 may supply the key to the answer. With the equation for n shown in figure 12, the results of figures 16 and 17 have been converted to load exceedance curves given in figure 18. In appraising the results of this figure, however, we also have a question similar to that asked in connection with figures 14-17; that is, of the various load exceedance curves, which is most appropriate for design consideration? Since the operational experience of the aircraft cannot be predicted precisely, it would appear that the answer is to choose the top or most conservative curve.

It is to be noted that the consideration of several possible missions in conjunction with the rigid body results of figure 9 offers a rather quick and simple way for establishing the more critical missions. The number of possible flight conditions which might be investigated has thereby been greatly reduced. As a result, detailed evaluation of the frequency response functions using actual structural and aerodynamic properties of the airplane configuration under study can be limited to the few flight conditions of the critical missions, thus saving considerable work.

8. CONCLUDING REMARKS

Discussion and results presented in this report deal with the problem of determining the frequency response functions and the associated structural parameters A and N_0 for gust response. A summary of some of the main points brought out, including certain additional concluding comments, is given in the following listing.

1. The determination of a specific frequency response function is a rather involved computational process, especially when lifting surface theory is used; simplified procedures are needed.

2. Comparisons of computed and measured frequency response functions indicate fair to reasonably good agreement. The magnitude of the peaks in the functions seems to be the most difficult to predict.

3. For flexible aircraft, treatment should include the lower frequency elastic modes, as well as the rigid-body modes.

4. There is not *a* frequency response function for an aircraft; rather, there are many.

5. Because of 4, listings indicating the A and N_0 value of aircraft should not be given, nor should the A and N_0 values of one aircraft be compared arbitrarily with the values of another. If a listing or comparison is made, care should be taken to cite the flight conditions for which the A and N_0 evaluations were made so that a meaningful comparison can be made.

6. Because there are many A and N_0 values for a given airplane, the selection of the appropriate A and N_0 values for use in design presents a real problem. Perhaps the best way to arrive at appropriate values is to consider various missions by simplified procedures and then to choose, for detailed evaluation, the mission which appears to lead to more severe load exceedance values.

REFERENCES

1. Houbolt, John C. — *Design Manual for Vertical Gusts Based on Power Spectral Techniques.* A.R.A.P. Report No.147, prepared for the Air Force Flight Dynamics Laboratory, Wright-Patterson AFB, Ohio, July 1970.

2. Watkins, Charles E. et al — *On the Kernel Functions of the Integral Equation Relating the Lift and Downwash Distributions of Oscillating Finite Wings in Subsonic Flow.* NACA Report 1234, 1955, (Supersedes NACA TN 3131).

3. Houbolt, John C. — *Some New Concepts in Oscillatory Lifting Surface Theory.* Technical Report AFFDL-TR-69-2, June 1969.

4. Albano, E Rodden, W.P. — *A Doublet-Lattice Method for Calculating Lift Distributions on Oscillating Surfaces in Subsonic Flows.* AIAA Jour., Vol.7, No.2, February 1969, pp.279-285.

5. Landahl, M.T. Stark, V.J.E. — *Numerical Lifting-Surface Theory – Problems and Progress.* AIAA Jour., Vol.6, No.11, November 1968, pp.2049-2060.

6. Kalman, T.P. et al — *Application of the Doublet-Lattice Method to Nonplanar Configurations in Subsonic Flow.* McDonnell Douglas Corp., Douglas Aircraft Co., Long Beach, Calif.

7. Steiner, R. Pratt, K. — *A Summary of Some Applications of Power Spectra to Airplane Turbulence Problems.* NASA Langley Research Center, Hampton, Va., presented at the AIAA Third Annual Meeting and Technical Display, Boston, Mass., November 29 – December 2, 1966.

8. Houbolt, John C. et al — *Dynamic Response of Airplanes to Atmospheric Turbulence Including Flight Data on Input and Response.* NASA TR R-199, June 1964.

9. Peloubet, R.P. Haller, R.L. — *Evaluation of Response Calculations for the B-58 Airplane by Comparison with Flight Data.* Presented at the NASA Langley Research Center, September 24-25, 1968.

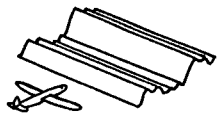

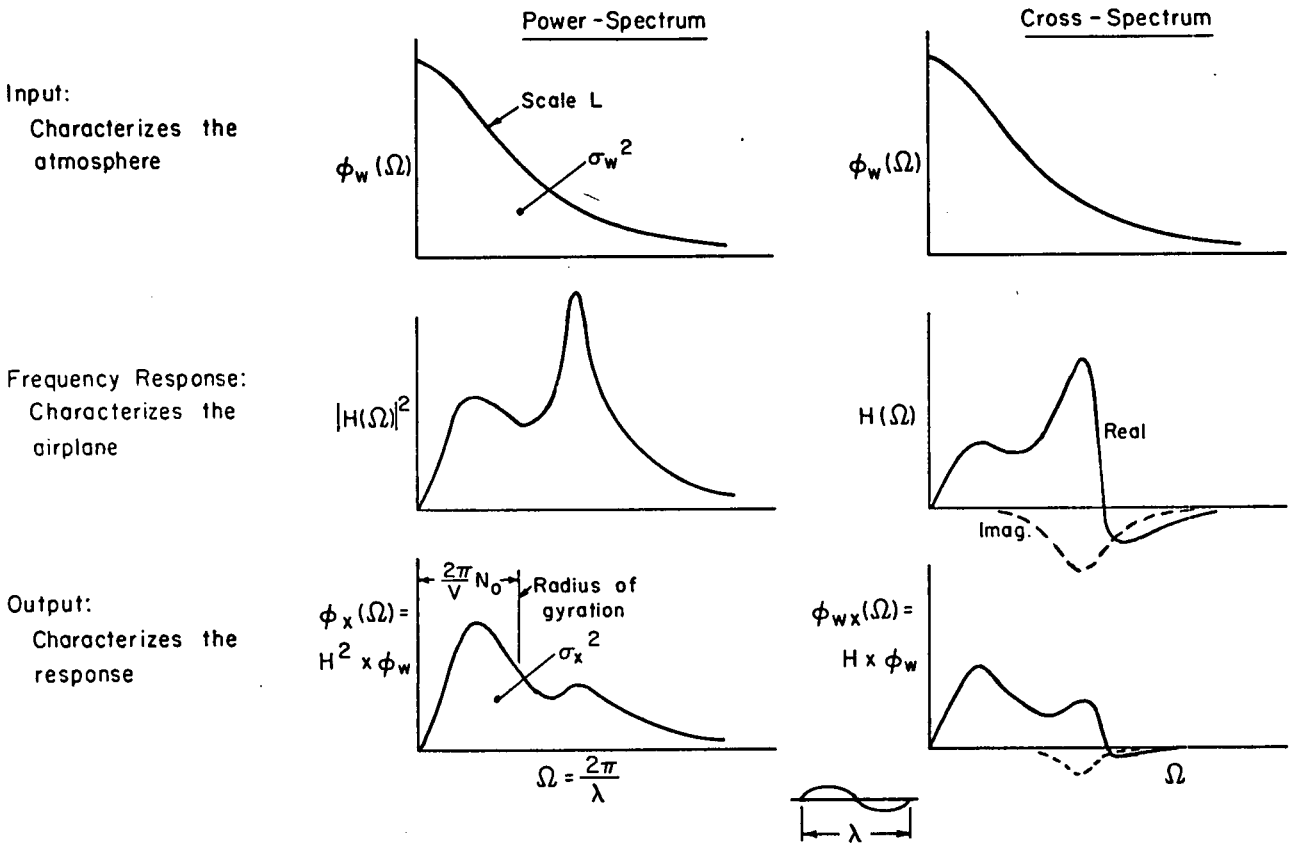

Fig.1 Input-output relations for gust response

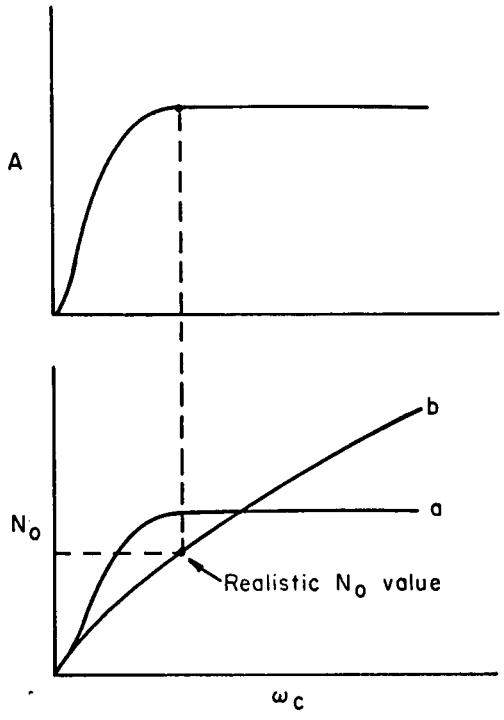

Fig.2 Establishment of A and N_o

Discrete Loads (Lumped Mass)

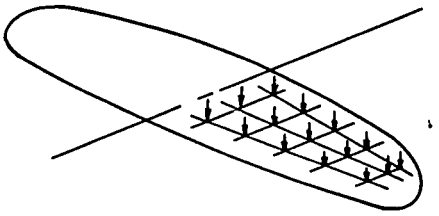

$$[D]\,|w| = \omega^2\,[m]\,|w| + |P|$$

Modal

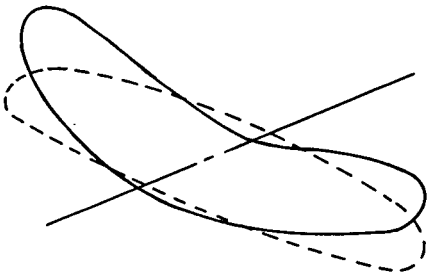

$$w = a_1 w_1 + a_2 w_2 + \cdots$$

$$M_n \ddot{a}_n + \beta_n \dot{a}_n + M_n \omega_n^2 a_n = \int p\,dS$$

Fig.3 Basic techniques for treating the structure

Strip theory

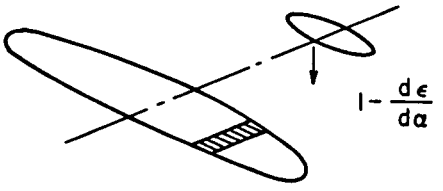

$$p = f_1(w)$$

Kernel unction

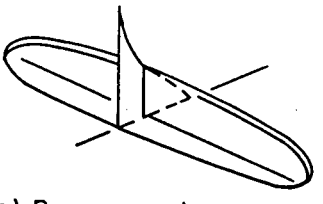

(a) Pressure mode

$$w = f_2(p)$$

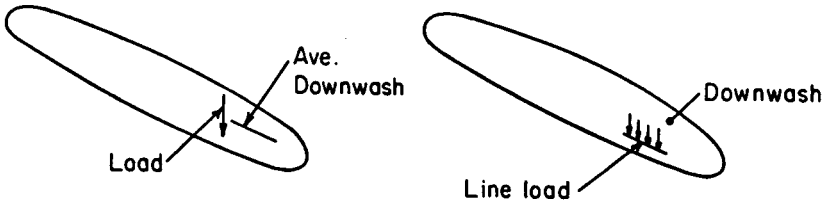

(b) Discrete element

$$|w| = |\bar{K}|\,|p|$$

or

$$|p| = |\bar{K}|^{-1}\,|w|$$

Fig.4 Basic means for treating the aerodynamics (in this figure p is pressure and w is downwash)

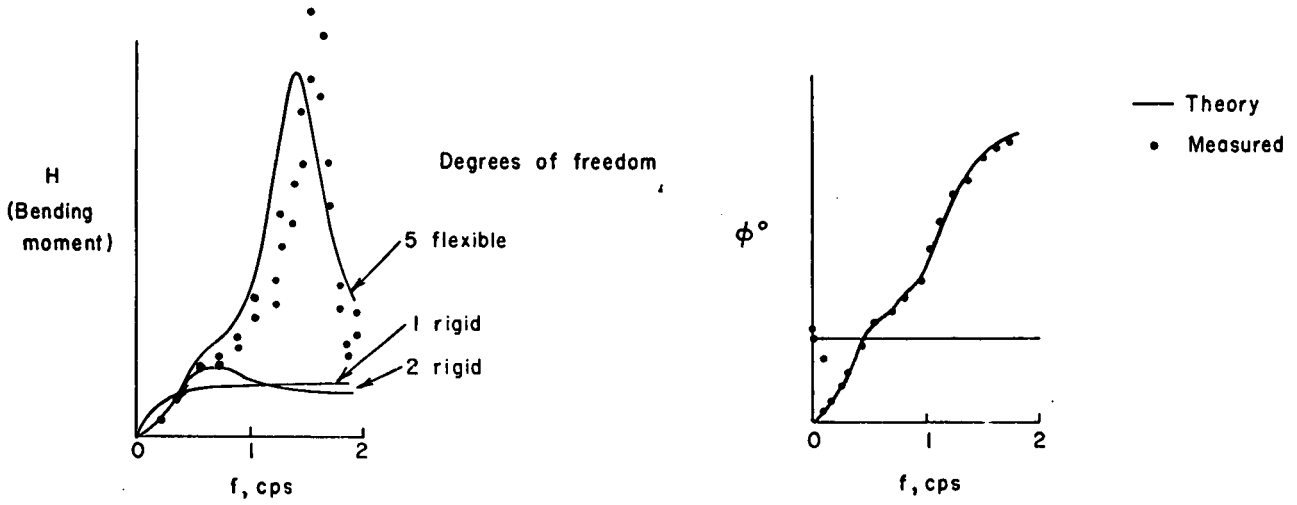

Fig.5 Calculated and measured frequency response function for a large swept-wing airplane

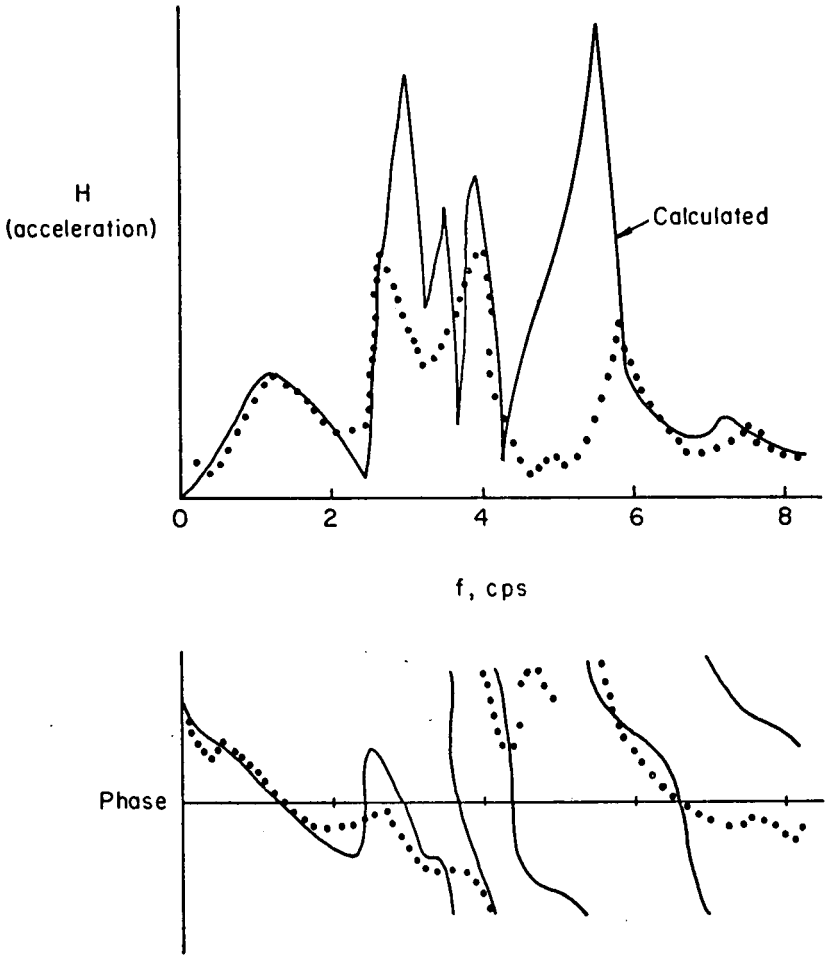

Fig.6 Calculated and measured frequency response functions for a large delta airplane

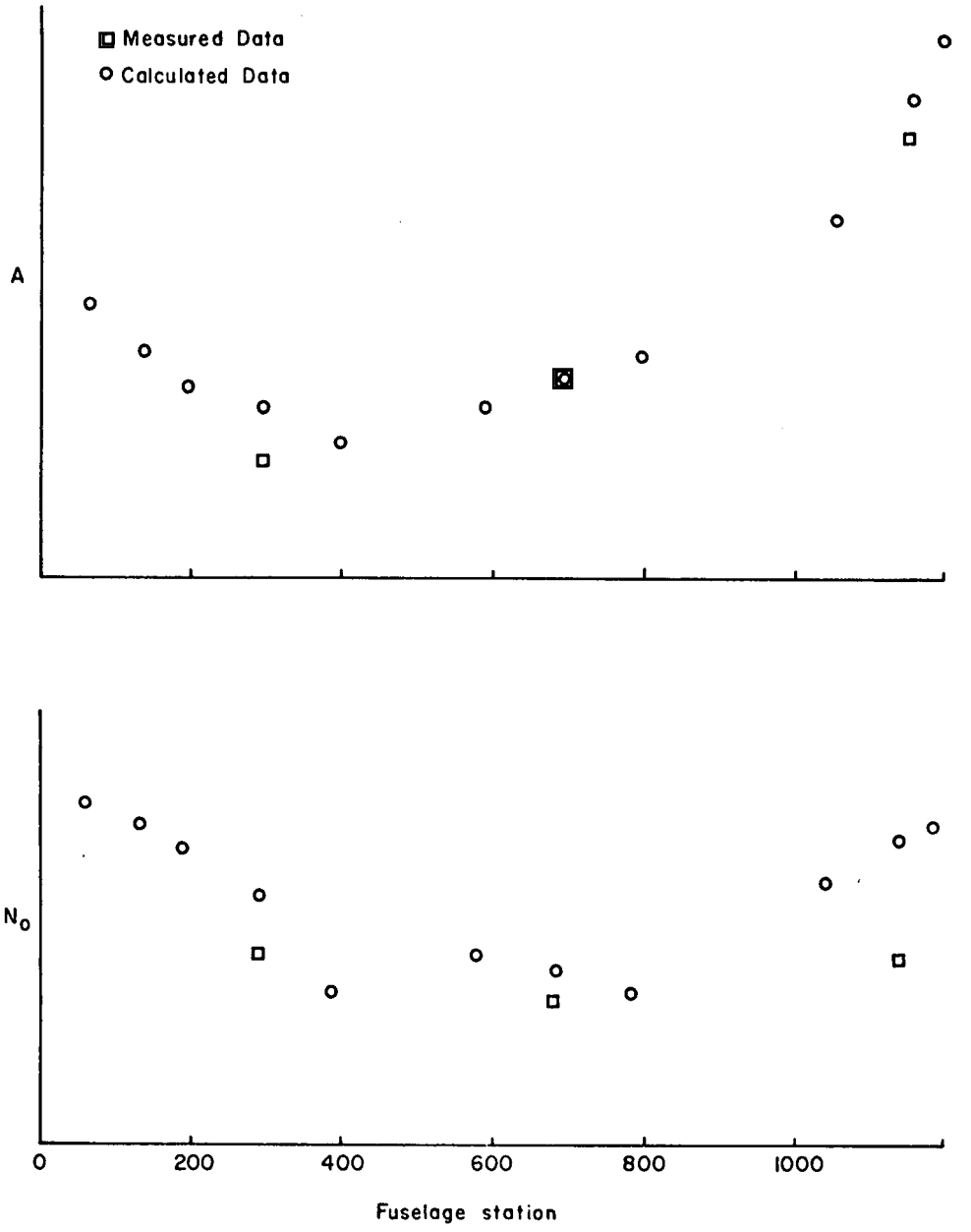

Fig.7 Calculated and measured A and N_o for a large delta airplane

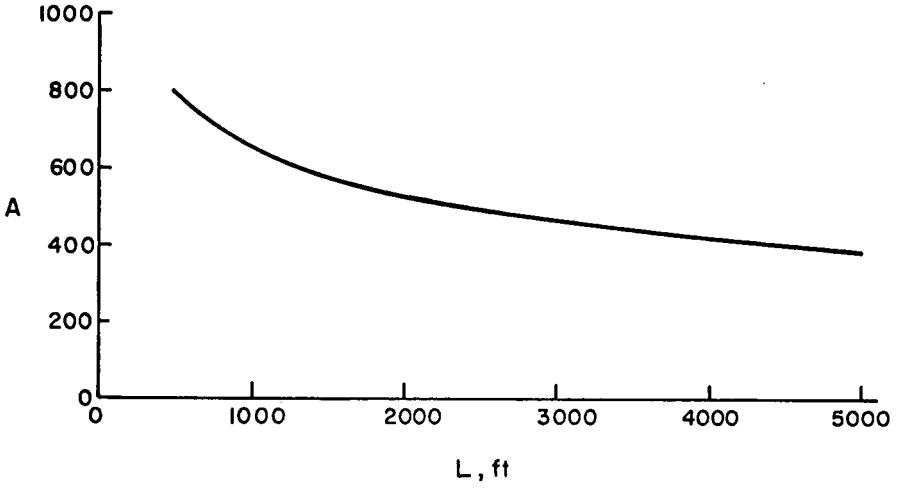

Fig.8 Variation of A with scale value L

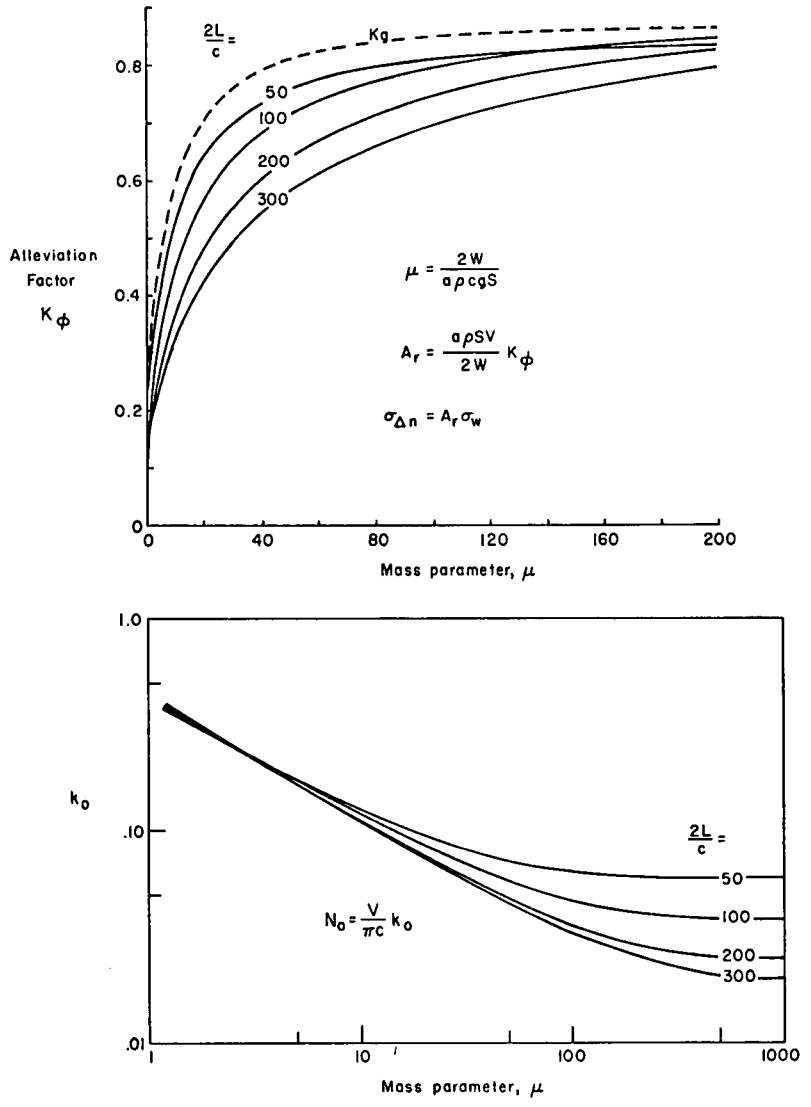

Fig.9 Gust-alleviation factor K_ϕ and zero-crossing values k_o

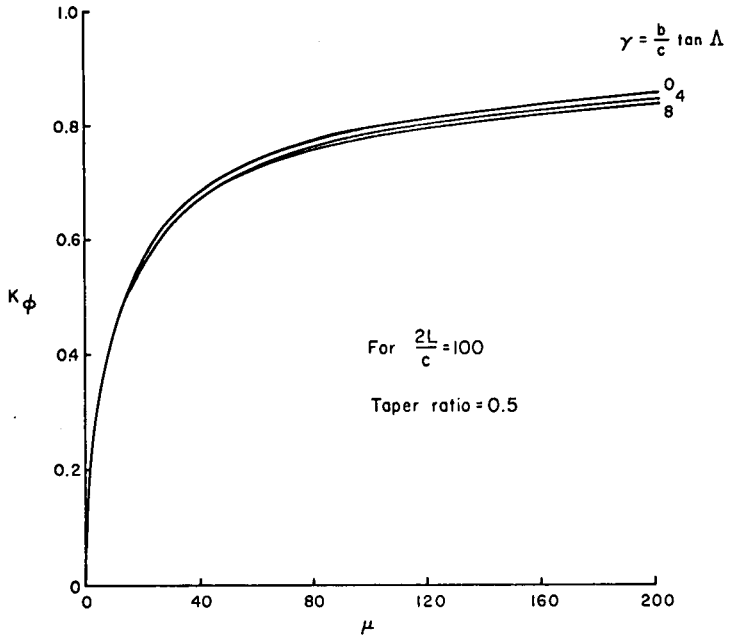

Fig.10 Effect of sweep on alleviation factor

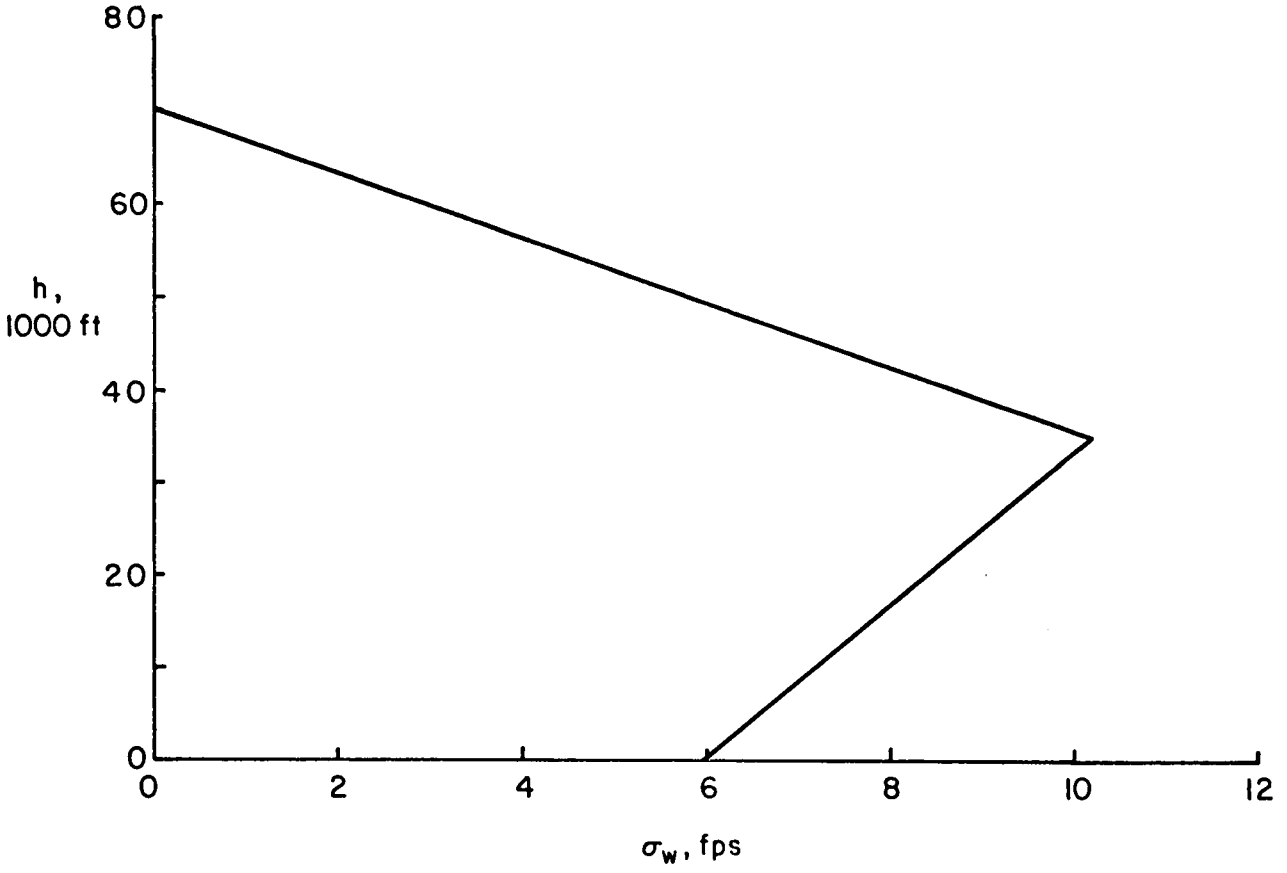

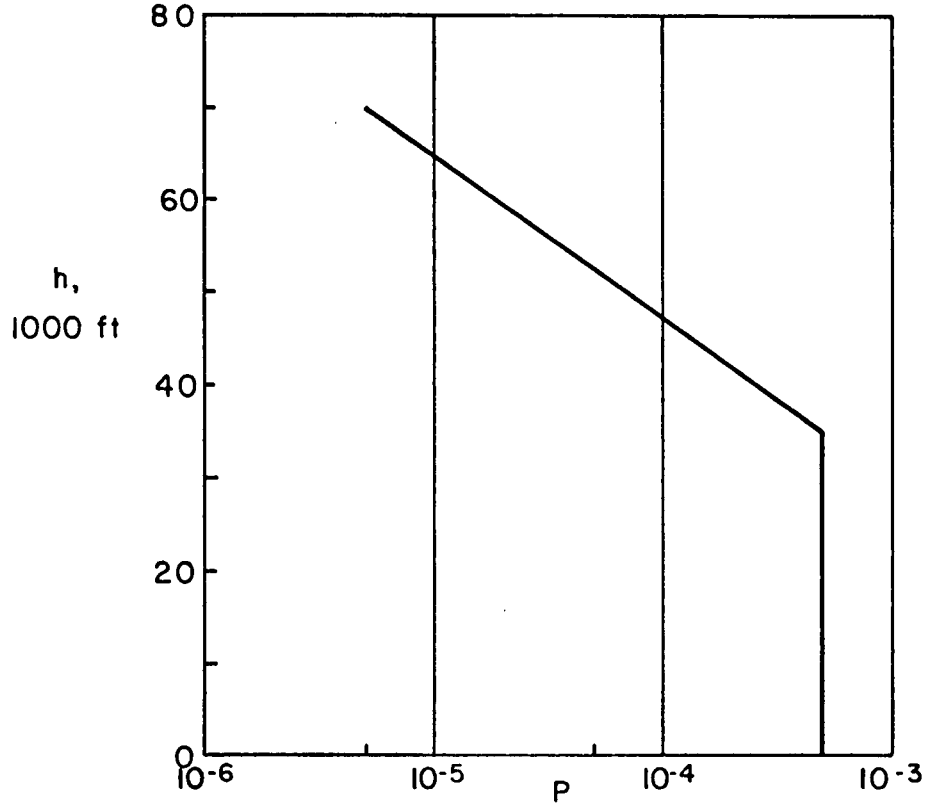

Fig.11 σ_w and P values for large load levels

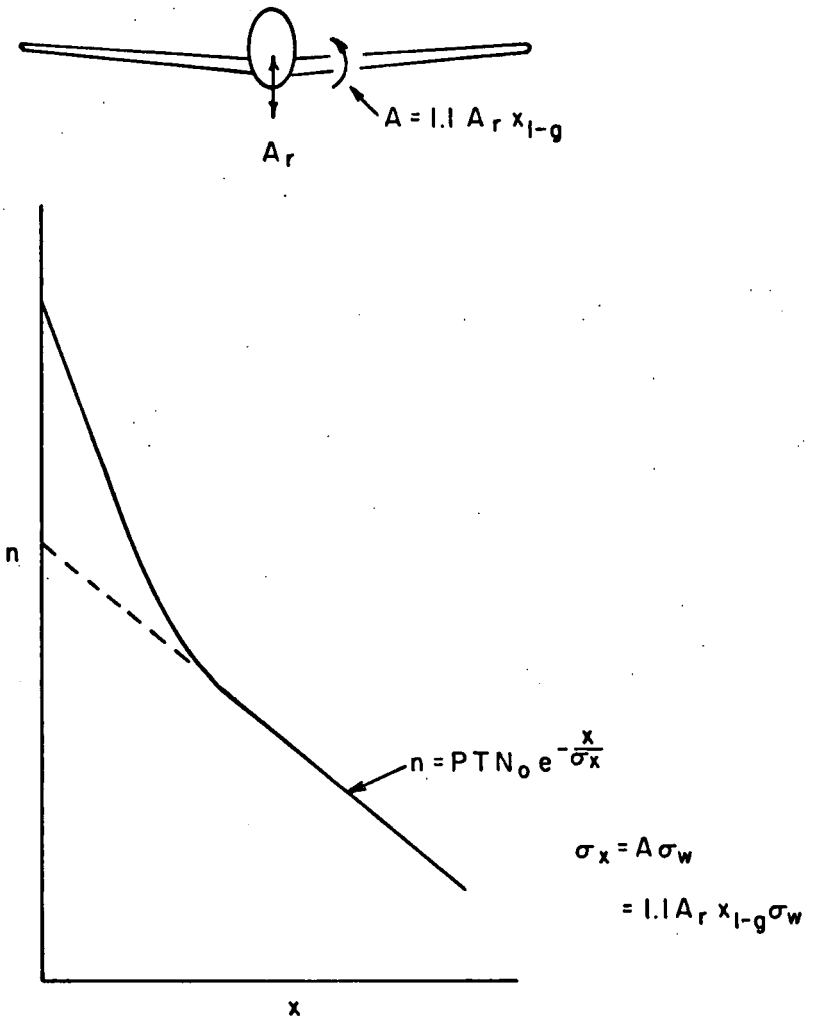

Fig.12 Representation of load exceedance curves for large load levels

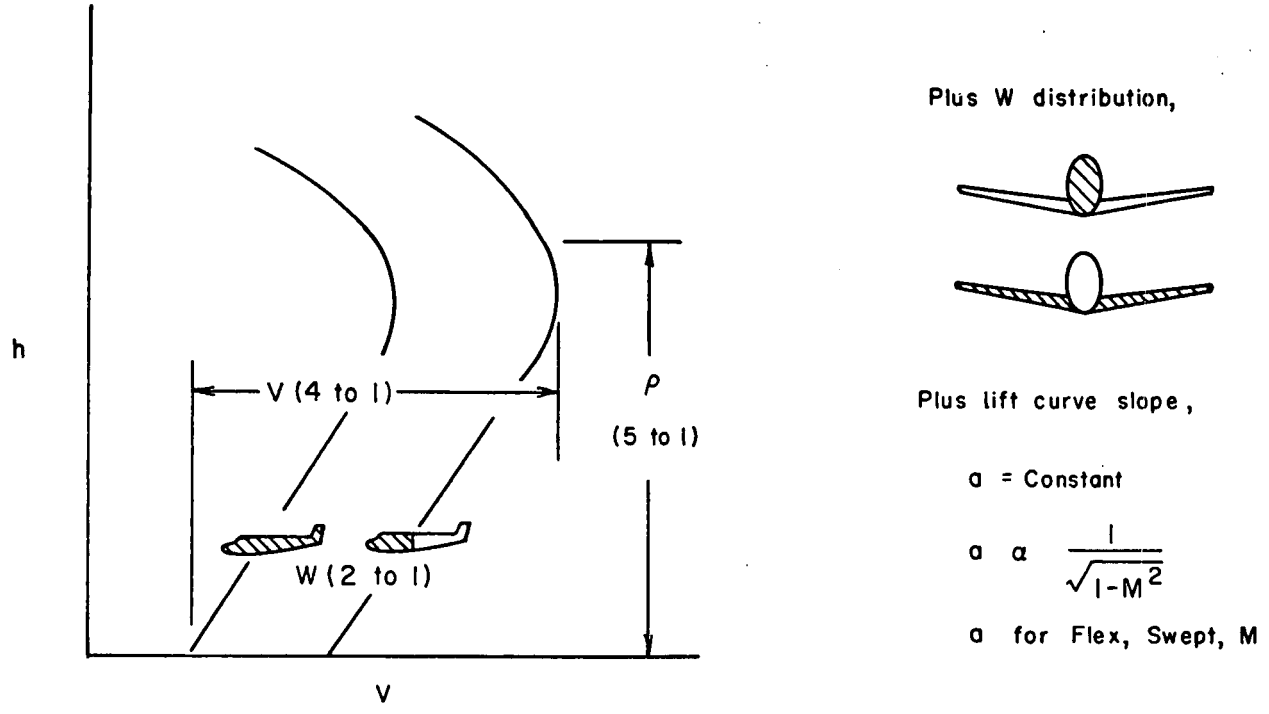

Fig.13 Variations in flight conditions leading to variation in A and N_o

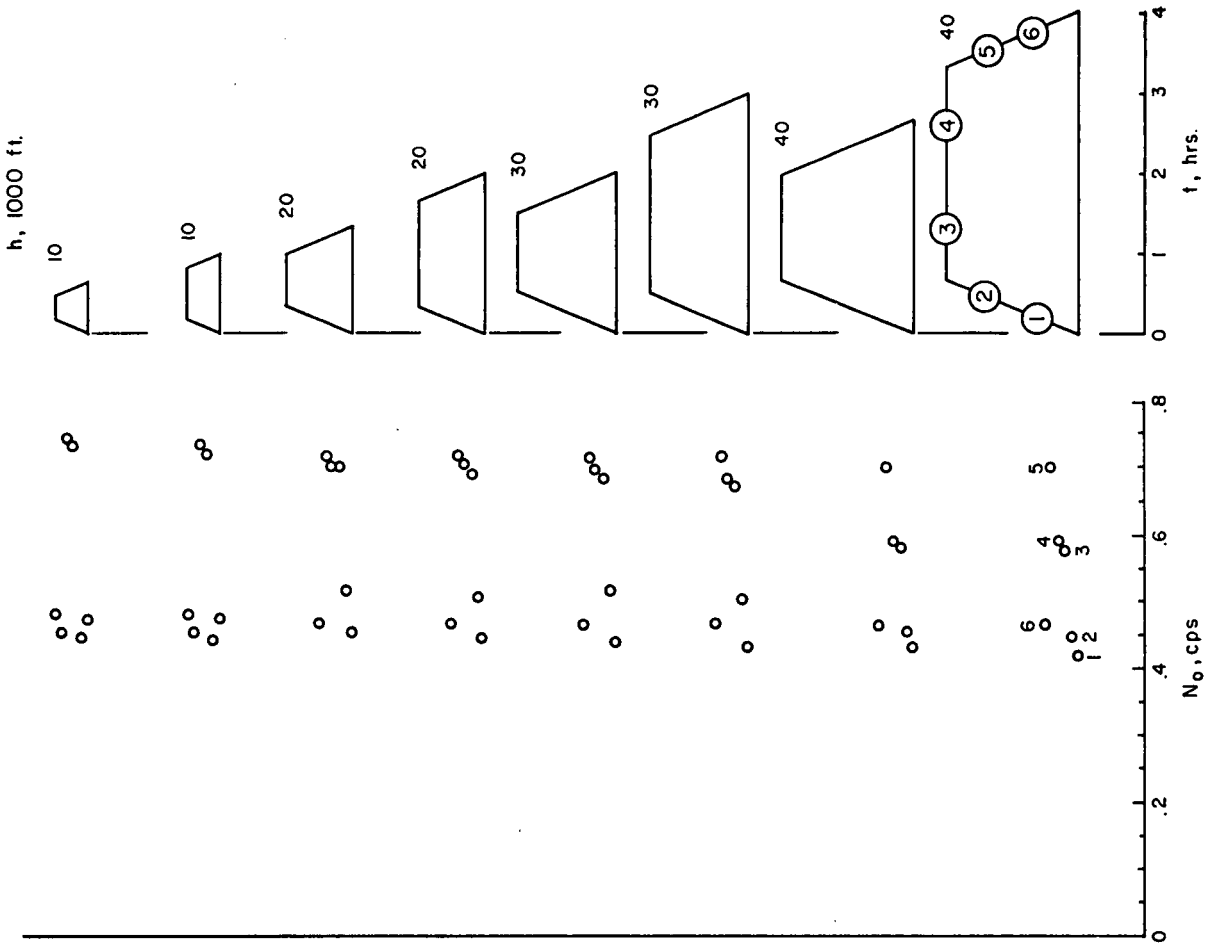

Fig.15 Variations of N_o for missions

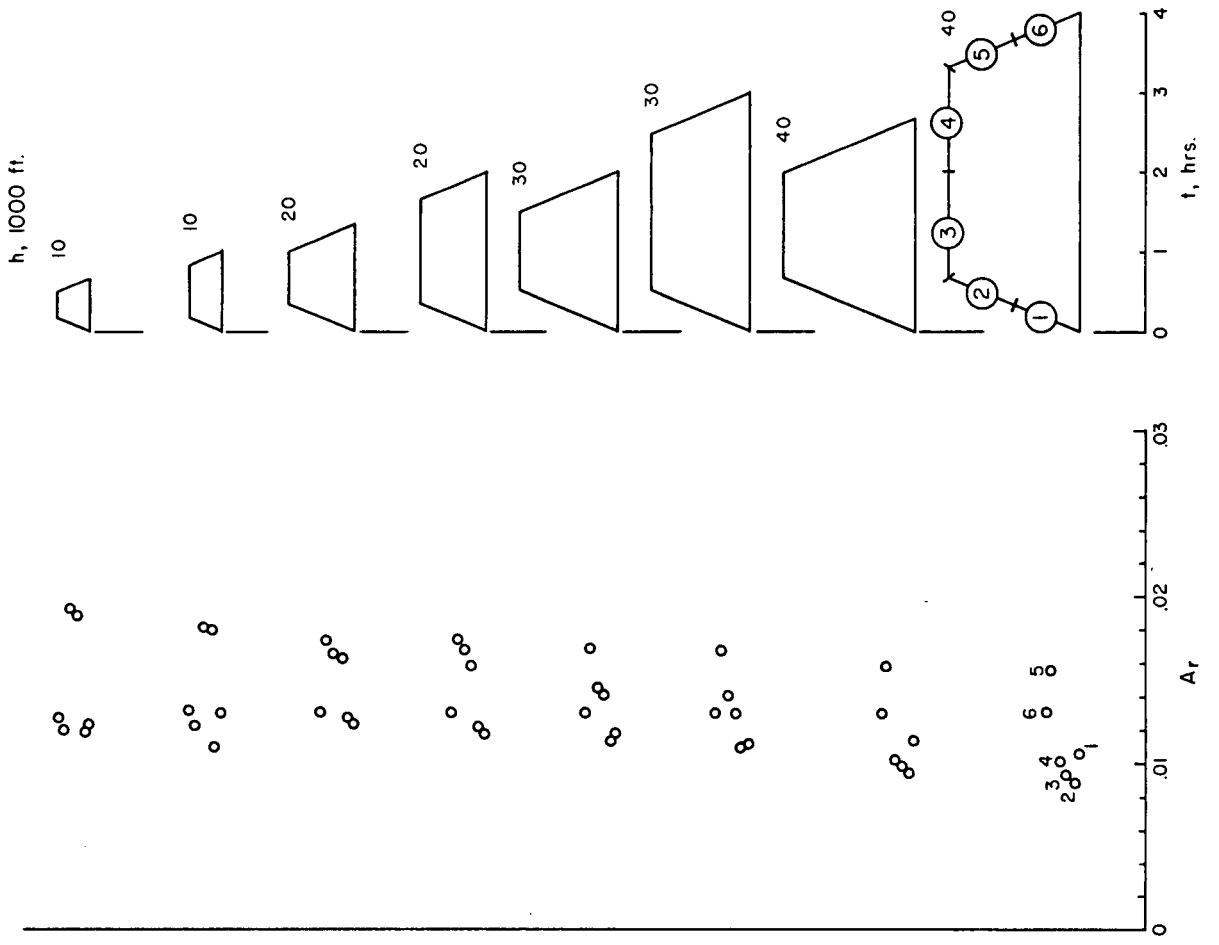

Fig.14 Variations of A_r for missions

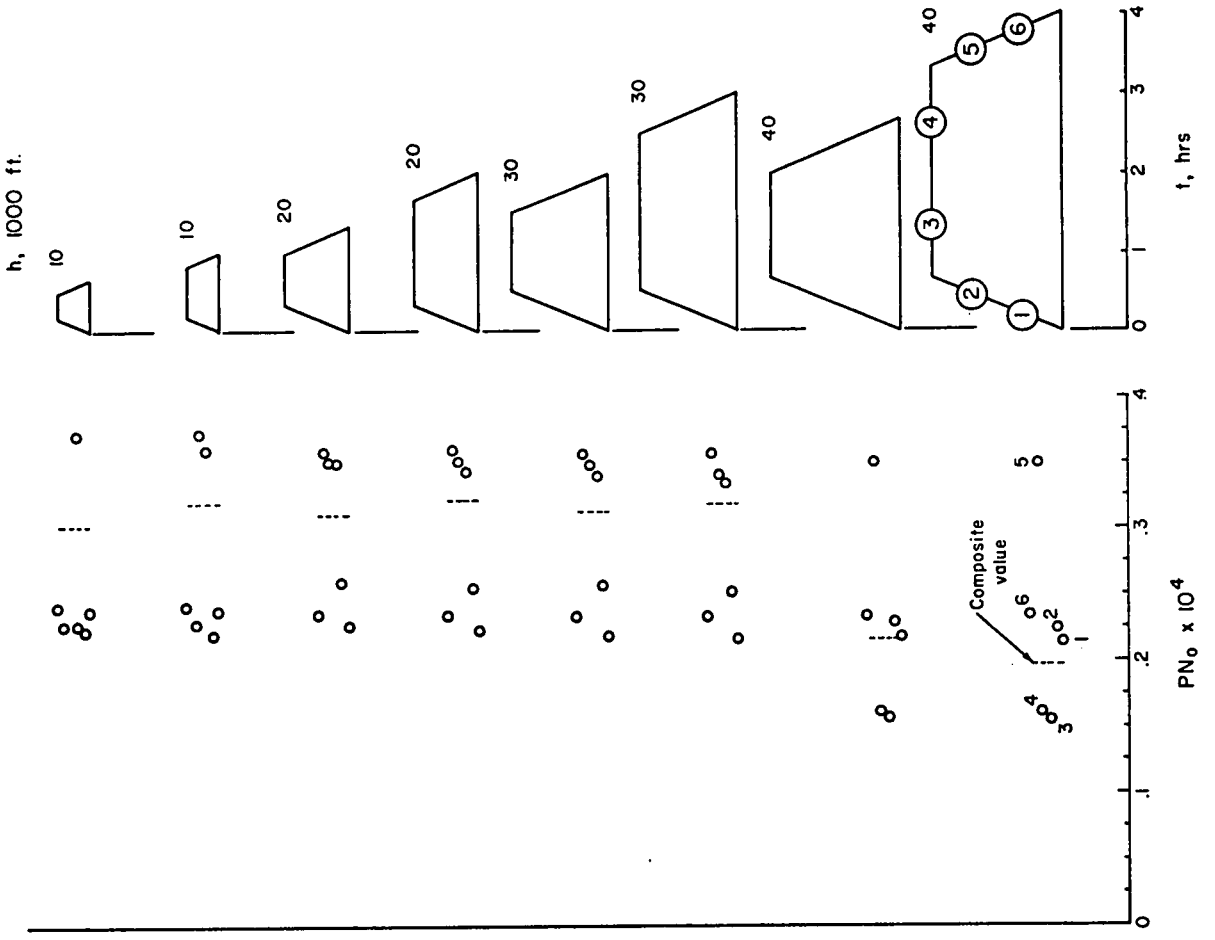

Fig.17 Variations of PN_o for missions

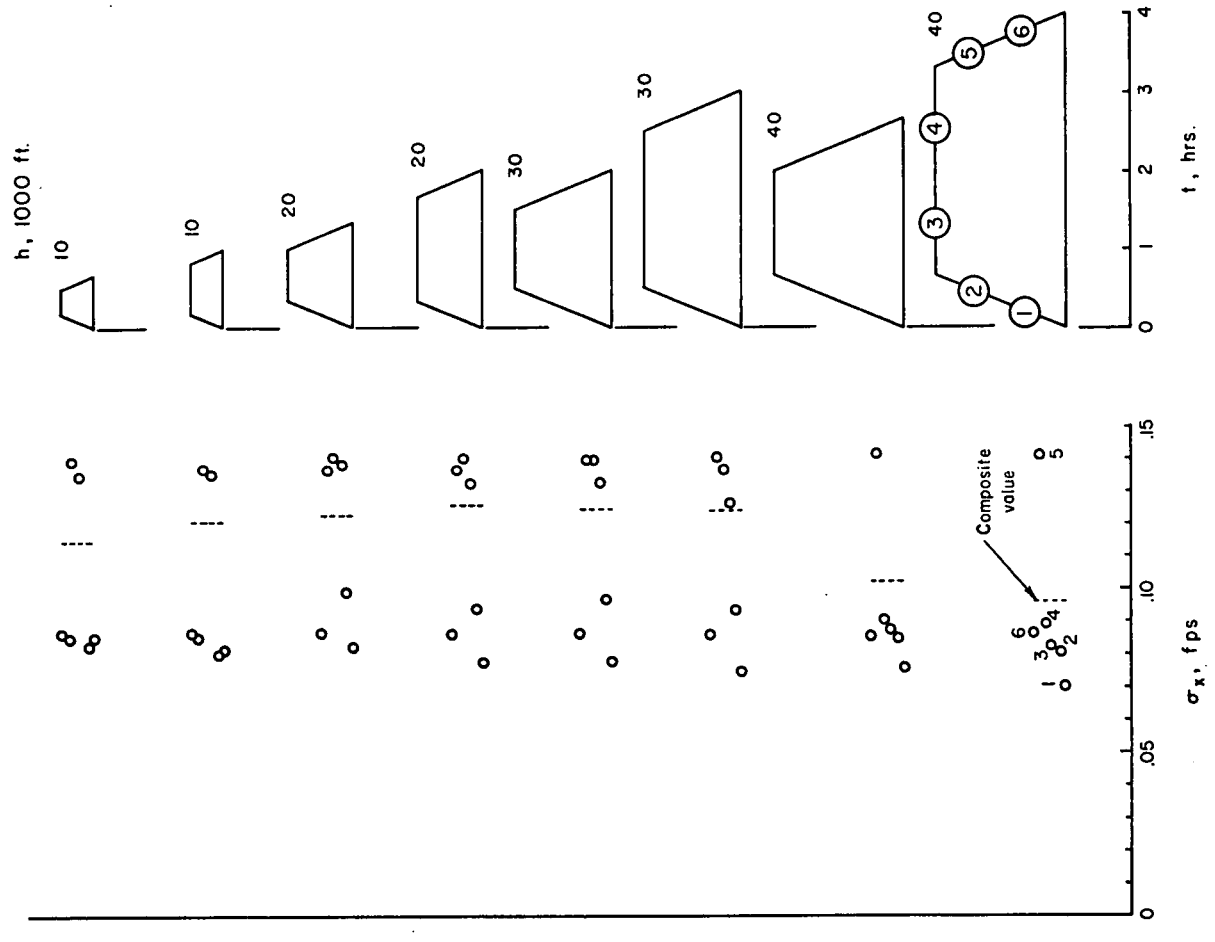

Fig.16 Variations of σ_x for missions

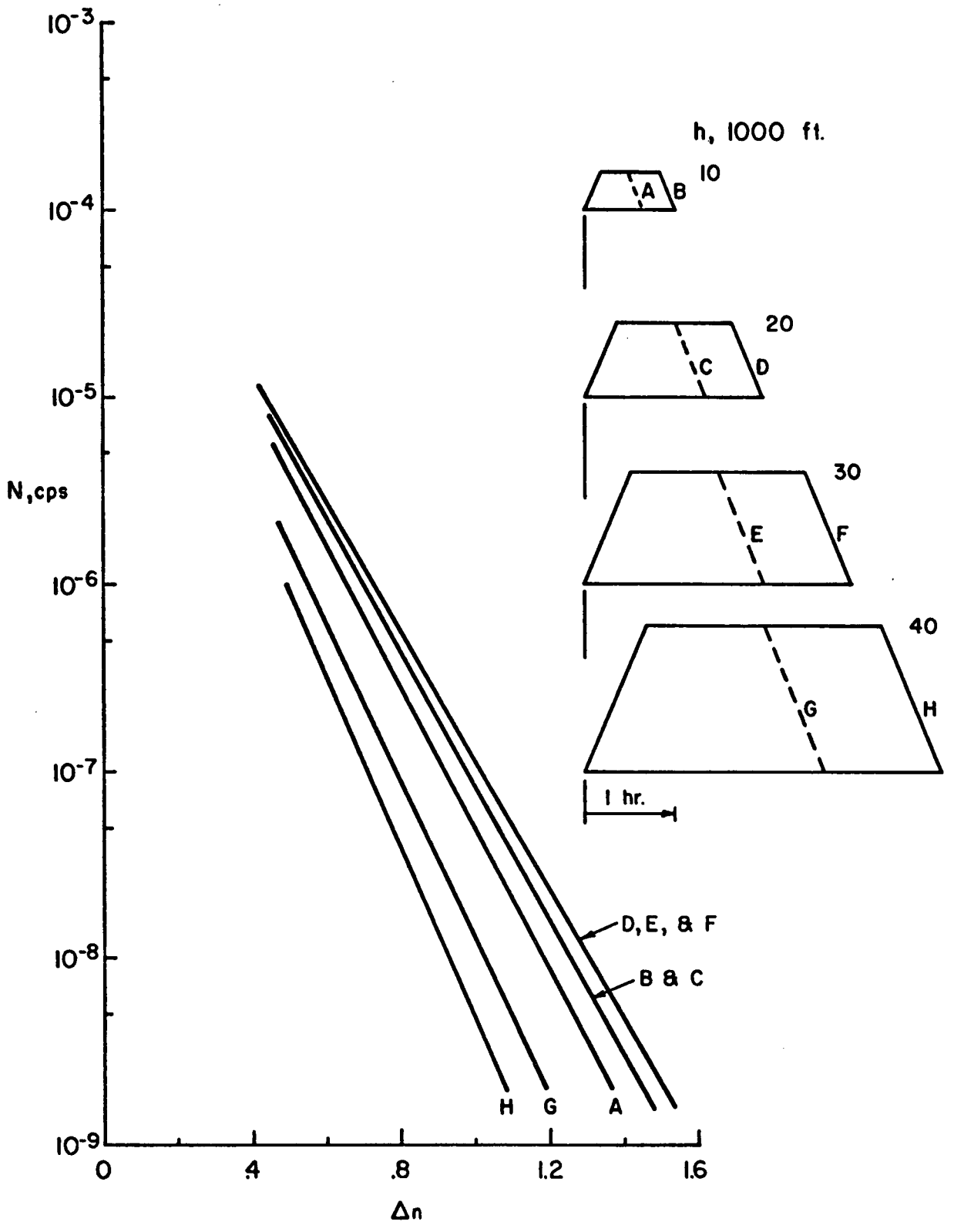

Fig.18 Number of load exceedances per second for various missions

THE EFFECT OF ACTIVE CONTROLS ON STRUCTURAL RESPONSES

by

Clifford F.Newberry
James I.Arnold
Gerald J.Kass

The Boeing Company,
Wichita, Kansas,
USA

SUMMARY

The use of an active control system on large flexible aircraft to improve flying qualities, ride qualities, and to alleviate loads require a good mathematical model. This paper deals with the selection of the mathematical model. The number of modes to be included is treated from a standpoint of stability and for structural loads evaluation. The verification of the model during flight testing is discussed. Frequency response, transient response, and random response techniques are presented. The paper presents two examples; one dealing with a lower structural mode frequency that affects the handling qualities and ride qualities of the aircraft and the other deals with a higher frequency mode that is a stability problem. Consideration for artificial damping of the flutter mode is also presented.

FOREWORD

This paper was prepared at the request of Lt Col Charles K.Grimes, Chief of Structures Division of the Air Force Flight Dynamics Laboratory, Wright-Patterson Air Force Base, Ohio, for delivery at the 31st Meeting of the Structures and Materials Panel of the Advisory Group for Aerospace Research and Development Working Group on Interaction of Handling Quality, Stability Control, and Load Alleviation Devices on Structural Loads, at Tønsberg, Norway, 2-6 November 1970. The work in this paper is a result of many people's effort within the Air Force and The Boeing Company. The authors merely summarize this work.

NOMENCLATURE

Symbol	Description
"A"	Normalized RMS gust response parameter
BS	Airplane Body Station
CPS	Cycles Per Second
DOF	Degrees-Of-Freedom
FCS	Flight Control System
FMCS	Flutter Mode Control System
FT	Feet
FUS	Fuselage
HT	Horizontal Tail
K	Feedback gain
LAMS	Load Alleviation and Mode Stabilization
NBFM	Narrow Band Frequency Modulation
PSD	Power Spectral Density
Q_i	i^{th} modal coefficient
RAD/SEC	Radians per second
RMS	Root Mean Square
SAS	Stability Augmentation System
T	Frequency response function
WBL	Wing Buttock Line
WG	Wing
W_g	Vertical gust velocity
KH (S)	Feedback electronic filter transfer function
$[N_o]$	Matrix of Generalized Structural Stiffness and Non-Circulatory Aerodynamic Stiffness Terms
$[N_1]$	Matrix of Generalized Non-Circulatory Aerodynamic Damping Terms
$[N_2]$	Matrix of Generalized Mass and Aerodynamic Apparent Mass
$[R_o]$	Matrix of Generalized Circulatory Aerodynamic Stiffness Terms
$[R_1]$	Matrix of Aerodynamic Coefficients defining the Generalized Air Forces due to Gusts

$[R_2]$	Matrix of Generalized Circulatory Aerodynamic Damping Terms
db	Decibels
fps	Feet per second
t	Time
$e^{j\lambda}$	Complex number
δ_e	Elevator deflection
δ_r	Rudder deflection
ζ	Structural damping ratio
$\dot{\theta}$	Pitch rate about wing elastic axis
τ	Time delay
$\dot{\psi}$	Rigid body yaw rate
$\dot{\psi}$ (S)	Yaw rate gyro transfer function
$\frac{q}{\delta_r}$ (S)	Transfer function relating airplane elastic bending to rudder deflection
$\frac{\psi}{\delta_r}$ (S)	Transfer function relating rigid body yaw to rudder deflection
$(S + a)$ $(S + \sigma \pm j\omega)$	Rigid body numerator transfer function zeros
$(S - b)$ $(S + c)$ $(S + \alpha \pm j\omega_{DR})$	Rigid body denominator transfer function poles
$(S + \beta_n \pm j\omega_{N_n})$	n^{th} structural mode numerator transfer function zeros
$(S + \gamma_n \pm j\omega_{D_n})$	n^{th} structural mode denominator transfer function poles

1.0 INTRODUCTION

The 1960's saw much interest in applying active controls to stabilizing structural modes on military aircraft. This interest was generated from the application of large flexible aircraft designed for high altitude operation to operation in a low altitude environment where the atmospheric turbulence excites the elastic modes of the aircraft. In some cases, these elastic modes were coupled to the pilot control inputs. As aircraft become more elastic and the frequency separation between the elastic and the rigid modes of the aircraft are reduced, the possibilities of the pilot coupling with elastic modes become greater.

Studies sponsored by the Air Force indicate that aerodynamic loads imposed on the airframe by environmental excitation of elastic modes can be alleviated by suitable control functions. These studies resulted in a more sophisticated analytical approach by the controls engineer to the airframe stability. The studies also forced communication between the control dynamics and the structural dynamics engineer which strengthed the two disciplines.

Artificially stabilizing elastic modes improves certain characteristics of the airframe. Ride characteristics are improved by increasing the damping or changing the frequency of troublesome elastic modes. A very elastic airframe will deflect in response to a gust which tends initially to reduce loading associated with the disturbance. If damping is low, the resulting overshoot in dynamic response will result in higher aerodynamic loads imposed on the airframe. Therefore, the control system should provide a compromise between resisting the first cycle load and minimize the overswing. As damping is increased, the number of cycles needed to damp the motion will be reduced, and consequently, fatigue damage will be lessened. The curves shown in Figure 1 illustrate this effect.

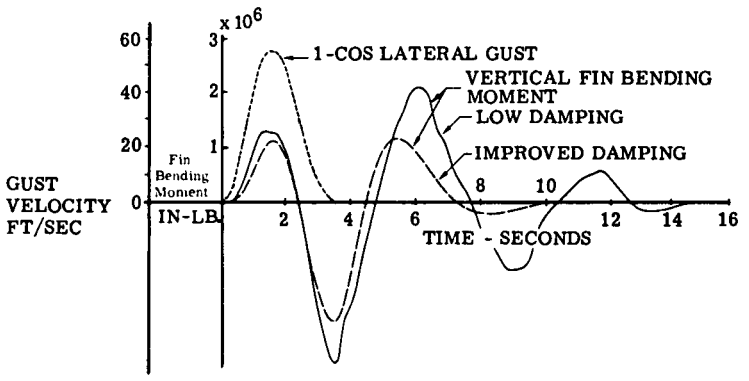

DAMPING EFFECT ON LOADS
FIGURE 1

The United States Air Force sponsored a study conducted by Boeing in 1964 and 1965 to determine if a Stability Augmentation System (SAS) could improve the structural life of a large elastic airplane. The design approach in this study is illustrated in Figure 2, wherein sensor locations, sensor types, and compensation networks are variables. Control surface sizes and locations were constrained to those existing on the aircraft. Since airplane geometry and structure were not significantly altered, basic airplane dynamic properties were also considered fixed. The system derived from this study was flight tested and is being incorporated in the B-52 fleet.

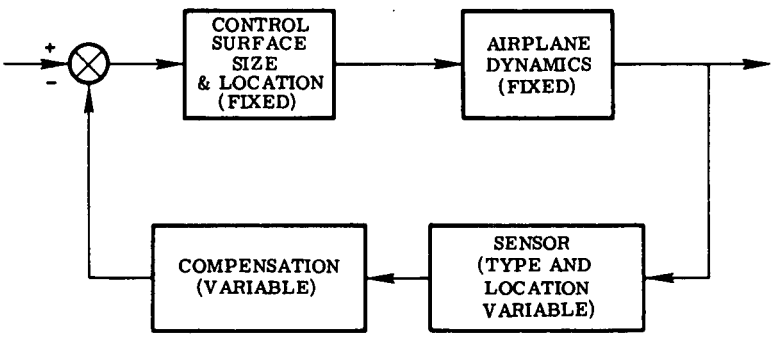

DESIGN APPROACH
FIGURE 2

Another Air Force sponsored program used a similar vehicle but allowed control surface modulation on the wings and variable pilot feel characteristics. A programmable analog computer was installed in the airplane with the capability to change stability augmentation system parameters in flight. Hardware devised for this study was also demonstrated in flight. In a third program, potential benefits of various control surface locations were assessed. The airplane dynamics is the only remaining block in Figure 2 to be treated as variable. This is the case if the Load Alleviation and Mode Stabilization (LAMS) concepts were applied in the conceptual design stages of an airplane.

Boeing is engaged in analytical studies that include evaluation of optimum surface, sensor locations, and types of sensors. The functional scope of the systems studied includes improved ride qualities, flutter stability, and reduced structural loads through maneuvering load control. Research studies are also under way to determine the application of modern control theory to the analysis of these control systems. This paper summarizes some of these studies and specifically emphasizes the mathematical model required to adequately study the effect of an active flight control system on the structural response of the aircraft. The effect of model size and composition is discussed with methods of validating the mathematical model through flight testing.

2.0 SELECTION OF MATHEMATICAL MODELS FOR ACTIVE CONTROL SYSTEM SYNTHESIS

Present computing capabilities provide the control system engineer with the tools to synthesize active control systems with great accuracy in performance predictions. However, the control system is defined in accordance with airplane models available, and therefore, the resultant system is only as good as the mathematical models used in the synthesis process. This section explores the active control system synthesis process and examines mathematical model effects on system stability and performance predictions.

2.1 Classical Rigid Body System Synthesis

For many years, the accepted approach to system synthesis has been to transform the airplane dynamic equations of motion into an equivalent set of Laplace operator equations. The Laplace transfer equations are then easily adapted to linear block diagram system synthesis techniques such as frequency response and root locus stability analysis.

The basic approach is to identify the airplane control surface and feedback sensor to be analyzed and formulate potential active control loops in terms of Laplace operator transfer functions. Typically, active control systems are employed to damp rigid body Dutch roll or short period response to improve airplane handling qualities. Figure 3 is a block diagram of a typical Dutch roll damper active control system.

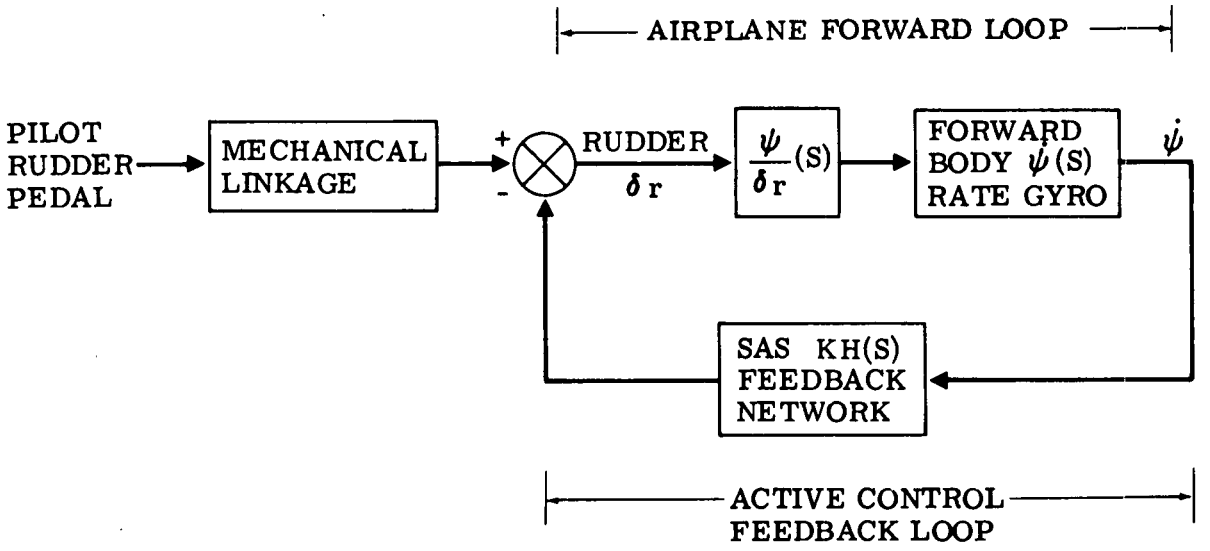

DUTCH ROLL DAMPER BLOCK DIAGRAM
FIGURE 3

Mathematical models necessary for the system synthesis are the airplane transfer function relating yaw to rudder inputs ($\dot{\psi}/\delta_r$), rate gyro input-output dynamic response, $\dot{\psi}(S)$, and the feedback electronic shaping filter dynamic characteristics KH(S). Representative transfer functions used in rigid airplane analyses for the study are:

AIRPLANE

$$\frac{\dot{\psi}}{\delta r}(S) = \frac{.2\,(S + .73)\,(S - .0085 \pm j.2825)}{(S - .0064)\,(S + .684)\,(S + .1147 \pm j1.098)} \quad \frac{\text{DEG/SEC}}{\text{DEG}} \tag{1}$$

ELECTRONIC SHAPING FILTER

$$KH(S) = \frac{\delta r}{\dot{\psi}}(S) = \frac{(8.9)(237)^S}{(S + .25)(S + 2.5)(S + 7.5)(S + 11.4)} \quad \frac{\text{DEG}}{\text{DEG/SEC}} \tag{2}$$

GYRO DYNAMICS

$$\dot{\psi}(S) = 1 \tag{3}$$

Frequency response characteristics of the airplane provide the necessary insight to the control system designer such that the frequency bandpass of the active control feedback can be postulated. Figure 4 typifies the rigid airplane lateral frequency response characteristics. The Dutch roll mode of interest peaks at .17 cps and the resultant Dutch roll damper bandpass must be adequate to pass only those frequencies in this range. Figure 5 is the Dutch roll damper frequency response relating rudder control surface deflection to a yaw rate sensor output. The gain is attenuated (washed out) below the Dutch roll frequency so that the system does not respond to steady state yaw rate commands from the pilot. The gain is attenuated above the Dutch roll frequency to prevent possible rudder response to airplane elastic bending. The high frequency gain attenuation is classically specified as attenuated at least 10 db from the midband gain at the lowest structural mode frequency.

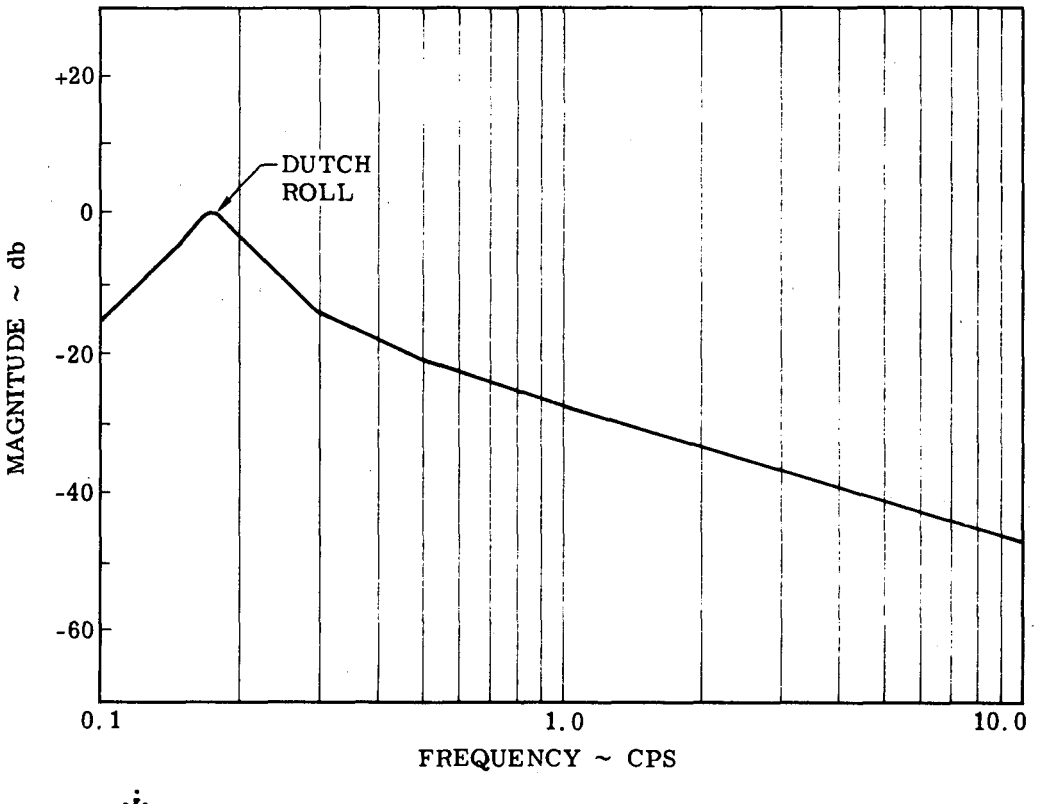

$\frac{\dot{\psi}}{\delta r}$ RIGID AIRPLANE FORWARD LOOP FREQUENCY RESPONSE
FIGURE 4

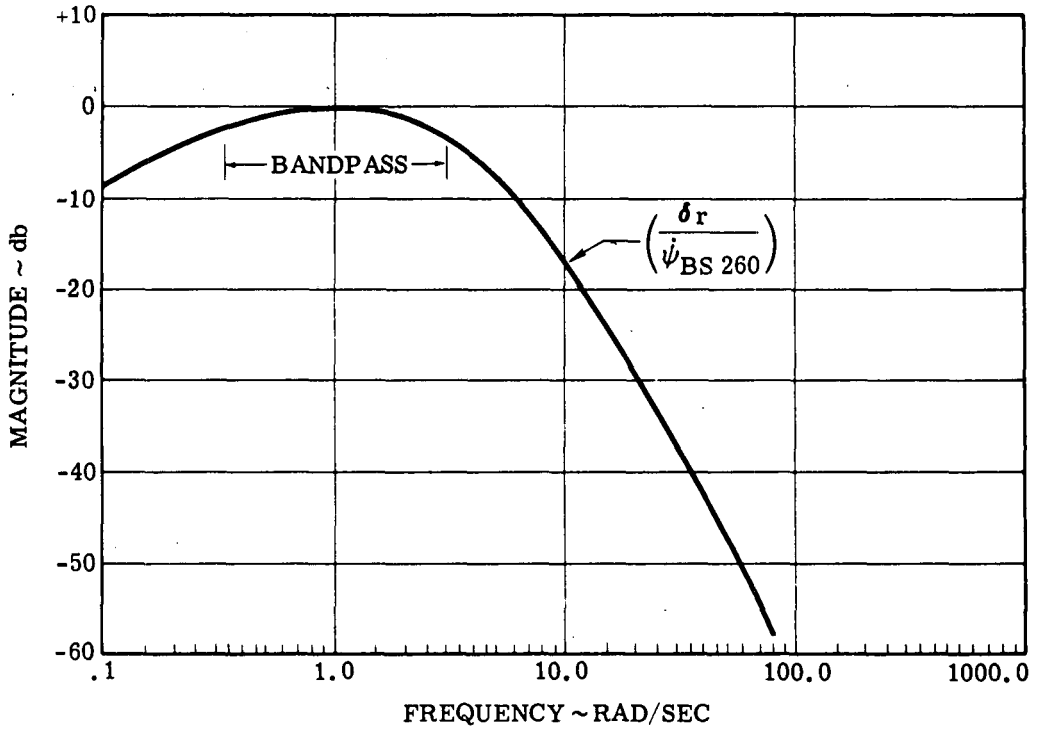

DUTCH ROLL DAMPER FREQUENCY RESPONSE
FIGURE 5

Root locus methods are used to define feedback system filter requirements, conduct stability analyses, and predict Dutch roll damping. The root locus is an analysis technique for evaluating the effects of control system feedback gain and phase shift on the airplane's dynamic response characteristics.

The airplane characteristic equation with the Dutch roll damper included is:

$$1 + KH(S)\frac{\dot{\psi}}{\delta r}(S) = 0 \tag{4}$$

As the Dutch roll damper feedback gain (K) is incremented, the roots of Equation 4 are plotted in the complex frequency domain. Figure 6 is a root locus for the Dutch roll damper; although, it is noted that the evaluation was performed on an elastic airplane model. For a rigid airplane model only, the Dutch roll mode stability can be predicted. This system concept improves the Dutch roll damping significantly, however, a check of elastic mode stability using an elastic airplane model shows the forward body lateral bending mode was destabilized with the Dutch roll damper. This indicates the importance of rigid and elastic airplane dynamic properties for active control system synthesis. In this case, there are two parameters that influence the system stability in the elastic mode frequency range. First, the feedback bandpass is not sufficiently attenuated and second, the choice of a yaw rate sensor in the forward body of the aircraft significantly magnifies the sensor pickup of the forward body lateral bending mode.

2.2 Elastic Airplane Mathematical Models

Elastic airplane mathematical models have existenced for many years to predict airplane gust loads and to evaluate fatigue and flutter characteristics. The airplane equations of motion are generally described by a set of coupled, linear, constant coefficient differential equations expressible in the following form:

$$\begin{aligned}&\left[N_2\right]\ddot{q}(t) + \left[N_1\right]\dot{q}(t) + \left[N_0\right]q(t) + \left[R_2\right]\left\{W(t)*\ddot{q}(t)\right\} + \left[R_3\right]\left\{W(t)*\dot{q}(t)\right\} \\ &+ \left[R_{1_{FUS}}\right]W_g(t-\tau_{FUS}) + \left[R_{1_{WG}}\right]\left\{K(t)*W_g(t-\tau_{WG})\right\} + \left[R_{1_{HT}}\right]\left\{K(t)*W_g(t-\tau_{HT})\right\} = 0\end{aligned} \tag{5}$$

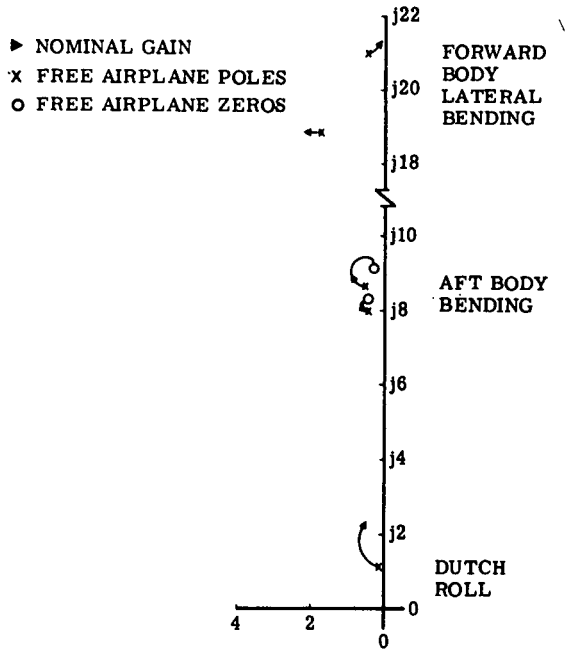

DUTCH ROLL DAMPER ROOT LOCUS
FIGURE 6

The square N and R matrices are numerical matrices containing elements that change with flight condition or airplane configuration. The column q matrices are the generalized coordinates and, for asymmetric motion, these are specified as:

$$\{q\} = \begin{Bmatrix} y \\ \phi \\ \psi \\ q_1 \\ q_2 \\ \cdot \\ \cdot \\ q_n \\ \delta_c \end{Bmatrix} \tag{6}$$

where: y airplane rigid body side translation

ϕ airplane rigid body roll angle

ψ airplane rigid body yaw angle

$q_1 \cdots q_n$ generalized antisymmetric structural displacements

δ_c control surface displacement

The notation $W(t) * \ddot{q}(t)$ and $W(t) * \dot{q}(t)$ indicates convolution with the Wagner lift growth function. The $K(t) * W_g(t-\tau)$ denotes convolution of a time delayed gust input with the Küssner lift growth function.

Airplane loads are related to the generalized elastic mode displacements by

$$\text{Airplane Load} = \sum_{i=1}^{n} C_i \, q_i \tag{7}$$

where: $n \equiv$ number of elastic modes

$C_i \equiv$ coefficient associated with the type of load, the location on the airplane, and the i^{th} elastic vibration mode.

A typical gust loads response obtained from these equations is shown in power spectral density in Figure 7. This result illustrates that a considerable portion of the wing bending moment response results from a 1 cps first wing bending mode. Therefore, loads predictions would be grossly in error if a rigid airplane representation were used to evaluate the load response. Since the early 1960's, there has been considerable interest in the idea of actively controlling airplane elastic mode responses to reduce loads due to atmospheric turbulence.

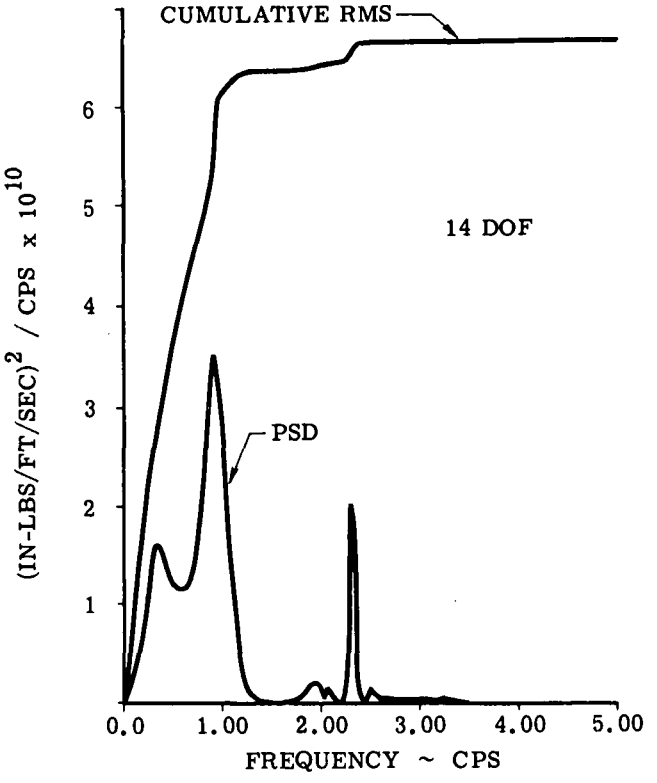

MID WING GUST LOAD PSD
FIGURE 7

An Air Force sponsored study was conducted by Boeing during 1964 and 1965 to determine if a Stability Augmentation System could provide meaningful improvements in the B-52 structural life. Analytical predictions showed that significant reductions in loading could be expected with a suitable modal damping system designed to actively control the rigid body and lowest frequency elastic airplane motions.

Accordingly, a pitch and yaw stability augmentation was designed based on the analyses, and the system was flight tested in 1967. Test results indicated gust loads were reduced as great or greater than predicted. As a result, the B-52G-H fleet is being retrofitted with the resultant system.

During the early feasibility phase of this program, an accurate airplane mathematical model was determined as the key to a successful result. Studies showed that system stability and performance prediction were greatly influenced by the number of elastic airplane modes included in the airplane mathematical model. Prior control system analyses did not consider airplane elasticity, therefore, the control system engineer had to develop new analysis techniques and adapt existing methods to the multiple degree-of-freedom elastic airplane equations.

2.3 Active Elastic Mode System Synthesis Approach

The synthesis approach for active modal suppression systems is primarily an adaptation of existing linear control theory to multiple loop feedback design. To examine closed loop stability and predict elastic mode frequency and damping, the generalized elastic equations of motion are transformed into equivalent Laplace operator expressions similar to the approach for rigid airplane analyses. Transfer functions are generated that characterize the desired airplane motion and control surface excitation. For elastic airplane analyses, more than 30 elastic modes are often required to adequately define airplane motion. Models of this size can result in greater than 100 order transfer functions.

Figure 8 is a block diagram of the elastic airplane transfer function model with active control system incorporated. The closed loop block diagram is similar to the Dutch roll damper example since the rigid body $\dot{\psi}/\delta_r$ loop still exists, but a feedback loop is represented for each additional elastic mode included in the analysis.

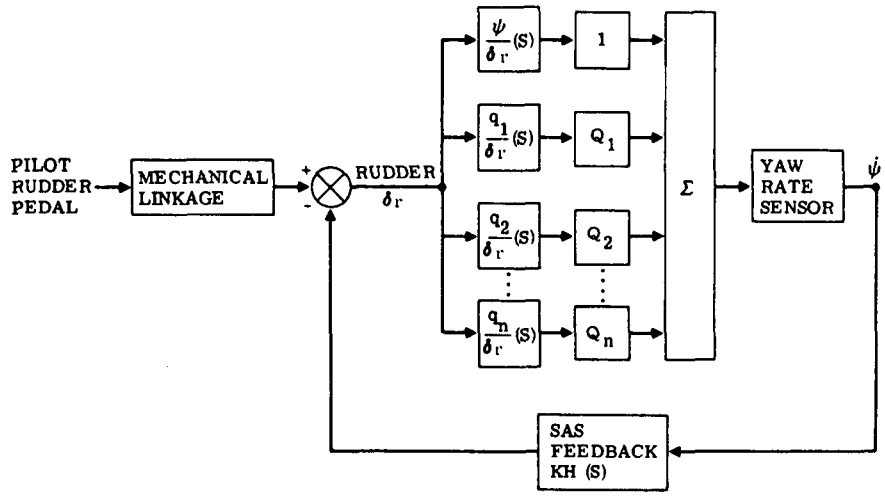

LAMS SYSTEM BLOCK DIAGRAM
FIGURE 8

From the control system synthesis viewpoint, each location on the airplane must be represented by a unique transfer function. For example, the yaw rate due to rudder transfer function at Body Station X is written:

$$\frac{\dot{\psi}_{STA_X}}{\delta_r}(S) = \frac{\dot{\psi}}{\delta_r}(S) + \sum_{i=1}^{n} Q_i(X) \frac{q_i}{\delta_r}(S) \qquad (8)$$

n ≡ number of structural modes

The constants Q_i (X), classically called model coefficients, are functions of airplane fuel distribution and location on the aircraft. Plots of typical modal coefficients versus airplane body station are illustrated in Figure 9. In terms of information sensed by a rate gyro, the modal coefficients provide relative weighting factors for each generalized coordinate. The contribution of each mode in the sensor pickup may be altered by moving the sensor location.

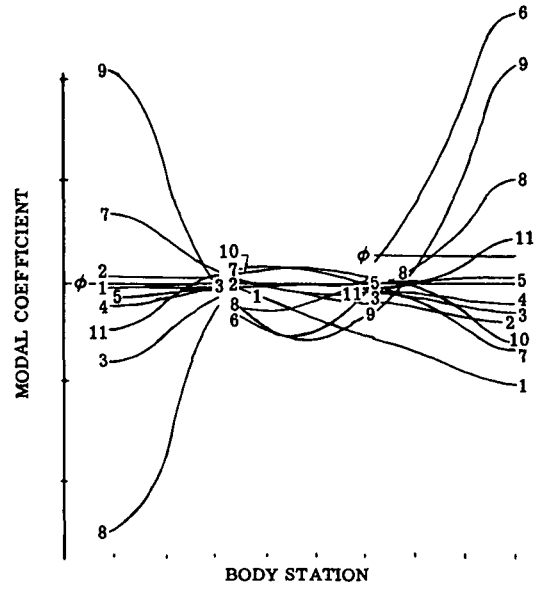

MODAL COEFFICIENTS FOR MODES 1 THRU 11
FIGURE 9

For an elastic airplane, a typical yaw rate due to rudder transfer function has the following form:

$$\frac{\dot{\psi}_{STA_X}}{\delta_r} = \frac{K(S+a)(S+\sigma \pm j\omega)(S+\beta_1 \pm j\omega_{N_1}) \cdots\cdots\cdots\cdots (S+\beta_n \pm j\omega_{N_n})}{(S-b)(S+c)(S+\alpha \pm j\omega_{DR})(S+\gamma_1 \pm j\omega_{D1}) \cdots\cdots\cdots (S+\gamma_n \pm j\omega_{D_n})} \tag{9}$$

Figure 10 is a frequency response comparison of the 24 degree-of-freedom elastic airplane at a midbody (BS 695) and aft body (BS 1307) sensor locations. The Dutch roll rigid body response is independent of sensor location, however, the first body bending response at 8 rad/sec is 10 times greater at BS 1307 than at BS 695.

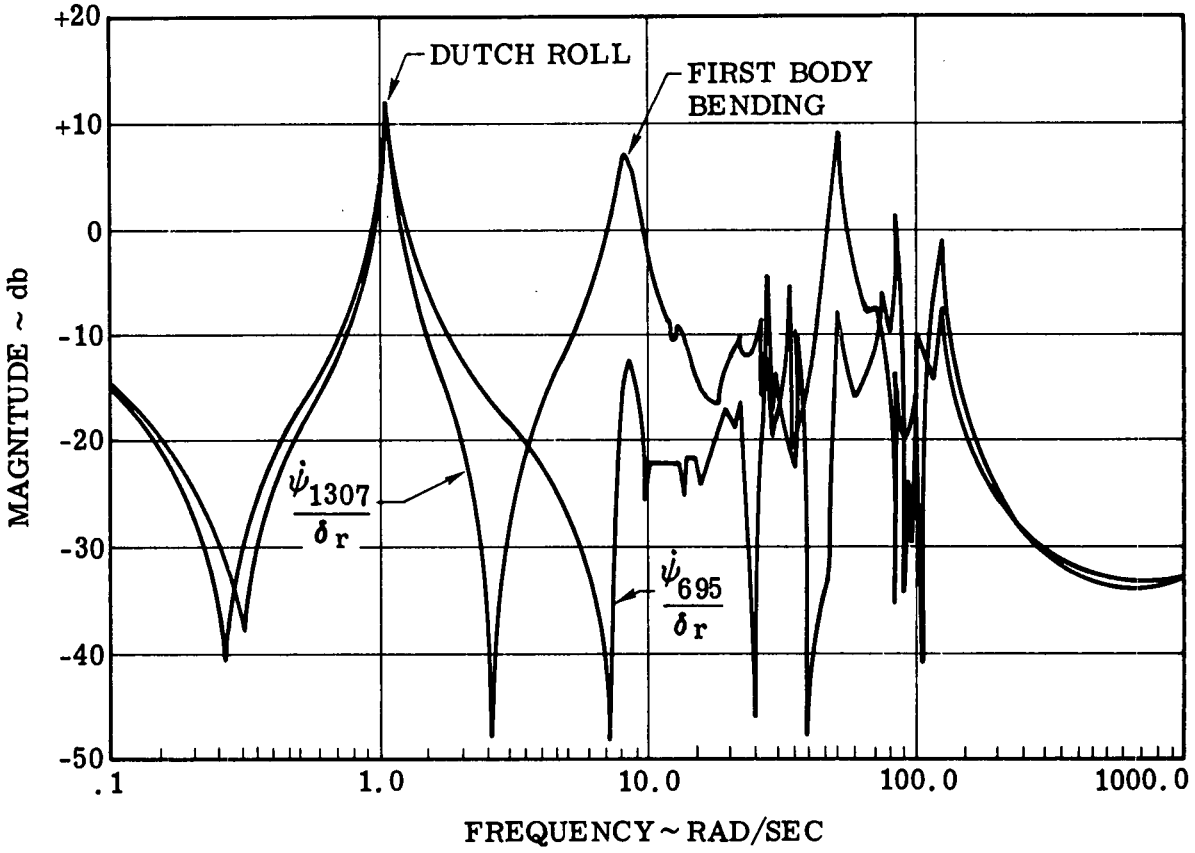

COMPARISON OF FORWARD LOOP AIRFRAME RESPONSE FOR TWO BODY LOCATIONS - 24 DOF ELASTIC AIRPLANE
FIGURE 10

The detailed control system analysis and synthesis employs the root locus method mentioned previously in the Dutch roll synthesis. For active elastic mode control, the root locus closed loop characteristic equation for a rate gyro feedback is

$$1 + KH(S)\left[\frac{\dot{\psi}}{\delta_r}(S) + \sum_{i=1}^{n} Q_i \frac{\dot{q}_i}{\delta_r}(S)\right] = 0 \tag{10}$$

A plot of the roots of Equation 10, as a function of the feedback gain K in the complex S plane, reveals to the control system analyst those elastic modes which are controllable with the selected sensor and feedback shaping filter.

Systems specifically employed to augment or control the higher frequency elastic modes are now commonly called Load Alleviation and Mode Stabilization Systems (LAMS). The technology involved in the system analyses and design is referred to as LAMS technology.

The function of a LAMS system is primarily to reduce gust induced airplane loads by improving rigid body and elastic mode damping. A LAMS system differs from a classical Dutch roll damper since it provides a higher frequency response bandpass and the feedback sensors are located strategically on the aircraft to sense elastic mode response.

Figure 11 compares the frequency response bandpass of a typical LAMS system designed to control the first aft body mode with a Dutch roll damper. The LAMS system has adequate rudder response to control airplane motions four times greater in frequency than the Dutch roll. However, the Dutch roll and lower frequency response is similar to the Dutch roll damper.

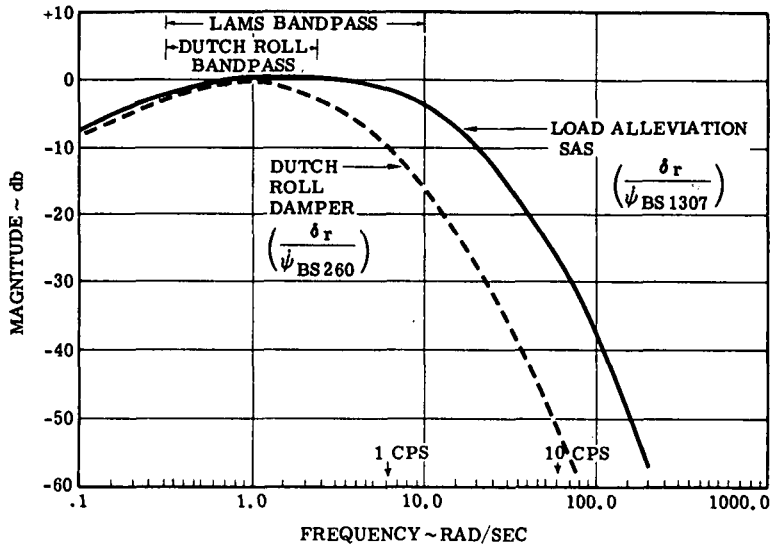

COMPARISON OF DUTCH ROLL DAMPER AND LAMS SYSTEM FEEDBACK BANDPASS
FIGURE 11

The feedback transfer function for the LAMS system is

$$\frac{\delta_r}{\dot{\psi}_{BS\ 1307}}(S) = \frac{KS}{(S+.25)(S+25)^2} \quad \frac{DEG}{DEG/SEC} \tag{11}$$

where: $\dot{\psi}(S) = 1$

A root locus showing the damping effect of the LAMS system on the Dutch roll and first aft body bending mode is shown in Figure 12.

The sensor location and feedback filter were selected such that all elastic modes above the 1.5 cps aft body bending are decoupled and feedback gain has little effect on free airplane roots.

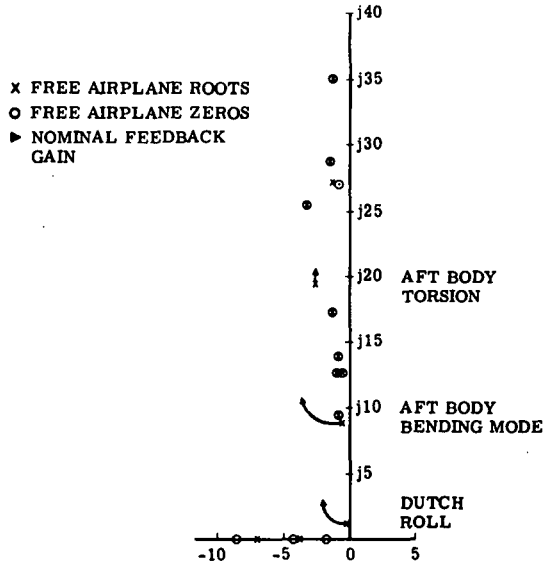

LOAD ALLEVIATION SAS ROOT LOCUS
FIGURE 12

Application of the active modal stabilization system to prevent flutter has also emerged in the past few years. A flutter mode control system (FMCS) employs essentially the same airplane elastic models and system synthesis approach as LAMS. However, flutter generally occurs at frequencies higher than the gust loads frequency range. Therefore, the FMCS must have a bandpass higher than the LAMS system as Figure 13 illustrates.

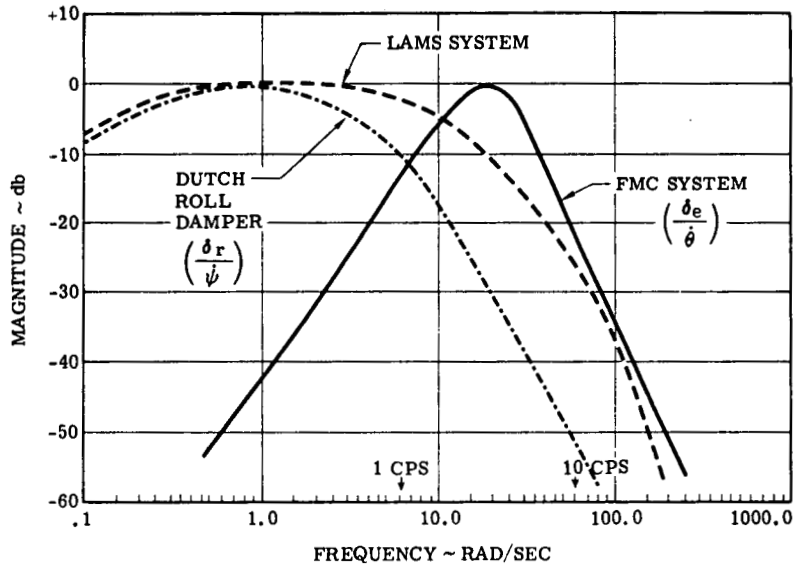

COMPARISON OF FMCS, LAMS AND DUTCH ROLL DAMPER FEEDBACK BANDPASS
FIGURE 13

This system concept uses a rate gyro located on the wing and an elevator control surface for symmetric flutter control. The transfer function representing the feedback loop is

$$\frac{\delta_e}{\dot{\theta}_{WBL\ 825}} = \frac{KS^2}{(S^2 + 12S + 144)(S^2 + 25S + 625)(S + 40)} \qquad (12)$$

The FMCS maintains positive damping on elastic modes in the flutter frequency range, therefore, the feedback is attenuated to prevent control surface response above and below the flutter frequency.

Figure 14 is a root locus which shows the effect of the FMCS on a 2.4 cps wing flutter mode. The unstable second wing bending and torsion root is driven to the stable region without significantly altering the lower frequency wing bending and short period roots.

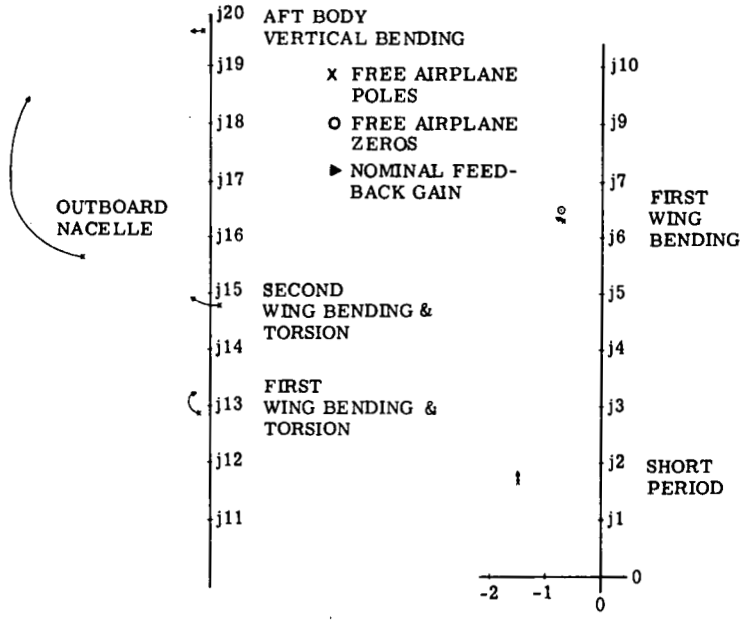

FLUTTER MODE CONTROL ROOT LOCUS
FIGURE 14

In view of the extended LAMS and FMCS system bandpass, it is essential that a complete and accurate elastic airplane mathematical model be available to cover the frequency range of feedback response. Prior to flight testing the system, sensor location, feedback filter and nominal feedback gains, are totally dependent on the analysis models. When flight testing begins, the system may be modified based on tests. In most instances, flight test time is available at a premium.

The root locus technique can be used to evaluate the effects of elastic mode selection on system stability and the sensitivity of mode damping predictions to tolerances in the airplane transfer function phase-gain characteristics.

Figure 15 shows the effect of mathematical model size on a LAMS root locus. An identical yaw rate feedback system was used for the 9 degree-of-freedom (DOF) and the 20 DOF models. Results show that increasing the model size introduces phase lag on the aft body bending and torsion modes which produces gross errors in structural damping and frequency predictions. An infinite gain margin is predicted for the 9 DOF case. However, the 20 DOF model predicts a 1.5 gain margin for the same system and the 10th degree-of-freedom at 6.5 cps limits the allowable system feedback gain.

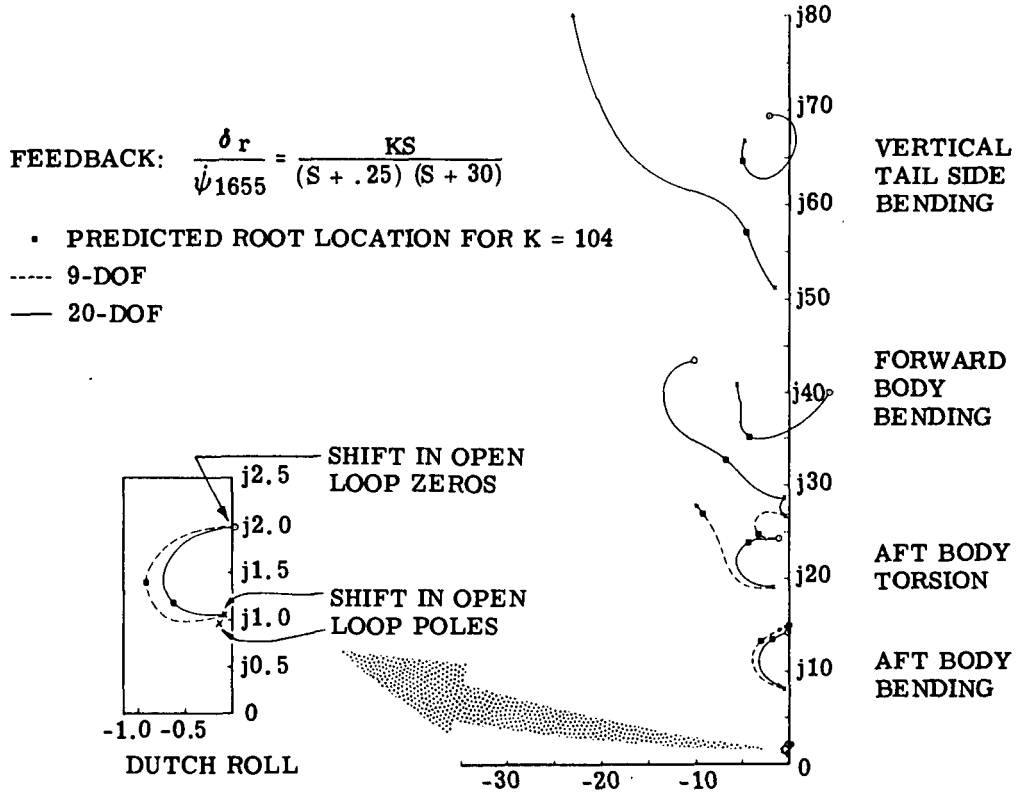

EFFECT OF AIRPLANE DEGREES OF FREEDOM ON ROOT LOCUS
FIGURE 15

This result is typical of the type and degree of errors expected when the airplane model size is not adequate. For Dutch roll damper synthesis, sensor placement and feedback filters can be selected to minimize structural motion pickup and reduce the requirement for a large mathematical model. However, LAMS and FMCS synthesis requires all elastic modes which couple with the control system under consideration. Generally, degrees-of-freedom that predominate at the sensor location should never be excluded.

After an airplane mathematical model is selected, a phase-gain root locus can be used to predict system sensitivity to tolerances in the airplane phase gain characteristics. The closed loop characteristic equation is obtained by replacing the feedback gain in Equation 10 with a complex gain, $Ke^{j\lambda}$. The resultant phase gain root locus equation is

$$1 + Ke^{j\lambda}\left[\frac{\dot{\psi}}{\delta_r}(S) + \sum_{i=1}^{n} Q_i \frac{\dot{q}_i}{\delta_r}(S)\right] = 0 \qquad (13)$$

Incrementing K for $\lambda = 0$ in Equation 10 corresponds to the familiar gain root locus. Non-zero values of λ have the effect of rotating the gain root locus in the S-plane. Figure 16 illustrates a typical phase-gain root locus.

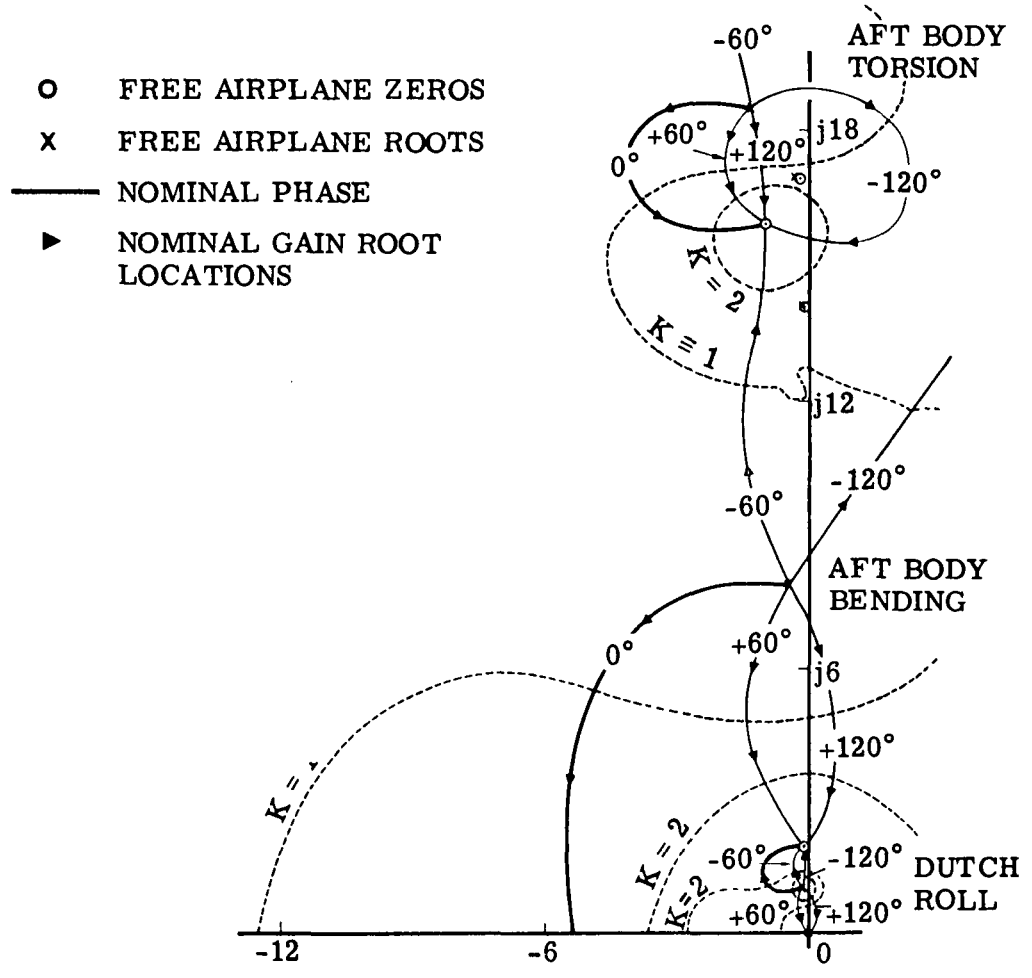

EFFECT OF FEEDBACK PHASE ON ROOT LOCUS
FIGURE 16

The nominal phase-gain airplane characteristics result in a predicted aft body damping ratio with LAMS of $\zeta = .67$. However, phase of -60 degrees lag at the 1.5 cps frequency results in an insignificant damping improvement. If the airplane's actual transfer function characteristics had been in error by -120 degree phase lag, the nominal system selected would actually be unstable in flight. When analysis predictions prove sensitive to model representation, a carefully controlled flight test evaluation of the airplane model is required.

3.0 FLIGHT VALIDATION OF THE MATHEMATICAL MODEL

The proof of any system is obtained through hardware validations accomplished by ground and flight tests. The system performance can then be compared to the theoretical predictions to determine the soundness and accuracy of the mathematical model and analytical techniques. This section discusses the various flight test techniques available for evaluating aircraft characteristics with active flight control systems.

3.1 Transient Response Testing

3.1.1 Purpose and Technique

Transient response testing has been used for many years as a tool to determine the stability of an aircraft. This testing determines experimentally the frequency and damping of the rigid-body and elastic modes of interest for comparison with theoretical analyses and proof of system performance.

Active flight control systems are generally of the form shown in Figure 17. To evaluate the system with or without SAS, control inputs are commanded to the control surfaces to upset the airframe dynamics. The aircraft responses are then monitored to determine system stability and performance.

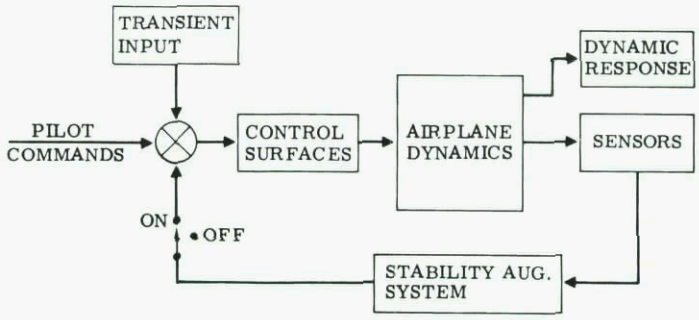

TRANSIENT RESPONSE TESTING BLOCK DIAGRAM
FIGURE 17

In general, the technique used in evaluating weapons systems has been through the manual control system in response to pilot induced control transients. However, two problems exist with this manual input procedure. One problem stems from the inability to obtain comparable inflight measurements of aircraft variables required to make factual tradeoff decisions. This information requires a defined and repeatable disturbance function. The other problem is that of extracting system dynamic information (frequency, damping, phasing, etc.) from a response that is a composite of several variables with characteristics in terms of frequency, amplitude, phasing, and damping. A combined response of this type is common when the input forcing function is not band-limited in frequency content.

A repeatable disturbance that excites the desired modes appears to be the simplest and most usable technique. This technique disturbs the aircraft and the output is displayed in a form suitable for immediate and direct evaluation in terms of SAS performance. A function generator, Figure 18, is used as the signal producing device capable of variable frequency, amplitude, number of cycles of excitation, and waveform (i.e. sine, ramp, square, or triangular). The output of the function generator can then be summed with the SAS signal into the autopilot or control surface actuators to excite the airframe at the desired frequency and mode of interest (i.e. Dutch roll, 1st wing bending, aft body bending, etc.). This technique can only work when the airplane autopilot or control surface actuators can accept the function generator electrical signal and these systems have adequate bandpass to provide excitation at the desired frequencies.

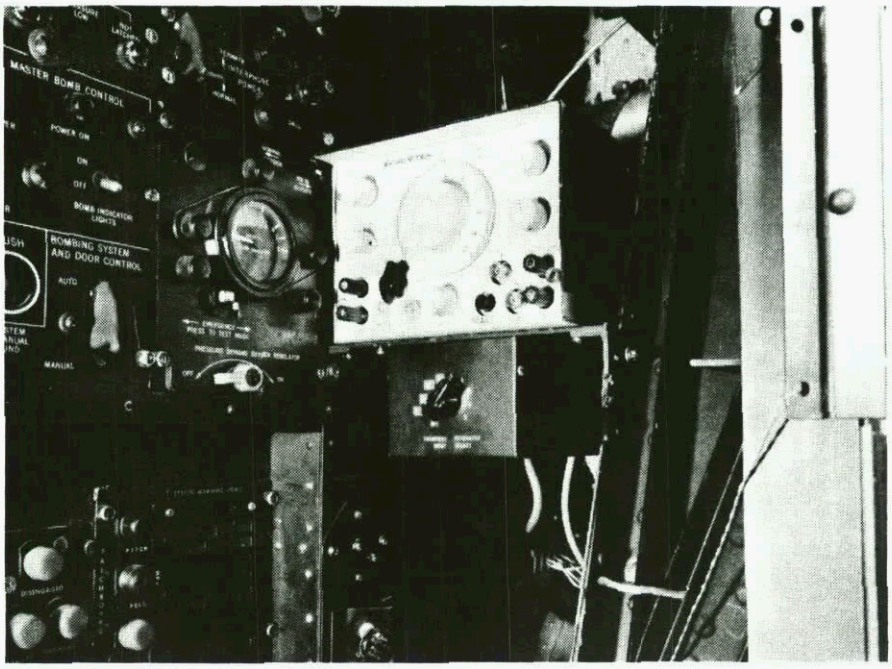

FUNCTION GENERATOR
FIGURE 18

3.1.2 Test Results

Boeing has used the transient response test technique to evaluate flight control systems, including SAS, to determine system performance. Typical results of using the function generator to excite discrete modes of interest for large flexible airplanes are shown in Figures 19, 20, and 21.

Figure 19 shows the effect of the SAS on the Dutch roll mode at a frequency of 0.16 cps. The input was commanded to the rudder for two cycles and then turned off to allow the airplane to respond as it would. The SAS-OFF airplane response shows little decay in oscillation after the excitation is terminated. As noted for the SAS-ON response, an immediate attenuation occurs when the SAS is engaged. Similar results are shown in Figure 20 for an aft body bending mode at a frequency of 1.4 cps. As noted, a significant improvement in modal damping is evident with the SAS engaged.

Figure 21 shows the effect of the SAS on a higher frequency wing-body mode at 2.6 cps. Again, an improvement is shown with the SAS-ON, but is not as dramatic as Figures 19 and 20 and indicates that the system was not designed for optimum performance at this frequency.

The results obtained during this testing provided frequency and damping data that could be explicitly compared with theory. Figure 22 shows a good comparison of system performance versus gain for the modes that needed SAS control to provide reduced airframe fatigue damage during flight through turbulence. Based on these results, a high degree of confidence exists that the SAS will perform adequately in random atmospheric turbulence.

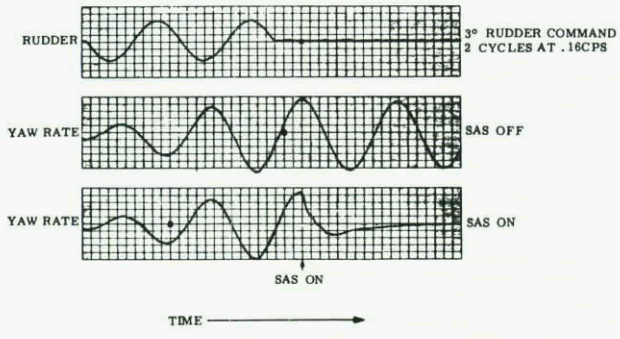

EFFECT OF SAS ON DUTCH ROLL MODE
FIGURE 19

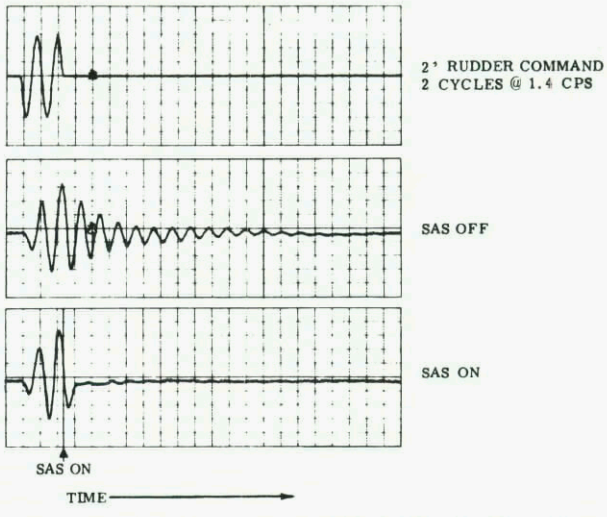

EFFECT OF SAS ON AFT BODY BENDING MODE
FIGURE 20

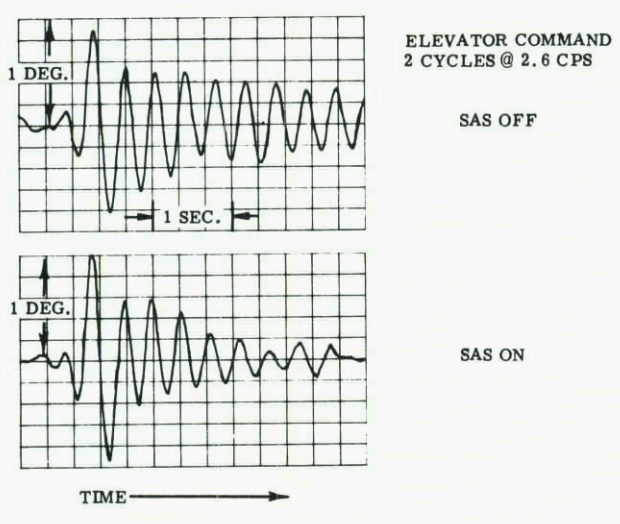

EFFECT OF SAS ON WING MODE
(ANGULAR DISPLACEMENT)
FIGURE 21

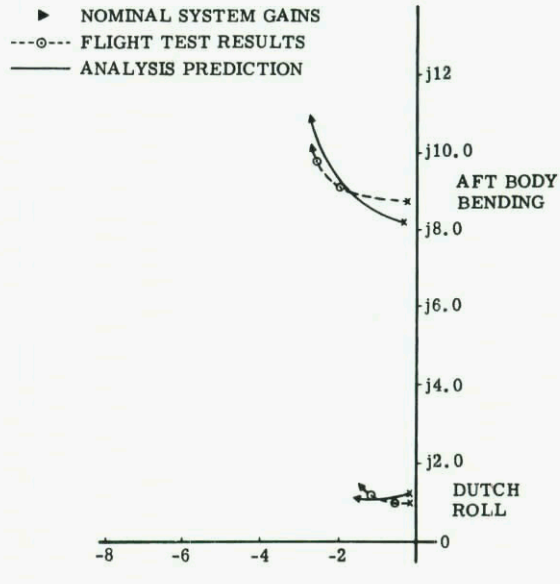

ROOT LOCUS RESPONSE COMPARISON
FIGURE 22

3.2 Frequency Response Testing

3.2.1 Purpose and Technique

As mentioned in the previous section, the primary concern was to identify the frequency and damping of various modes to determine the system performance. This technique is adequate for a narrow bandwidth SAS from 0-2 cps. However, wide bandwidth SAS (0-10 cps) are more complex and, therefore, the experimental test techniques must be capable of providing comparative performance data to check the mathematical model or, if needed, provide data to correct the model.

Typical response data is shown in Figure 23 for the aft fuselage acceleration due to a one degree elevator deflection. As noted from this figure, there are numerous elastic modes between 1 and 10 cps which must be controlled to reduce the airplane fatigue damage problem. To accurately define the response function, a continuous sinusoidal sweep can be accomplished over the frequency spectrum between 0.5 and 10.0 cps while continually recording the response parameters. To accomplish this testing a function generator similar to that shown in Figure 18 is required and incorporated into the system as depicted in Figure 17. This function generator must have the added feature of automatic sweep rate similar to laboratory vibration test equipment. The sweep rate should be established such that near steady-state responses will be achieved throughout the frequency spectrum tested.

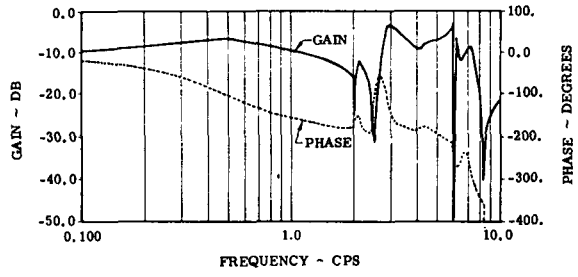

RESPONSE FUNCTION OF AFT FUSELAGE ACCELERATION PER DEGREE ELEVATOR DEFLECTION
FIGURE 23

The test excitation equipment is somewhat more complex and data obtained can be used by the controls engineer. This data will be used to compare the response function of the experimental and theoretical basic airplane (SAS-OFF) to confirm the math model used in the SAS synthesis studies.

As an alternate approach, a discrete frequency response technique can be used and does not require the complex excitation equipment of the continuous sweep test technique described in the previous paragraph. This technique requires the aforementioned function generator with a capability of running for many cycles of excitation so that near steady-state responses are attained at the selected frequency of oscillation. This technique has been used by Boeing to evaluate the basic airframe dynamics. Phasing of the SAS was a suspect at the frequencies to be controlled by the SAS. Figure 24 shows some typical data obtained using this technique and shows good agreement between theory and experiment below 2 cps with a significant deviation above 2 cps. Additional testing could be accomplished using this technique and approach the sweep test technique by obtaining data at many frequency intervals.

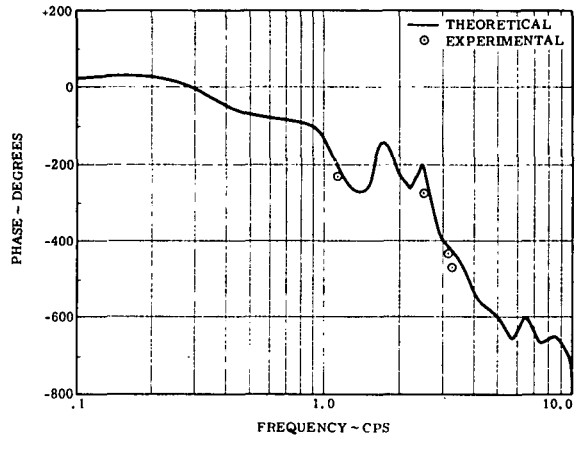

PHASE RESPONSE OF AFT FUSELAGE PITCH RATE DUE TO SPOILER DEFLECTION
FIGURE 24

3.3 Random Testing

3.3.1 Purpose

The previous sections discussed evaluation of the airplane mathematical model and system performance through evaluations based on system responses due to control excitations. These techniques are required by the controls engineer to determine the system performance. However, the system final proof-of-performance still depends on how the system performs in the real world of atmospheric turbulence in terms of loads, accelerations, and fatigue damage reductions. Since the testing is accomplished in random turbulence, statistical methods must be used in the data analyses for comparison with the analytical results. This requires considerable time and money to produce the final results.

3.3.2 Test Procedure and Data Reduction

The airplane system to be evaluated is flown through atmospheric turbulence as shown in Figure 25 with or without the SAS engaged. The airplane responses are recorded on Narrow Band FM (NBFM) tape for system performance evaluation using appropriate ground station computer techniques. In addition to the airplane responses, a gust probe similar to the one shown in Figure 26 is required to reduce the raw recorded response data to frequency response functions per unit gust velocities. Representative gust velocity time histories for the three earth referenced axes are shown in Figure 27. The frequency response function in terms of accelerations and bending moments are independent of the input spectrum and can be compared for various flight segments although gust environments of individual samples were not identical. The frequency responses were computed using the cross-spectral approach.

$$T_r/g(i\,\omega) = \frac{\Phi r,g(i\,\omega)}{\Phi g,g(i\,\omega)} \qquad (14)$$

where: $T_r/g(i\,\omega)$ is the complex frequency response of "r" with respect to the input "g"

$\Phi r,g(i\,\omega)$ is the complex cross-spectral density of "r" and "g"

$\Phi g,g(i\,\omega)$ is the auto-spectral density of the input "g"

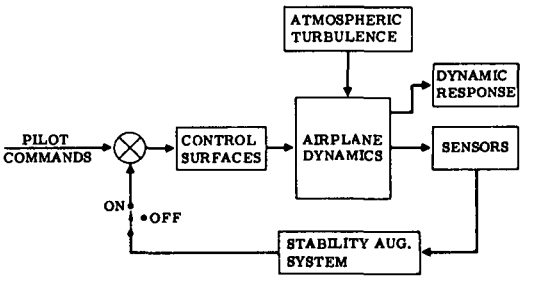

RANDOM TESTING BLOCK DIAGRAM
FIGURE 25

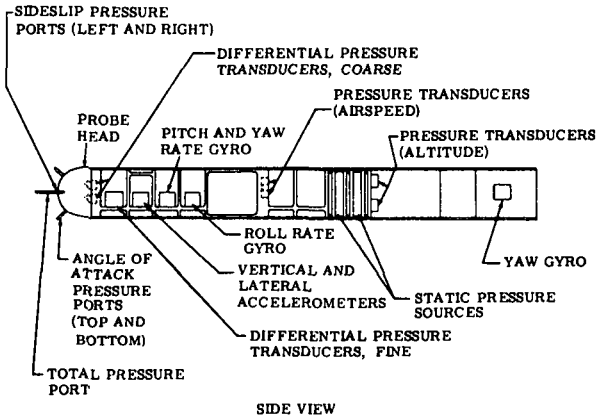

GUST PROBE INSTRUMENTATION
FIGURE 26

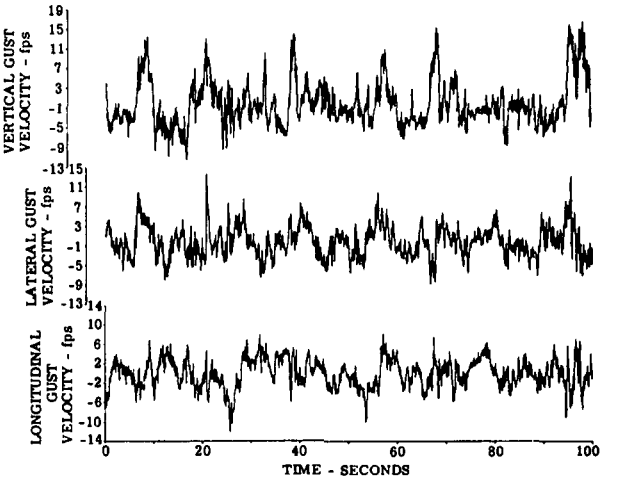

REPRESENTATIVE GUST VELOCITY TIME HISTORIES
FIGURE 27

The cross spectral method of data reduction eliminates all response information not statistically coherent with the selected gust component as measured at the probe.

Assumptions inherent in turbulence response testing are that:

- The airframe, aerodynamics, actuators, recorders, etc., are within their linear ranges
- All gust measurements have an adequate signal-to-noise ratio
- Pilot inputs are incoherent with gust inputs
- Vertical and lateral turbulence components are statistically independent
- The gust components on the aircraft are perfectly coherent with the respective gust components at the probe

The linearity assumption is considered valid for RMS gust intensities of less than 10 fps. Signal-to-noise ratios for the gust components are estimated by comparing power spectral density calculations in still air to that in turbulence as shown in Figure 28. A turbulence signal 10 times that of the smooth air signal is considered adequate to define the gust environment. The cross-spectral analysis technique removes the pilot effects which leave only the gust response data when the pilot inputs are not coherent with the gust components. Testing has shown the vertical and lateral gust velocities to be statistically independent of each other when comparing the calculated coherency function between simultaneously recorded time histories. This calculation shows near zero correlation and verifies the statistical independence.

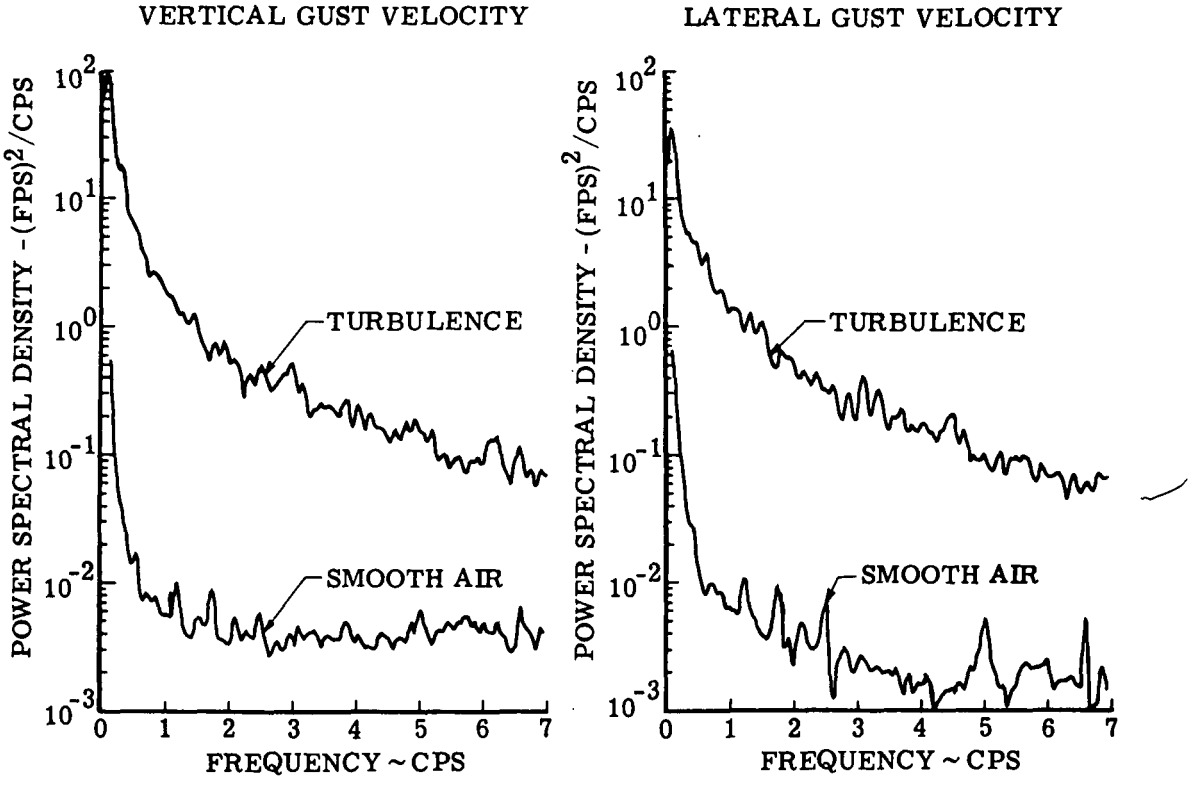

SIGNAL TO NOISE COMPARISON
FIGURE 28

3.3.3 Test Results

Typical response function results acquired during Boeing programs are shown in Figure 29 and 30 for the three configurations tested (i.e., basic airplane - No SAS; the baseline SAS; and the LAMS Flight Control System) and are compared with the theoretical results. Good agreement exists in the frequency spectrum below 3 cps. However, all of the test frequency response functions show a roll-off of amplitude versus frequency as depicted in Figure 31. This was a direct result of a reduced coherency with increasing frequency and is probably caused by the reduced coherency between gust components as calculated at the probe versus the gust at various locations across the aircraft.

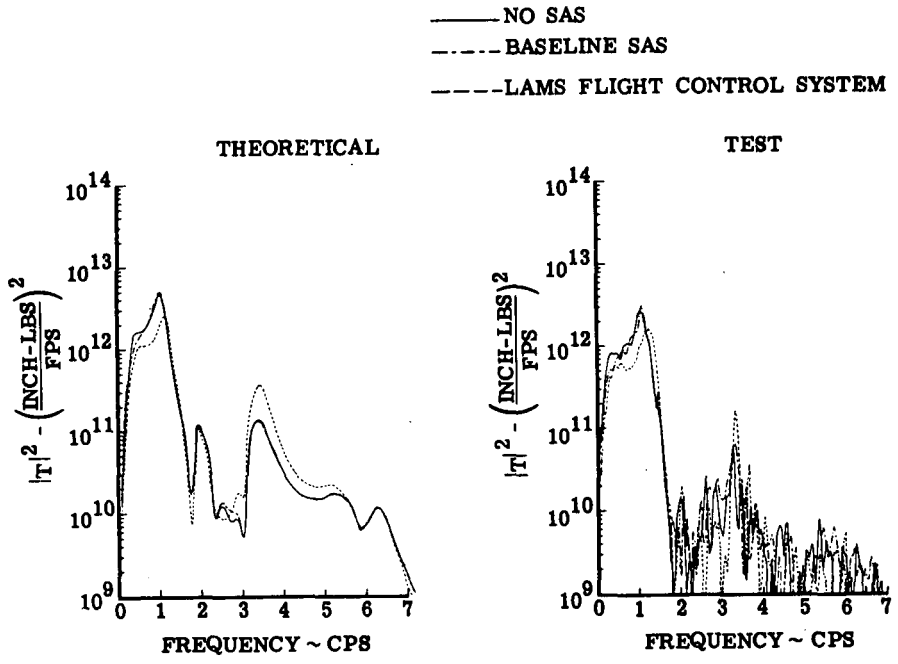

WING VERTICAL BENDING MOMENT RESPONSE
DUE TO VERTICAL GUST
FIGURE 29

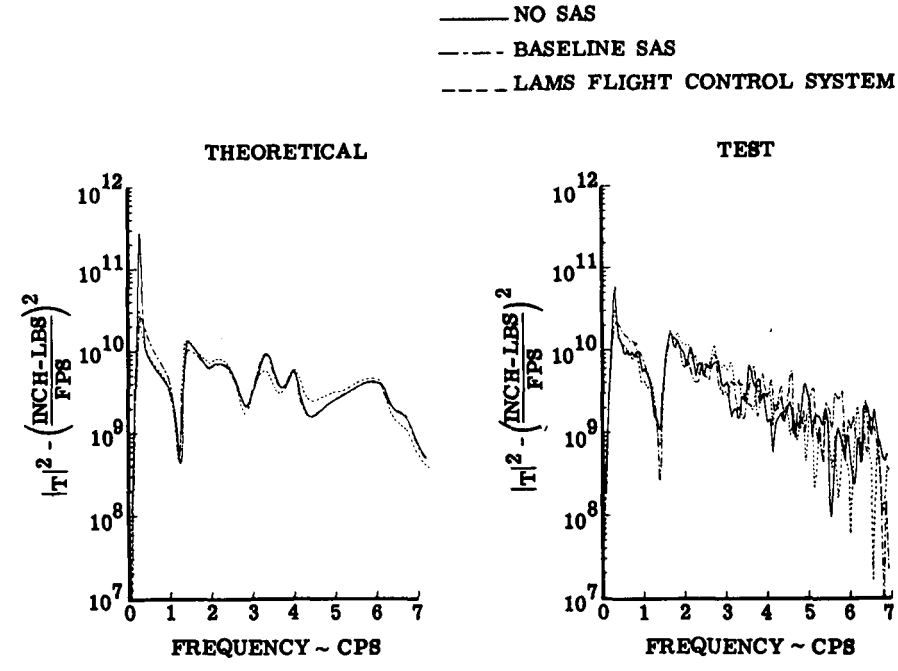

VERTICAL TAIL BENDING MOMENT RESPONSE
DUE TO LATERAL GUST
FIGURE 30

Due to the lack of coherency with the gust at higher frequencies, the normalized rms gust response parameter "A" was calculated two ways. The first value was computed from the total frequency response using raw time-history data and the other using only the data coherent with the gust. These data, shown in Figure 32, are compared with the theoretical calculations. The cross spectral "A" values based on gust coherent data are lower than predicted as a result of the following:

- The coherent data reduction method reduces the responses due to pilot inputs (the primary reason for requiring coherent data reduction)

- There is a lack of coherency between gust components at the gust probe and various points on the aircraft for the higher frequencies, further reducing the response functions.

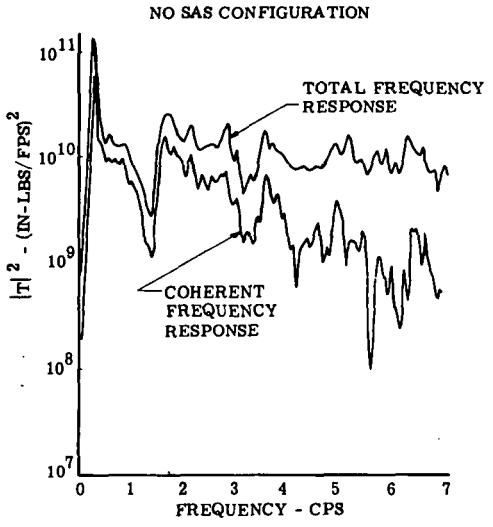

COMPARISON OF TOTAL AND COHERENT FREQUENCY RESPONSE FUNCTIONS - BENDING MOMENT OF VERTICAL TAIL
FIGURE 31

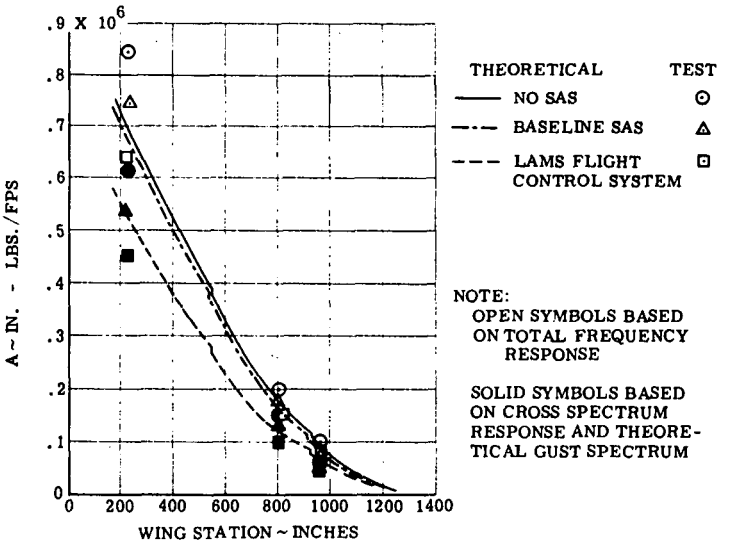

WING RMS VERTICAL BENDING MOMENT DUE TO VERTICAL GUST
FIGURE 32

The summation of the two effects listed above results in responses below that predicted. The two sets of "A" values obtained generally bracket the predicted response and show the trends as predicted. It is apparent that the spanwise and time variations of the turbulence components cannot be measured with a single gust probe. Less than perfect coherence results in lowered frequency response amplitudes as computed from the single-input cross-spectral equation.

The apparent coherency between gusts at the probe and response decrease as the wave length of turbulence decreased. Therefore, this data reduction technique can only provide a measure of the relative reduction in accelerations, loads, and fatigue damage for evaluating active flight control systems. This is an area that requires more refined techniques to provide a better comparison between theory and experiment.

4.0 CONCLUDING REMARKS

An analysis can not be better than the mathematical model representing the system or components under investigation. However, the analyst is faced with the limitations of computer size and economies of time and money required to analyze the large mathematical models. The effect of active controls on the structural responses is clearly a coupling problem and the analyst must evaluate the modes that directly couple with the control system. Any secondary effects, such as eliminating one structural mode from the model, influence the responses of another structural mode. Although certain rule of thumbs are available, no precise approach has been devised that totally eliminates the reiterative processes.

In general, the structural modes influenced by the active control system must be accurately represented in the mathematical model from a phase and gain relationship. The frequencies beyond the range of active control will generally be gain stabilized. Unless these are investigated, often a phasing with small amplitude changes will severely deteriorate the damping. Therefore, it is recommended that the system be evaluated with the most complete mathematical model available after the control system is selected and the model verified by testing to the extent possible.

BIBLOGRAPHY

1. Boeing Document D3-6950, "Stability Augmentation System Analysis", G. E. Hodges, O. E. Visor, J. I. Arnold, W. J. Wattman; September 1967

2. R. P. Johannes and P. M. Burris, "Flight Controls Damp Big Aircraft Bending", Control Engineering, September 1967

3. J. I. Arnold, "Automatic Control for Damping Large Aircraft Elastic Vibrations", NAECON Paper, May 1968

4. J. B. Dempster and J. I. Arnold, "Flight Test Evaluation of an Advanced Stability Augmentation System for the B-52 Aircraft", Paper No. 68-10 AIAA 5th Annual Meeting and Technology Display, 21 October 1968.

5. AFFDL-TR-68-158, "Aircraft Load Alleviation and Mode Stabilization (LAMS)' , December 1968

6. Clifford F. Newberry, "Consideration of Stability Augmentation Systems for Large Elastic Aircraft", Presented to The AGARD Flight Mechanics Panel 1969 Spring Meeting, April 1969

7. R. B. Holloway, P. M. Burris, and R. P. Johannes, "Aircraft Performance Benefits from Modern Control System Technology", AIAA 1st Aircraft Design and Operations Meeting, Paper No. 69-767, July 1969

8. Lewis H. Pasley and Gerald J. Kass, "Improved Airplane Performance Through Advanced Flight Control System Design", CASI/AIAA Meeting on the Prospects for Improvement in Efficiency of Flight, Paper No. 70-875, July 1970

9. Robert P. Johannes, "Adaptive Control of Flexible Aircraft Structural Modes" Presented to The AGARD Flight Mechanics Panel, Fall Meeting, September 1968.

FONCTIONS DE TRANSFERT D'UN AVION SOUPLE A LA TURBULENCE

par

G.Coupry

Office National d'Etudes et de Recherches Aérospatiales (ONERA)
92 Châtillon, France

RESUME

L'exposé dévoloppe les méthodes de calcul et de mesure de la fonction de transfer d'un avion souple à la turbulence atmosphérique. Après avoir rappelé quels sont les modèles de turbulence utilisables, on montre que le calcul du transfert en turbulence isotrope n'est guère plus compliqué que le calcul du transfert en turbulence uniforme. A la fin, les méthodes de mesure en vol de ce transfert sont indiquées.

SUMMARY

The paper deals with the computation and the measurement of the transfer function of an aircraft flexible to atmospheric turbulence. After a survey of the usable turbulence models, the computation of the transfer function for isotropic turbulence is discussed; it is shown that it is hardly more complicated than in the case of uniform turbulence. Finally, the methods for measuring the transfer function are described.

INTRODUCTION

La première question que nous poserons au début de cet exposé est la suivante : quelle est l'origine du renouveau d'intérêt porté à la turbulence atmosphérique, sujet qui a pourtant fait l'objet de nombreux travaux depuis plus de trente ans ? En fait, les effets de la turbulence atmosphérique préoccupent les constructeurs d'avions en raison de leur importance de plus en plus grande comme facteur de dimensionnement des appareils en projet ou en construction.

Les nouveaux problèmes auxquels ils ont à faire face viennent essentiellement de l'évolution des structures et des domaines de vol, et sont liés au fait que l'énergie que la turbulence transmet à l'avion est d'autant plus importante que les longueurs d'onde intéressées sont grandes. Comme les longueurs d'onde Λ sont associées à la vitesse de vol V et à la fréquence f qu'elles excitent par la relation :

$$\Lambda = V/f$$

On sait, d'après la figure 1, qu'à l'évolution actuelle des dimensions des avions correspondent des charges de plus en plus grandes dues à la turbulence. Par ailleurs, l'expérience montre que l'intensité de la turbulence est spécialement forte au voisinage du sol ; la tendance des opérations militaires à des vols au ras du sol a donc elle aussi une influence néfaste sur les charges auxquelles est soumise la structure.

La prévision des réponses d'un avion à la turbulence atmosphérique s'avère donc nécessaire, dès le stade du projet, en vue de tenter de préciser :

- les charges limites induites par la turbulence ;
- le dommage cumulatif causé par les rafales et, par conséquent, la durée probable de résistance de la structure à la fatigue ;
- les conditions limites de manoeuvrabilité et de pilotage ;
- les niveaux de vibrations susceptibles d'affecter le confort de l'équipage et des passagers, ainsi que la tenue des équipements ;
- les conditions d'environnement que devraient représenter les simulateurs de vol et auxquelles devraient faire face les pilotes automatiques et les systemes d'atterrissage par tous temps ;
- les systèmes possibles d'absorbeurs automatiques de rafales et les gains qu'ils permettent d'espérer.

L'exposé s'efforcera de faire apparaître les difficultés que présente la prévision de la réponse d'un avion à la turbulence atmosphérique, en insistant plus spécialement sur les désaccords qui existent encore entre théorie et expérience.

La première partie sera consacrée à la description des modèles de turbulence à partir desquels s'effectuent les calculs prévisionnels de réponse de l'avion.

Nous poursuivrons en développant les méthodes qui sont à la disposition des constructeurs pour effectuer ces calculs ; nous insisterons spécialement sur les toutes nouvelles théories qui permettent de rendre compte de l'isotropie de l'excitation.

L'exposé se terminera par l'analyse, dans quelques cas, de la comparaison entre théorie et expérience en vol.

1. DESCRIPTION PHENOMENOLOGIQUE DE LA TURBULENCE

1.1 - Les modèles locaux

Les théories statistiques de la turbulence qui ont été développées par Heisenberg, Kolmogoroff et Von Karman sont relatives à des "pavés" d'espace pour lesquels le phénomène est supposé homogène, stationnaire et gaussien. Dans le cadre de ces hypothèses, la notion de dégradation des grands tourbillons en petits tourbillons permet de prévoir que, dans le domaine inertiel (fig. 2), la densité spectrale d'énergie décroît comme la puissance -5/3 du nombre d'onde $2\pi/\Lambda$. L'absence de toute information sur le domaine des grandes longueurs d'onde (domaine de la création des grands tourbillons) et sur le domaine des très petites longueurs d'onde (qui correspondent à l'extinction des petits tourbillons par viscosité) oblige l'ingénieur à "inventer" des modèles aussi représentatifs que possible de la réalité.

Les modèles utilisés par les ingénieurs peuvent tous être représentés par le modèle général de Bullen qui donne respectivement, pour la fonction d'auto-corrélation et pour la densité spectrale de puissance de la composante transverse W de la turbulence, les expressions :

$$K_{ww}(\xi) = \left[(\xi/a)^p / 2^{p+1}\,\Gamma(p)\right]\left[2K_p(\xi/a) - (\xi/a)K_{p-1}(\xi/a)\right]$$

$$S_w(k) = \sigma_w^2 L \;\frac{1+8\pi^2(p+1)a^2k^2}{(1+4\pi^2a^2k^2)^{p+3/2}}$$

où a est lié à l'échelle macroscopique L de la turbulence par la relation :

$$a = \Gamma(p)\,L/\sqrt{\pi}\;\Gamma(p+1/2)$$

Les deux modèles locaux les plus utilisés dans l'industrie sont :

- le modèle de Dryden ($P = 1/2$) :

$$r_{ww}(\xi) = (1 - \xi/2L)\exp(-\xi/L)$$

$$S_w(k) = \sigma_w^2 L \frac{1 + 3(2\pi k L)^2}{[1 + (2\pi k L)^2]^2}$$

- le modèle de Karman ($P = 1/3$)

$$r_{ww}(\xi) = [2^{2/3}(\xi/a)^{1/3}/\Gamma(1/3)][K_{1/3}(\xi/a) - (\xi/2a)K_{-2/3}(\xi/a)]$$

$$S_w(k) = \sigma_w^2 L \frac{1 + \frac{8}{3}(2,678\,\pi k L)^2}{[1 + (2,678\,\pi k L)^2]^{11/6}}$$

Quels que soient les avantages que présente le modèle de Dryden du point de vue analytique, du fait que la densité spectrale s'exprime sous forme de fraction rationnelle, on devra en principe lui préférer le modèle de Karman dont le comportement asymptotique (loi de puissance en -5/3) est conforme aux théories relatives au domaine inertiel. Les mesures en vol de la turbulence atmosphérique permettent par ailleurs de s'assurer que le modèle de Karman est bien représentatif de la réalité dans pratiquement tous les cas (l'exception étant la pénétration en orage). A titre d'exemple, une comparaison entre modèle de Karman et densité spectrale mesurée est donnée dans la figure 3.

1.2 - Les modèles globaux de l'atmosphère

N'importe quel passager d'un avion commercial peut se rendre compte, après quelques vols, que la turbulence n'est pas un phénomène homogène : l'avion vole la plupart du temps en air calme, et rencontre occasionnellement un "pavé" de turbulence. Zbrozek, partant des documents existants, a abouti à une estimation de la proportion du temps de vol passé en turbulence, suivant l'altitude. La figure 4 résume ses conclusions.

En conséquence, la turbulence ne peut en aucun cas être considérée, dans son ensemble, comme un processus stationnaire, ni même gaussien. H. Press a, pour lever cette difficulté, proposé un modèle dans lequel la turbulence est considérée comme un processus localement stationnaire et gaussien. On assimile l'atmosphère à un ensemble de pavés stationnaires et gaussiens, ayant tous même échelle de turbulence et même forme de densité spectrale, mais différant par la variance du phénomène. Le comportement global de l'atmosphère est alors totalement défini, du point de vue statistique, si l'on connaît la densité de probabilité des écarts types des différents pavés. Si l'on appelle $P(\sigma_w)$ cette densité de probabilité, si on note par N_{ow} le nombre moyen de zéros par unité de longueur du processus dans chaque pavé, et par $N_w(x)$ le nombre moyen de fois par unité de longueur où le processus global a dépassé le niveau x, on aboutit au résultat :

$$N_w(x) = N_{ow} \int_0^{+\infty} P(\sigma_w) \exp\left(-\frac{x^2}{2\sigma_w^2}\right) d\sigma_w$$

Un des modèles les plus séduisants pour représenter $P(\sigma_w)$ a été présenté par Dempster :

$$P(\sigma_w) = \sqrt{\frac{2}{\pi}}\left[\frac{P_1}{b_1}\exp\left(-\frac{\sigma_w^2}{2b_1^2}\right) + \frac{P_2}{b_2}\exp\left(-\frac{\sigma_w^2}{2b_2^2}\right)\right]$$

Dempster a défini P_1 , P_2 , b_1 , b_2 à partir des résultats disponibles à l'époque :

Altitude	P_1	b_1	P_2	b_2
0-1 km	0,80	3,6	0,20	4,2
9-12 km	0,13	1,8	0,01	4,8

En fait, des travaux coopératifs se poursuivent au sein même de l'AGARD, en vue de réunir le maximum d'informations sur les statistiques de la turbulence par tranche d'altitude et par saison. Ces travaux sont fondés sur l'exploitation systématique des enregistrements V.G.H. (Velocity, Gravity, Height) effectués sur les avions commerciaux au cours de vols d'exploitation courante. Une technique nouvelle, qui consiste à étalonner ces avions, en tant qu'instruments de mesure de la turbulence, a été mise au point et permet d'améliorer sérieusement la qualité des dépouillements.

2. CALCUL DE LA REPONSE D'UN AVION

2.1 - Calcul formel de la réponse

Considérons un avion souple volant dans un des "pavés" stationnaires et gaussiens de turbulence que nous avons décrits plus haut. Si l'on suppose la structure linéaire, la réponse en tout point sera elle-

même un phénomène stationnaire et gaussien, et pourra se représenter sous la forme :

$$(1) \qquad z(M,t) = \sum_i q_i(t)\,\psi_i(M)$$

où les $\psi_i(M)$ sont les formes propres associées aux modes d'ensemble et de déformation, et les $q_i(t)$ les réponses des coordonnées généralisées aux forces généralisées d'excitation induites par la turbulence.

La corrélation de la réponse $z(M,t)$ au point M s'exprime alors par :

$$(2) \qquad R_{zz}(M,\tau) = \sum_{i,j} R_{q_i q_j}(\tau)\,\psi_i(M)\,\psi_j(M)$$

où $R_{q_i q_j}(\tau)$ est la corrélation croisée entre les coordonnées généralisées q_i et q_j .

Appelant $D_{ik}(t)$ la réponse impulsionnelle en vol calme du mode i à une impulsion sur le mode k , la réponse $q_i(t)$ peut s'exprimer par :

$$q_i(t) = \sum_k \int_{-\infty}^{+\infty} D_{ik}(\alpha)\,Q_k(t-\alpha)\,d\alpha$$

où $Q_k(t)$ est la force généralisée d'excitation sur le mode k due à la turbulence. On aurait de même :

$$q_j(t+\tau) = \sum_\ell \int_{-\infty}^{+\infty} D_{j\ell}(\alpha')\,Q_\ell(t+\tau-\alpha')\,d\alpha'$$

On en déduit que :

$$(3) \qquad R_{q_i q_j}(\tau) = \sum_k \sum_\ell D_{ik}(-\tau) * D_{j\ell}(\tau) * R_{Q_k Q_\ell}(\tau)$$

où le symbole $*$ représente le produit de convolution, et où $R_{Q_k Q_\ell}(\tau)$ est la corrélation croisée de force généralisée due à la turbulence sur les modes k et ℓ .

Appelant $P(M',t)$ la pression induite par la turbulence au point M' , au temps t , on peut calculer la force généralisée associée sur le mode k , qui est :

$$Q_k(t) = \iint_A \psi_k(M')\,P(M',t)\,dM'$$

On aurait de même :

$$Q_\ell(t+\tau) = \iint_A \psi_\ell(M'')\,P(M'',t+\tau)\,dM''$$

D'où :

$$(4) \qquad R_{Q_k Q_\ell}(\tau) = \iint_A \iint_A \psi_k(M')\,\psi_\ell(M'')\,R_{PP}(M',M'',\tau)\,dM'\,dM''$$

Nous allons maintenant reporter l'expression (4) dans l'équation (3), et reporter le résultat ainsi obtenu dans l'équation (2). Il viendra alors :

$$R_{zz}(M,\tau) = \sum_{i,j,k,\ell} \psi_i(M)\,\psi_j(M)\,D_{ik}(-\tau) * D_{j\ell}(\tau) * \iint_A \iint_A \psi_k(M')\,\psi_\ell(M'')\,R_{PP}(M',M'',\tau)\,dM'\,dM''$$

Nous effectuerons alors la transformation de Fourier des deux membres par rapport à τ , en notant par $\phi_{rs}(\omega)$ la transformée de Fourier $R_{rs}(\tau)$ et en rappelant que la transformée de Fourier de la réponse impulsionnelle $D_{ik}(\tau)$ est la fonction de transfert $T_{ik}(\omega)$ du mode i de l'avion en air calme à une force généralisée unité sur le mode k .

Compte tenu de ces remarques, on obtient :

$$\phi_{zz}(M,\omega) = \sum_{i,j,k,\ell} \psi_i(M)\,\psi_j(M)\,T^*_{ik}(\omega)\,T_{j\ell}(\omega) \iint_A \iint_A \psi_k(M')\,\psi_\ell(M'')\,\phi_{PP}(M',M'',\omega)\,dM'\,dM''$$

On sait en conséquence que la densité spectrale de déplacement au point M est parfaitement connue si l'on sait calculer la densité spectrale croisée de pression $\phi_{pp}(M',M'',\omega)$ induite sur l'aile par la turbulence atmosphérique.

2.2 - Calcul de la densité spectrale croisée de pression

Nous allons montrer que la densité spectrale croisée de pression entre deux points M et M' de l'aile peut être déterminée dès que l'on connaît la densité spectrale croisée de la composante verticale W de la turbulence atmosphérique.

On part de la théorie de la surface portante qui permet d'exprimer l'angle d'attaque $\alpha(M,\omega)$ induit en tout point de l'espace par un champ de pression harmonique $p(\mu,\omega)$ sur l'aile :

$$\alpha(M,\omega) = \iint k(M,\mu;\omega)\, P(\mu,\omega)\, d\mu$$

Depuis plusieurs années, on sait résoudre cette équation intégrale après une transformation qui ramène l'aile à un carré, et un développement polynomial de $p(\mu,\omega)$ limité à ses n premiers termes. La solution, qui se présente sous forme matricielle, exprime sous cette forme la relation intégrale directe :

$$P(M,\omega) = \iint_A G(M,\mu,\omega)\,\alpha(\mu,\omega)\, d\mu. \tag{5}$$

En effectuant la transformation de Fourier inverse par rapport à ω, on déduit de l'équation (5) la pression induite au point M, au temps t, par une variation d'angle d'attaque localisée au point μ, au temps τ :

$$\tilde{P}(M,t) = \iint_A \tilde{G}(M,\mu,t) * \tilde{\alpha}(\mu,t)\, d\mu.$$

Pour le problème qui nous intéresse, le champ de pression est induit par une turbulence responsable de l'incidence induite :

$$\tilde{\alpha}(M,t) = \frac{W(M,t)}{V_0}$$

et, en conséquence :

$$\tilde{P}(M,t) = \frac{1}{V_0}\iint_A \tilde{G}(M,\mu,t) * w(\mu,t)\, d\mu. \tag{6}$$

On aurait de même, au temps $t+\tau$ et au point M' :

$$\tilde{P}(M',t+\tau) = \frac{1}{V_0}\iint_A \tilde{G}(M',\mu',t+\tau) * w(\mu',t+\tau)\, d\mu' \tag{7}$$

Partant de ces deux équations, et calculant la corrélation croisée de pression

$$R_{PP}(M,M',\tau) = E\left(\tilde{P}(M,t)\,\tilde{P}(M',t+\tau)\right)$$

on obtient :

$$R_{PP}(M,M',\tau) = \frac{1}{V_0^2}\iint_A\iint_A \tilde{G}(M,\mu,-\tau) * \tilde{G}(M',\mu',\tau) * R_{WW}(\mu,\mu';\tau)\, d\mu\, d\mu'$$

Après transformation de Fourier, on déduit finalement :

$$\phi_{PP}(M,M',\omega) = \frac{1}{V_0^2}\iint_A\iint_A G^*(M,\mu,\omega)\, G(M',\mu',\omega)\, \phi_{WW}(\mu,\mu',\omega)\, d\mu\, d\mu' \tag{8}$$

Revenant au langage matriciel et introduisant les matrices de coefficients d'influence aérodynamiques calculées à l'occasion des problèmes de flottement, on sait que la matrice ϕ_{PP} qui représente d'une manière discrète la densité spectrale croisée de pression sur l'aile s'exprime en fonction de la matrice ϕ_{WW} qui représente d'une manière discrète la densité spectrale de la turbulence par :

(9) $$\phi_{pp} = G^{*} \phi_{ww} G$$

La connaissance de la matrice de coefficients d'influence aérodynamique G, déterminée à l'occasion des calculs de flottement, permet donc de calculer la densité spectrale croisée de pression en fonction de la densité spectrale croisée de la turbulence.

2.3 - Les diverses méthodes de calcul

La figure 5 résume les deux principales méthodes de calcul que l'on peut envisager, que nous appellerons méthode de la turbulence uniforme en envergure et méthode de la turbulence isotrope.

a) Méthode de la turbulence uniforme en envergure

C'est pratiquement la seule méthode utilisée par les constructeurs ; elle consiste à supposer que l'avion vole à travers une turbulence qui se présente sous forme de vagues cylindriques de génératrices perpendiculaires à l'axe du vol.

Dans ces conditions, compte tenu de l'hypothèse de Taylor qui suppose la turbulence statistiquement figée pendant la durée de vol de l'avion, associant ainsi la longueur d'onde à une période excitatrice τ par la formule :

$$\xi = V_0 \tau$$

on peut exprimer la corrélation croisée de turbulence entre deux points $M(x,y,h)$ et $M'(x',y',h')$ grâce au modèle de Karman par :

$$R_{ww}(M,M',\tau) = \eta_w\left(\tau - \frac{x-x'}{V_0}\right)$$

Effectuant la transformée de Fourier de cette équation, on obtient la densité spectrale croisée $\phi_{ww}(M,M',\omega)$ en fonction du spectre de Karman :

(10) $$\phi_{ww}(M,M',\omega) = \exp\left[-i\frac{\omega}{V_0}(x-x')\right] S_w\left(\frac{\omega}{V_0}\right)$$

Il ne reste plus qu'à reporter cette expression dans l'équation (8) pour en déduire la densité spectrale croisée du champ de pression sur l'aile et résoudre le problème du transfert.

b) Méthode de la turbulence isotrope

La méthode qui vient d'être exposée est utilisée par les constructeurs en raison de la forme extrêmement simple qu'elle donne de la densité spectrale croisée du champ de turbulence. Elle doit cependant être examinée soigneusement du fait qu'elle présente au départ une incohérence marquée. Cette incohérence réside dans le fait que l'on suppose la turbulence uniforme en envergure, et que les modèles spectraux utilisés présupposent par contre que la turbulence est isotrope. Une analyse serrée du problème montre que l'approximation qui précède est valable pour tous les modes tels que la longueur $1{,}5\ \frac{V_0}{\omega_i}$ soit grande par rapport à l'envergure.

Quand il n'en est pas ainsi, l'erreur faite sur la réponse de ces modes peut être très importante.

Pour lever cette difficulté de principe, il est préférable de supposer (fig. 5) la turbulence isotrope et d'effectuer le calcul correspondant.

La turbulence étant isotrope, sa corrélation croisée entre les points M et M' de l'aile ne dépend (fig. 6) que de la distance PM', c'est-à-dire de la longueur :

$$\sqrt{(x-x'-V_0\tau)^2 + (y-y')^2}$$

Cette corrélation croisée s'exprime alors, en fonction du modèle de Karman, par :

$$R_{ww}(M,M',\tau) = \eta_w\left(\sqrt{\left(\tau - \frac{x-x'}{V_0}\right)^2 + \left(\frac{y-y'}{V_0}\right)^2}\right)$$

Grâce à des propriétés bien connues de la transformation de Fourier, on en déduit la densité spectrale croisée de turbulence, soit :

(11) $$\phi_{ww}(M,M',\omega) = \exp\left(-i\frac{\omega}{V_0}(x-x')\right)\left[S_w\left(\frac{\omega}{V_0}\right) - \frac{|y-y'|}{V_0}\int_0^{+\infty} J_1\left(\frac{|y-y'|}{V_0}v\right) S_w\left(\sqrt{v^2+\omega^2}\right) dv\right]$$

Cette expression est plus complexe que celle donnée dans la formule (10) pour une turbulence uniforme en envergure. Elle ne présente cependant aucune difficulté de calcul sur ordinateur. En reportant cette expression dans l'équation (8) on obtient la densité spectrale croisée de pression induite sur l'aile par une turbulence isotrope.

Contrairement aux craintes des constructeurs, il apparaît par conséquent qu'une fois connues les matrices de coefficients d'influence aérodynamiques, il n'est pas plus difficile de calculer le transfert à une turbulence isotrope qu'à une turbulence uniforme en envergure.

Les figures 7 et 8 donnent une comparaison du transfert de Concorde à la turbulence, transfert calculé par les deux méthodes.

3. MESURE DU TRANSFERT D'UN AVION

3.1 - Principe de la méthode

Les méthodes de mesure en vol de la fonction de transfert d'un avion à la turbulence atmosphérique sont fondées sur l'utilisation de deux formules usuelles de la théorie du transfert linéaire des processus aléatoires.

Appelant $\mathcal{C}_{yx}(i\omega)$ la fonction de transfert d'un système linéaire excité par une variable $X(t)$ et répondant par la variable $Y(t)$, on sait que la densité spectrale d'entrée est reliée à la densité spectrale de sortie par la relation :

$$\phi_{yy}(\omega) = |\mathcal{C}_{yx}(i\omega)|^2 \phi_{xx}(\omega)$$

Il suffit dès lors de mesurer la turbulence et la réponse, de calculer d'une manière quelconque leurs densités spectrales respectives pour en déduire :

$$|\mathcal{C}_{zw}(i\omega)|^2 = \phi_{zz}(\omega) / S_w(\omega)$$

L'inconvénient de cette méthode réside dans le fait que l'on suppose a priori que l'avion n'est excité que par la turbulence, ce qui est en général faux, puisque l'appareil est sollicité aussi par les manoeuvres du pilote. On est donc amené, quand c'est possible, à employer la formule :

$$\phi_{yx}(\omega) = \mathcal{C}_{yx}(i\omega)\, \phi_{xx}(\omega)$$

qui relie la densité spectrale croisée "entrée-sortie" à la densité spectrale directe d'excitation. Appliquant cette formule à la réponse d'un avion à la turbulence, on détermine la fonction de transfert par :

$$\mathcal{C}_{zw}(i\omega) = \phi_{zw}(\omega) / S_w(\omega)$$

Par cette méthode, on se débarrasse des excitations parasites, à condition qu'elles ne soient pas elles-mêmes corrélées à la turbulence.

3.2 - Application pratique et résultats

Pour appliquer ces méthodes à la mesure en vol de la fonction de transfert d'un avion à la turbulence atmosphérique, il est nécessaire de mesurer l'entrée, c'est-à-dire la turbulence qui excite l'avion en même temps que la sortie qui peut être une réponse quelconque en accélération, contrainte locale, etc...

La mesure de la réponse ne présente aucune difficulté à partir du moment où l'on dispose à bord de l'instrument de mesure approprié, accéléromètre ou pont de jauges. Pour connaître l'entrée, c'est-à-dire de la turbulence, on devra disposer de moyens quelconques de mesure de l'angle d'attaque α, de l'accélération $\dot{z}$ et de la vitesse de tangage apparente θ au même point.

Utilisant alors l'équation cinématique locale du fluide :

$$\alpha = \theta - \frac{\dot{z}}{V_o} + \frac{W}{V_o}$$

on pourra, par voie analogique ou digitale, calculer la composante $W(t)$ de la turbulence à chaque instant.

Ayant mesuré en fonction du temps l'entrée et la réponse on dispose de méthodes générales pour calculer les densités spectrales directes correspondantes, ainsi que la densité spectrale croisée "entrée-sortie".

A titre d'exemple, nous donnons dans les figures 9, 10 et 11 une comparaison entre les fonctions de transfert mesurées sur un Mirage III et un Transall, et les fonctions de transfert calculées en supposant la turbulence uniforme en envergure. On voit, pour les deux comparaisons qui portent sur le Mirage III, avion très rigide dont la souplesse n'intervenait pas, que la prévision théorique de la fonction de transfert est très bonne dans le domaine des fréquences correspondant à la mécanique du vol. La confrontation entre théorie et expérience pour le Transall est beaucoup plus décevante. Il s'agit d'un avion très souple qui comprend plusieurs modes de déformation dans la gamme des fréquences considérées. Il apparaît que la fonction de transfert mesurée est beaucoup moins "montagneuse" que la fonction de transfert prévue ; il est, par conséquent, probable que des calculs en turbulence isotrope, qui n'ont malheureusement pas encore pu être effectués, auraient amélioré la comparaison.

4. CONCLUSIONS

Nous avons tenté de résumer ici les méthodes dont dispose le constructeur pour calculer, ou vérifier en vol, le transfert d'un avion à la turbulence atmosphérique. Le premier point que nous soulignerons est que la comparaison entre une théorie fondée sur l'hypothèse d'uniformité en envergure, et l'expérience, est décevante pour l'avion souple. Nous avons par ailleurs proposé une méthode de calcul qui tient compte de l'isotropie de la turbulence. Cette méthode laisse prévoir des tendances qui amélioreraient sûrement la prévision théorique, mais la confrontation entre la théorie fondée sur l'isotropie et l'expérience n'a malheureusement pas pu encore être menée à bien.

De nombreux travaux restent encore à faire, d'une part, en vue de tenir compte de la réponse des modes antisymétriques dans le cas de l'excitation par une turbulence isotrope, d'autre part, en vue de mesurer non plus les modules des fonctions de transfert, mais les fonctions de transfert elles-mêmes. L'O.N.E.R.A. pense, au cours des mois qui viennent, aboutir dans ces deux domaines.

Rappelons enfin, pour terminer, que théorie et mesure destinées à prévoir la réponse de l'avion à une excitation latérale sont pratiquement inexistantes.

BIBLIOGRAPHIE.

[1] - H. PRESS - An Approach of the Prediction of the frequency distribution of Gust Loads on Airplanes in normal operations.
N.A.C.A., TN 2660, 1952.

[2] - J.B. DEMPSTER et C.A. BELL - Summary of flight load environmental data taken on B 52 fleet aircraft.
A.I.A.A. Paper 64-165, 1964.

[3] - J.M. FIREBAUGH - Evaluations of a spectral gust model using V.G.H. and V.G. flight data.
Journal of Aircraft, Vol. 4, n° 6, Nov.-Dec. 1967.

[4] - R. DAT, L. DAROVSKI et B. DARRAS - Considérations sur la solution matricielle du problème portant instationnaire en subsonique, et applications aux gouvernes.
O.N.E.R.A., Note Technique n° 135 (1968).

[5] - G. COUPRY - Pression induite sur une surface portante par une turbulence atmosphérique isotrope.
C.R. Ac. Sc. Paris, t. 268, série A, - (1969), p. 343-344.

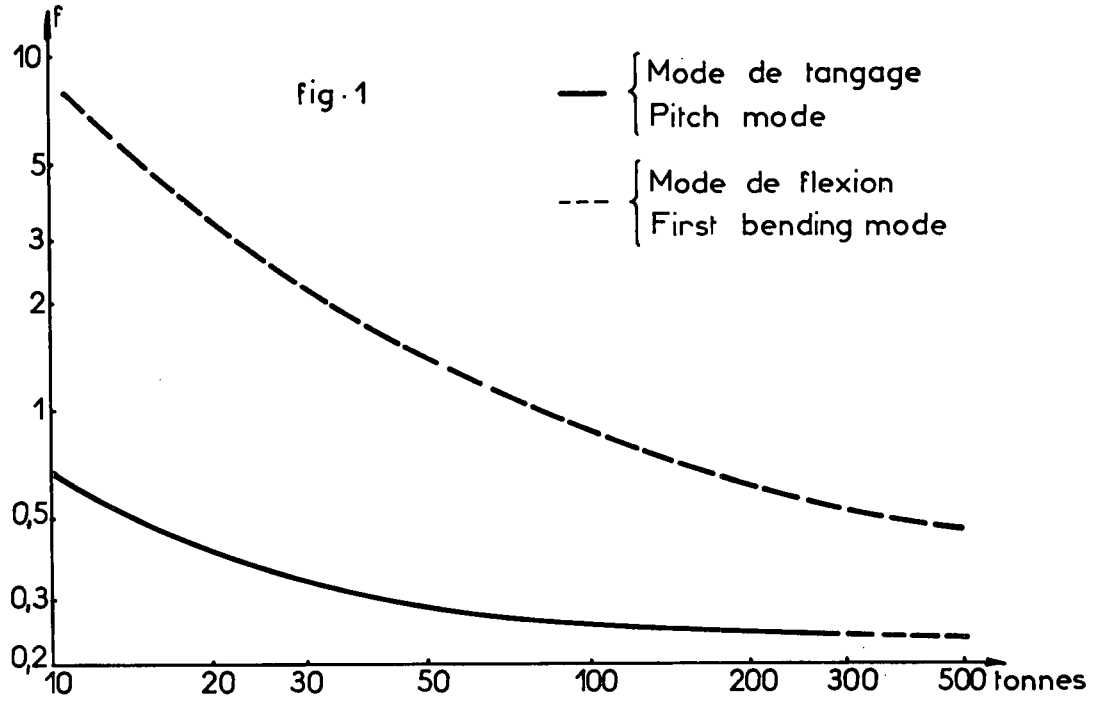

TENDANCE DES FREQUENCES DE TANGAGE ET DE FLEXION
TRENDS OF THE PITCH FREQUENCIES AND THE FIRST BENDING MODE FRENQUENCY

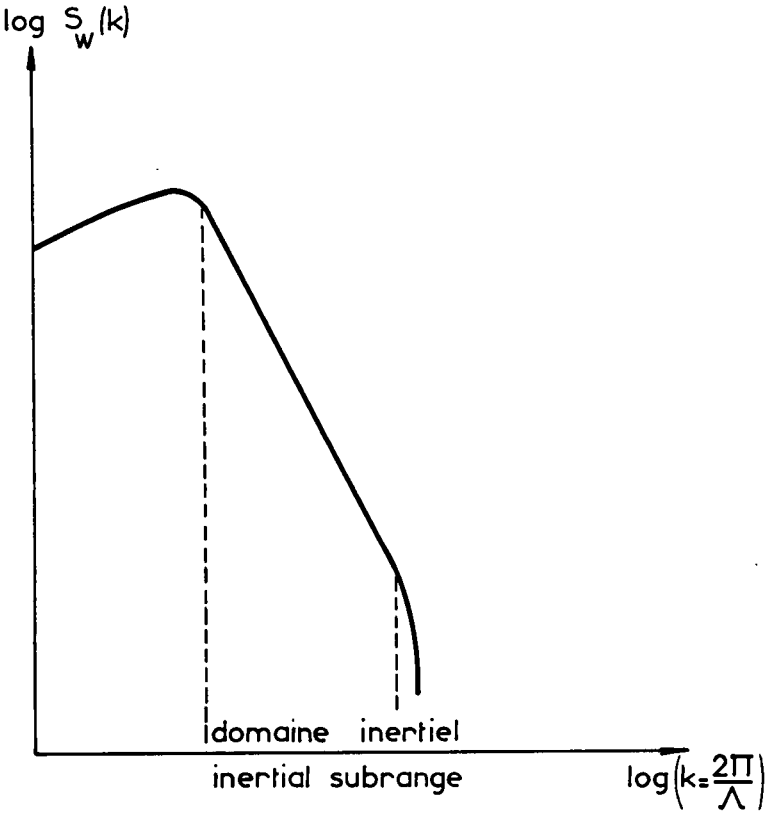

ALLURE D'UN SPECTRE DE TURBULENCE
TRENDS OF THE SPECTRUM OF ATMOSPHERIC TURBULENCE

fig. 2

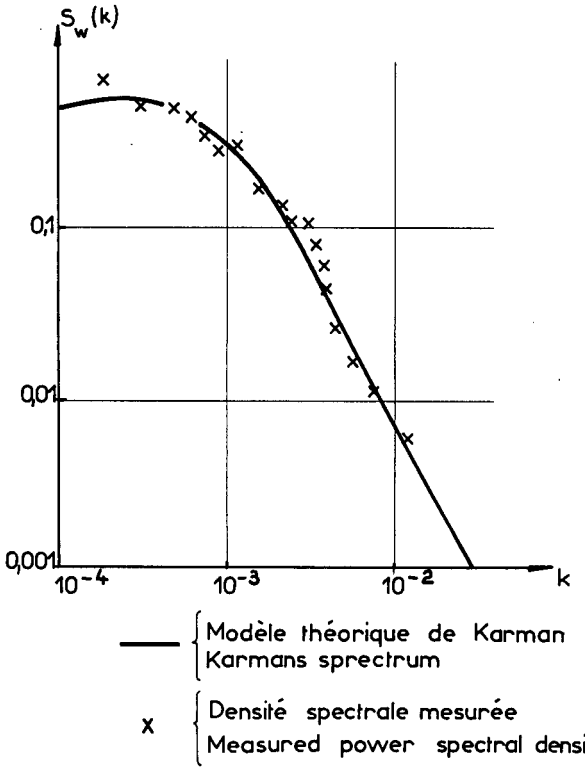

fig. 3

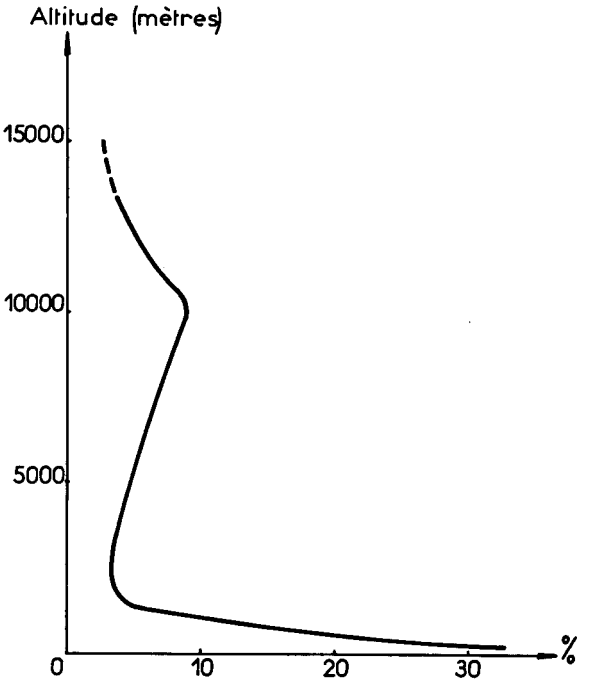

POURCENTAGE DU TEMPS PASSE EN TURBULENCE
PERCENTAGE OF TIME SPENT IN TURBULENCE

fig. 4

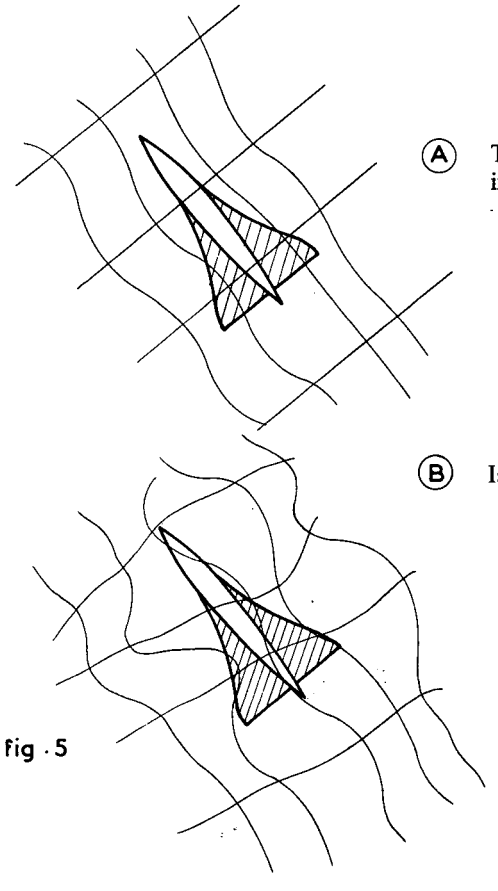

fig. 5

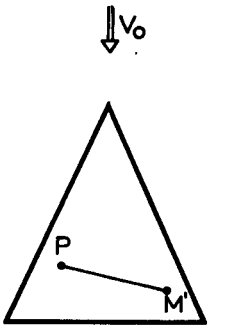

fig. 6

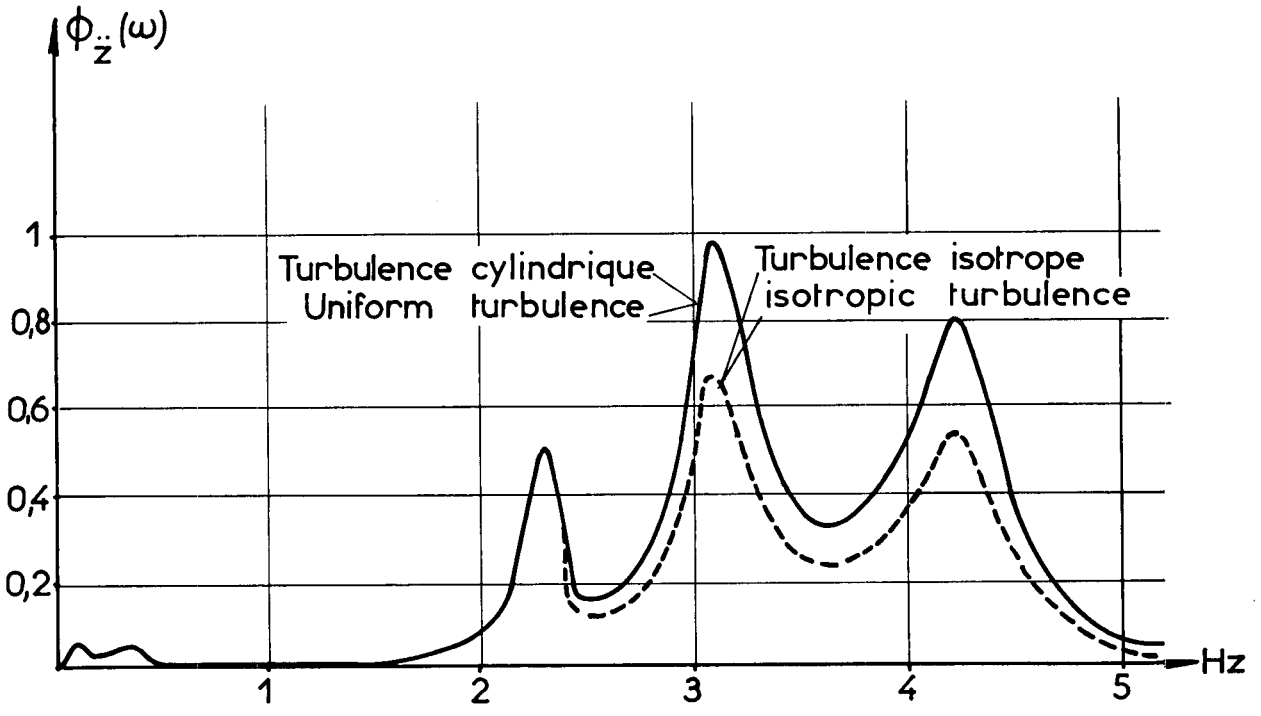

Avion Concorde M = 0,8 Echelle de turbulence 200 m
Concorde Mach number 0,8 ; scale of turbulence : 200m

fig.7

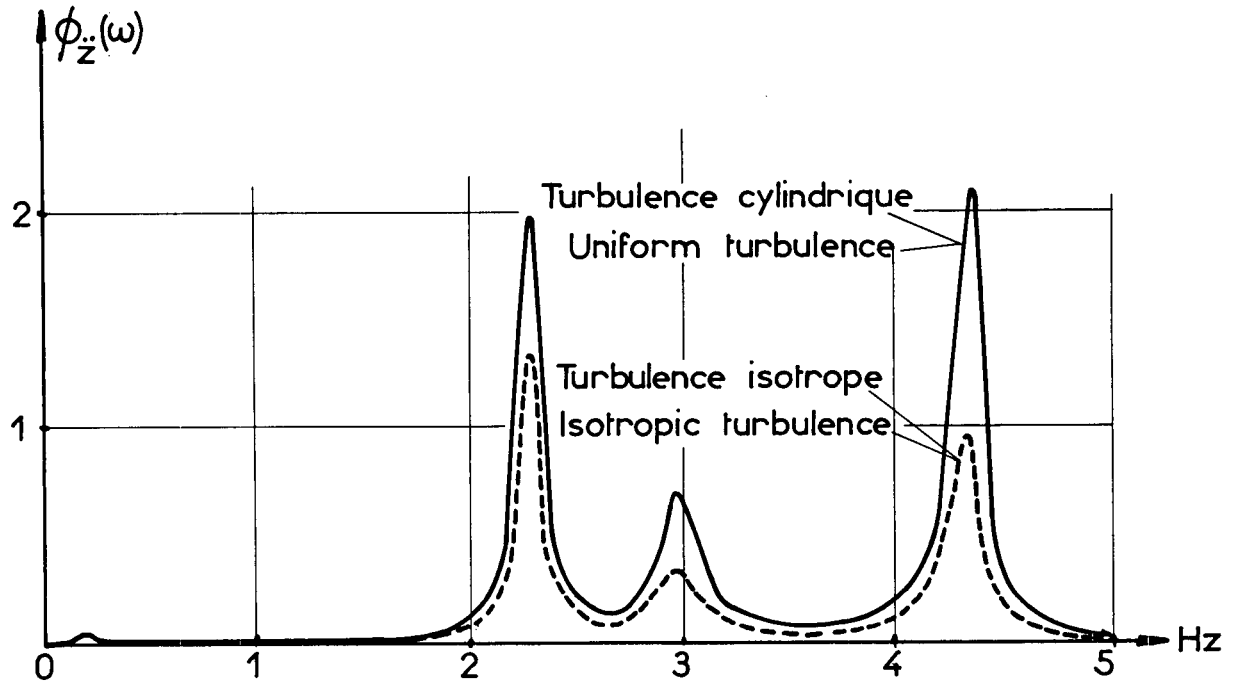

Avion Concorde M = 0,4 Echelle de turbulence : 105 m
Concorde Mach number 0,4 Scale of turbulence : 105m

fig.8

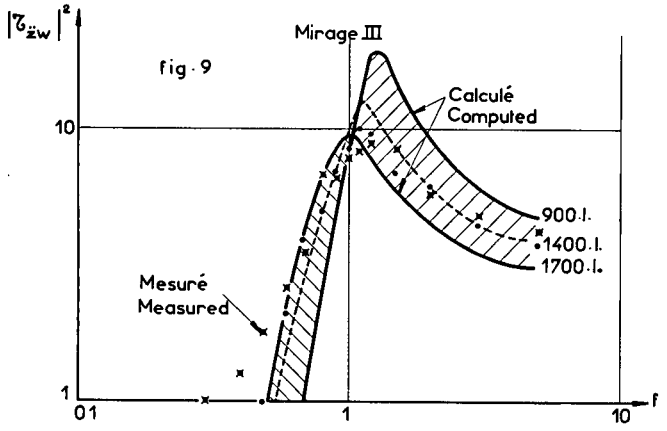

fig. 9

Fonction de transfert de l'accélération
C.g. acceleration transfer fonction

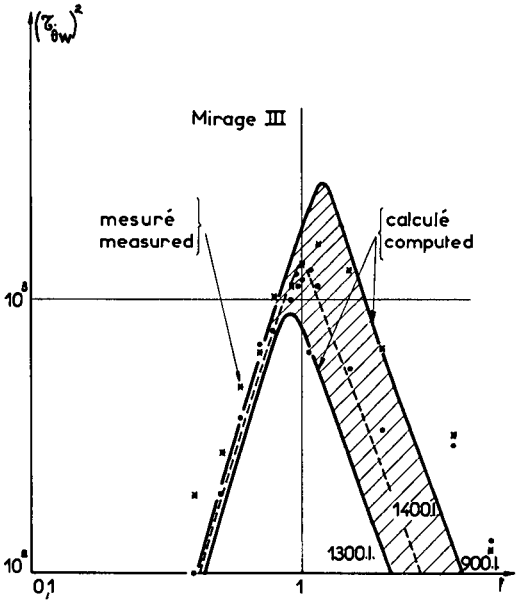

Fonction de transfert de vitesse de tangage
Pitch rate transfer fonction

fig. 10

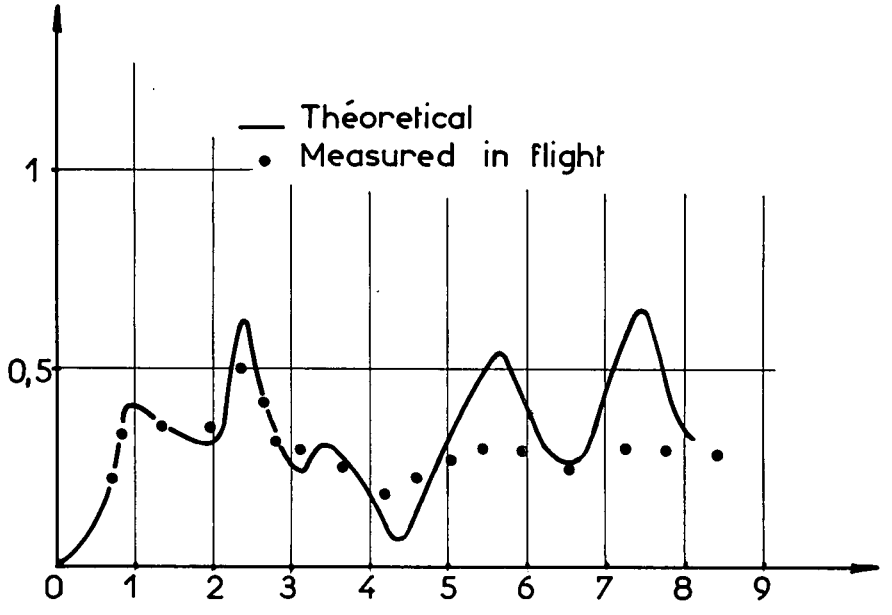

Transall V_o = 420 km/h

Transfer fonction for c.g. acceleration
Fonction de transfert de l'accélération

fig. 11

HUMAN PILOT MODELLING

by

Dr H.F.Huddleston

Human Factors Group,
RAE Farnborough
Hampshire, UK

HUMAN PILOT MODELLING

Dr H.F.Huddleston

1. INTRODUCTION

It would be unrealistic to attempt a detailed review of either the empirical data or the input-output theory which has been published on the problem of modelling the human pilot. Since Costello and Higgin's (1966) 236 – item bibliography, there have been some 10 to 20 papers a year, depending on one's criteria for selection (see, eg McRuer and Weir, 1969). What I want to convey is an impression of how human factors specialists might currently describe engineering attempts to define pilot 'transfer functions'.

I have found no good reason to disagree with Sadoff's (1966) view that, for the most part, modelling has been quasi-linear in method and single-axis in content. There have been notable models involving two or more axes (eg Baron and Kleinman, 1968; Todosiev et al, 1966) and notable attempts to tackle human non-linearity (eg Stapleford et al, 1969; Seifert and Miller, 1968) but there has not been that fundamental leap forward which many workers feel to be necessary. An additional difficulty lies in the fact that human behaviour is notoriously non-stationary (in terms of both the gain and time constants in attempted linear models) a fact which seems to be too difficult to treat just yet. (see, eg, Young 1969).

A few illustrations will help to define our terms. By quasi-linearity, I mean a linear model containing terms which are allowed to change over time. If a pilot were a linear system, the superposition theorum would fit, and we should be able to say, for example, that since a given height offset (one axis) elicited a stick input A and a given heading offset (a second axis) elicited B , the two errors together would evoke (A + B). This basic modelling simplification is rarely applicable, however. As to trends over time, it is known that human response changes for five main reasons:

(a) adaptation to a given level of input (eg not noticing the skin effects of ambient 1g except in the first few seconds of settling on to a seat);

(b) habituation to a class of inputs (eg overcoming a startle reaction by repeatedly experiencing negative g effects during training);

(c) boredom and fatigue (eg finding nothing of interest to do at some point in a 5 hour trans-oceanic flight);

(d) learning (eg realising that a visual crosscheck between attitude indicator and outside view permits a high level of flying control in a particular type of turbulence);

(e) modifying performance criteria (eg unexpectedly finding that a ground target has already been destroyed).

We know of no compelling reasons why these five causes of non-stationarity could not all operate more or less simultaneously.

Taking a broad overview, input-output engineering studies have reminded us that man as a tracker:

(a) behaves like a low-pass amplifier;

(b) has a built in reaction time delay;

(c) can, in some circumstances, generate substantial lead or lag characteristics;

(d) behaves as if he responded to some events about twice a second.

Not one of these points is, in any sense, a discovery for the human biologist. They are all, rather, impediments in the way of good control engineering.

2. PROBLEMS OF LOGIC

Let us pretend the universe contains two kind of logic, deductive and inductive. Deductive logics are those algebras or calculi which are closed, self-supporting systems; conventionally accepted definitions. For example, we do not allow 2 + 2 to be anything but 4, or it would be too difficult and inelegant to continue to accept 1 + 1 + 1 + 1 = 4 or any parallel "exception". Consistent rules of this kind, like science, have a psychological not a logical necessity. Inductive logic is, in one sense, the setting up of deductive algebras or calculi. The function of brains is, in particular, inductive; to model what might be "out there" and formulate techniques for testing the model for flaws.

Efficient control engineering, as a method, is surely deductive. We agree, for example, to describe a linear servo system as the ratio of the Laplace transform of its output to that of its input. Human psychophysiology, as a method, tries to be deductive too. (Hence, pilot modelling should be a happy event, the confluence of biologist and engineer on common ground, but it rarely is). Unfortunately, both professional practitioner and test material are, in this case, free to lock inductive antlers with each other. The printed instructions to subjects in some psychological experiments even go so far as to say: "Please do not run an experiment inside the experiment".

2.1 Specifying Pilot Input

A black box input is, comparatively speaking, easily specified to an acceptably complete degree. In almost all successful attempts to reach "the pilot transfer function" the experimenter has seen to it that the tracking input has been very nicely specifiable indeed. Normally it is random-appearing, albeit to some extent reproducible (as, for example, the sum of three incommensurable sines or white noise filtered at some low corner frequency). Also, it is usually delivered to a compensatory tracking display, for in pursuit tracking the operator shapes the error signal, too, and it is hence more complex to determine just what he does do, even in the laboratory.

Real life is rather different. The approach and landing flight phase could be a good example to consider. Before we go into more detail, however, note that the pilot is not merely concerned with a tracking task. He has a hierarchy of aims (see, eg, Carel 1965) and can neglect the sheer stick-pulling if this seems an appropriate thing to do.

2.1.1 Visual Input

The most obvious characteristic of signals in cockpit instruments is that they are not random-appearing. Very often, a pilot will achieve a high level of predictive ability by repeatedly observing, for example, the deflections of ILS needles. Nearly equally obviously, a pilot need not treat an instrument as one exclusive information channel just because it is single-axis. As an example, he does not control height in isolation just because an altimeter displays nothing else.

How well a display is human engineered can, of course, alter the pilot's behaviour. As an example, a display which gives information about error rate, as well as basic errors, will elicit a different controlling strategy. Similarly, with all types of aided, quickened, or predictor displays. We have already noted the compensatory-pursuit distinction.

But these seem trivial difficulties indeed when one comes to consider the pilot's use of the view outside his cockpit. Here, it is nearly impossible to specify what the visual inputs actually are, let alone quantify them. In the late stages of approach and landing the following inputs are thought to be involved:

(a) the horizon and separations between it and imaginary extensions of aircraft axes may be prime attitude sources (eg, front horizon view plus aircraft longitudinal production gives pitch);

(b) the apparent size and brightness of known objects, and their rates of change, help to give altitude, range and rate of closure with the impact point;

(c) the surface texture and texture gradient contribute to altitude, attitude and flight path;

(d) parallax, parallax motion and relative motion cues give an impression of altitude (very low down) and convey flight path towards the aiming point and rate of closure with the impact point;

(e) the detection of the "zero motion point", plus an appreciation of the surrounding "streaming" effect, signals flight path towards the impact point and separation between the impact and aiming points;

(f) at very low altitudes, angular details (eg the verticality of buildings, the squareness of field corner) convey altitude and attitude cues.

An important feature of this complex list of input signals is that it is still hotly argumentative. Were it accepted, however, it would still be no mean task to define interrelationships among these visual inputs as they changed, say, during the landing.

2.1.2 Vestibular and Somaesthetic Inputs

Given present knowledge, a specification of whole-body position and motion perception is likely to be no more successful than that of visual world perception. Broadly speaking, cockpit acceleration forces allow a faster appreciation (than cockpit instruments do) that some uncontrolled-for out-of-trim event has occurred. They do not, in any trustworthy sense, signal aircraft velocity or attitude changes. On the whole, though, pilots seem to find it difficult to disregard motion cues as completely as their training personnel would have them do.

To a first approximation, the three vestibular canals signal angular accelerations, while the utricle joins forces with the more widely distributed somaesthetic receptors (for touch, pressure, and joint position sense) to signal linear accelerations and position with respect to 1g ambient. One cannot categorically state, however, that the canals are not stimulated by linear forces, nor that somaesthesis does not accurately convey rotational sensations if conditions are favourable.

A yet greater problem in the way of specifying pilot input emerges if one considers the visual and vestibular-somaesthetic senses together. There is by now no doubt that the two interact. As examples, one knows that strong vestibular sensations elicit eye movements (nystagmus; counter-rolling) and that visual perception modifies the way in which position and motion sensations are interpreted (as witness the prevalent flight simulation technique whereby the attitude display continues to be driven following only a brief cockpit rotational acceleration in, say, the roll axis).

I am not, of course, saying that models to date have neglected motion cues as an input (see, eg, Bergeron, 1970; Sadoff and Dolkas, 1967) but merely that knowledge is too scant to permit adequate modelling.

Somaesthetic sensations, as well as contributing to cockpit position and motion perception, are also involved in the perception of control "feel". While the "feel" of a control has a well-established part to play in determining the pilot's tracking behaviour, the topic has so far defied adequate quantification.

2.1.3 Inputs from other Sensory Modalities

I need only mention audition, briefly. It is, of course, common knowledge that aerodynamic and engine noises constitute information useful to the pilot. Speech, in particular, can be an input of overriding importance however. As an example, consider the change in piloting criteria and technique which could result from a GCA controller's message that one was, after all, 1 and not 4 miles from runway threshold.

2.1.4 Inputs Referable to Stress

It is a defensible, though not a universally adopted position, to treat flight stresses as though they constituted irrelevant inputs. Vibration and sustained acceleration are obvious examples, causing as they do motion effects which do not so much form usable information as disrupt good vision and interfere with manual skills. These two stresses are amongst the simplest to treat, however; at the limit, the motion platform is switched on and a re-investigation of some aspect of physiology (from about 1880) commences.

At the far end of some intuitive spectrum are those elusive, almost un-researchable stresses such as failure stress, anxiety, and naked fear. Each could constitute a near-overwhelming input. It is problematic to make any general scientific statement whatever about the action of such stresses, however. My personal guess, from the sparse research which I consider acceptable, is that it would be worth investigating whether tracking inputs decreased in frequency of occurrence, increased in amplitude and force, and became bewilderingly non-linear under these conditions.

2.2 Specifying Pilot Output

The output of a black box can be, comparatively speaking, satisfactorily specified. In successful pilot modelling investigations, stick position or display error are acceptable parameters, so long as one is careful to study only a short time sample (eg 50 sec) of practiced tracking activity.

Poulton (1962) was the first to state bluntly, a fact known then and still extant, that the most important parts of behaviour are *not* servo-like. Jordan (1963) probably agrees with me in thinking that, in aircraft control the pilot is given a tracking task not because it suits his abilities, intellectual needs, or anything else, but because we are all too backward and clumsy to couple him appropriately. Hence statements of the kind "Man performs best when he has least to do" (ie he should be given an amplifying or attenuating function, solely) can stand only because of the thoroughly proscribed context in which they are written.

A practical consequence for transfer function analysis has been listed by Fogel (1963), the possibility of a stick output intended specifically for system investigation or pilot reassurance. I have personally watched a student test pilot maintain a control "dither" for 20-odd minutes with great apparent success (Huddleston, 1965).

It might be as well at this point to turn to the topic of pilot criteria mentioned in the Introduction. The sine qua non of successful pilot modelling is the tracker's acceptance of an unusually limited mandate. He must, for example, ".... keep that pitch error as small as possible ...." or something similar. Even in laboratory experiments of a deeply applied nature, pilots generally allow themselves a broader ambition. In evaluating alternative director displays, for instance (Huddleston and Samuel, 1967), one needs a credible, numerical comparison, such as heading error, but pilots agree there is no uniquely good form of co-ordinated ascending turn to starboard, or whatever. Tracking error measurements then have to be made as departures from an arbitrarily defined flight path which does not outrage good piloting practice. (Only by such explicit definition of aims can one employ a measurement computer at all, by the way, since all it can do is deduce inside a closed, consistent logic).

A pilot's aims are rarely explicit. Often, he is capable of truthfully reporting that, broadly, he is anxious to conserve fuel, or time, or at pains to give rear passengers a smooth ride. Perhaps equally often, though, he does not realize he is being aggresive, or exhibitionist, or out to amuse himself. In the absence of data, one can only speculate that controlling strategies should differ substantially across situations of this kind. How measurement baselines should be modified from one situation to another is not at all easy to see, however.

3. INDIVIDUAL DIFFERENCES

3.1 Some Physiological Determinants of Skill

The more quantitative reviews of human tracking characteristics (eg, Young and Stark, 1965) have found it helpful to consider underlying physiological capabilities such as hand dynamics and eye movement control.

It will illustrate human variety if we take an example from this latter area. One of the constituents of eyeball control seems to be accounted for by postulating a velocity pursuit system. In my own studies of this assumed system (Huddleston, 1969) it has been confirmed that, for a 1 Hz sine-wave target, the average eye travels through about 0.8 of the target amplitude and has a phase lag of something less than 10°. Of course, I found nobody in my group of 38 people who had that average eye. At one extreme, one individual consistently demonstrated a phase lag of 50° with an amplitude of 0.65, while at the other was an individual with a phase lead of 15° and an amplitude of 0.92.

One of the intriguing physiological events which can take place with familiarity at a motor skill is the near-abolition of a conscious pattern of physical movements and the establishment of a quasi-ballistic motor response in some "lower" motor loop(s). Fleishman, in particular, has contributed to an understanding of this type of problem for some time (see, eg, Fleishman and Fruchter, 1965) by analysing the components of skill at various stages in skill acquisition and practice. Certainly, this is a kind of human learning with profound implications for pilot modelling. A successful transfer function investigation would be one which selected only 2 or 3 individuals, all closely comparable in experience, and allowed them only very limited exposure to a motor task which showed nearly no predictable components. This would be no way to achieve a respectable population estimation, and no way to mimic the flight task at all. Even so, a relatively simple averaged parameter (gain) could range between values like 2.4 and 10.4 (Burgett, 1969).

3.2 Some Psychological Determinants of Skill

Human psychological variety is, arguably, more perplexing than physiological variety; certainly in terms of human variability (one individual from occasion to occasion) this seems to be true.

In this context it would be cowardice not to attempt some statement on that most bewildering topic, personality theory and research. Intelligence aside, the major British worker, Eysenck, finds he is able to summarize stable personality traits by recourse to only 2 parameters, while the major American worker, Cattell, achieves a satisfactory fit by analysing these 2 down into about 16. If I mention Eysenck's 2, the Extravert-Introvert and Stable-Neurotic continua, this should suffice.

Broadly speaking, extraverts might be expected to behave in an aircraft-controlling situation as if they were:

(a) readier to accept advice or solutions from fellow crew members, ground controllers, etc;

(b) more willing to make decisions on sparse evidence, or in a hurry;

(c) relatively resistant to disorientation, or the apprehension of a stress situation;

(d) less ambitious;

compared to introverts. Stable individuals, compared to neurotic ones in the normal population, might be expected to control as if they were:

(a) less upset by frustration or failure;

(b) relatively unaffected by the prospect of a personal evaluation;

(c) resistant to (normal) anxiety and conflict situations;

(d) more adaptive, but also abler to put out continuous effort in pursuit of a given plan.

I must say, however, that none of these theoretical expectancies has been borne out in any defensible human tracking investigation that I know of. This is far from saying they are irrelevant, though.

4. CONCLUSIONS

I fear that my paper may infuriate rather than inform. I hope to have shown that asking for a pilot transfer function is, regrettably, like asking the human biologist how a pilot flies. It is not yet time to lay claim to such wisdom, nor is it in our interests to condone this ignorance.

REFERENCES

BARON, S.
KLEINMAN, D.L. — *The human as an optimal controller and information processor.* National Aeronautics and Space Administration, Washington DC, Report NASA CR-1151. 1968.

BERGERON, H.P. — *Investigation of motion requirements in compensatory control tasks.* IEEE Transactions on Man-Machine Systems, Vol.MMS-11, 1970, pp.123-125.

BURGETT, A.L. — *A study of human operator performance using regression analysis.* National Aeronautics and Space Administration, Washington DC, Report NASA CR-1259, 1969, pp.164-166.

CAREL, W. — *Pictorial displays for flight.* Hughes Aircraft Company, Culver City, Calif., Technical Report 2732.01/40, especially Figures 2 and 3. 1965.

COSTELLO, R.G.
HIGGINS, T.J. — *An inclusive classified bibliography pertaining to modeling the human operator as an element in an automatic control system.* IEEE Transactions on Human Factors in Electronics, Vol.HFE-7, 1966, pp.174-181.

FLEISHMAN, E.A.
FRUCHTER, B. — *Component and total task relations at different stages of learning a complex tracking task.* Perceptual and Motor Skills, Vol.20, 1965, pp.1305-1311.

FOGEL, L.J. — *Biotechnology,* chapter 9, especially page 243. Englewood Cliffs, NJ, Prentice-Hall. 1963.

HUDDLESTON, H.F. — *Oculomotor pursuit of vertical sinusoidal targets.* Nature, Vol.222, 1969, p.572.

HUDDLESTON, H.F. — *Inter-subject differences in manual flight control.* Ministry of Defence, RAF Institute of Aviation Medicine, Farnborough, Scientific Memorandum S68, 1965, p.9.

HUDDLESTON, H.F.
SAMUEL, G.D. — *Attempts to improve perceptual clarity in an aircraft display.* Nature, Vol.215, 1967, pp.787-788.

JORDAN, N. — *Allocation of functions between man and machines in automated systems.* Journal of Applied Psychology, Vol.47, 1963, pp.161-165.

McRUER, D.
WEIR, D.H. — *Theory and manual vehicular control.* Ergonomics, especially Bibliography Vol.12, 1969, pp.599-633.

POULTON, E.C. — *On simple methods of scoring tracking error.* Psychological Bulletin, Vol.59, 1962, pp.320-328.

SADOFF, M. — *A survey of selected research on human controller characteristics.* NATO Advisory Group for Aerospace Research and Development, Paper to AGARD Ad Hoc Panel on Guidance and Control, Paris. 1966.

SADOFF, M.
DOLKAS, C.B. — *Acceleration stress effects on pilot performance and dynamic response.* IEEE Transactions on Human Factors in Electronics, Vol.HFE-8, 1967, pp.103-112.

SEIFERT, R.
MILLER, U. — *Investigations of the term "Remnant Spectrum" of the human control output function.* NATO Advisory Group for Aerospace Research and Development, AGARD Conference Proceedings 55, Paper 8. 1968.

STAPLEFORD, R.L.
et al. — *Experiments and a model for pilot dynamics with visual and motion inputs.* National Aeronautics and Space Administration, Washington DC, Report NASA CR-1325. 1969.

TODOSIEV, E.P.
et al — *Human tracking performance in uncoupled and coupled 2-axis systems.* National Aeronautics and Space Administration, Washington DC, Report NASA CR-532. 1966.

YOUNG, L.R. — *On adaptive manual control.* IEEE Transactions on Man-Machine Systems, Vol.MMS-10, 1969, pp.292-331.

YOUNG, L.R.
STARK, L. — *Biological control systems – a critical review and evaluation.* National Aeronautics and Space Administration, Washington DC, Report NASA CR-190. 1965.

NATIONAL DISTRIBUTION CENTRES FOR UNCLASSIFIED AGARD PUBLICATIONS

Unclassified AGARD publications are distributed to NATO Member Nations through the unclassified National Distribution Centres listed below

BELGIUM
General J.DELHAYE
Coordinateur AGARD – V.S.L.
Etat Major Forces Aériennes
Caserne Prince Baudouin
Place Dailly, Bruxelles 3

CANADA
Director of Scientific Information Services
Defence Research Board
Department of National Defence – 'A' Building
Ottawa, Ontario

DENMARK
Danish Defence Research Board
Østerbrogades Kaserne
Copenhagen Ø

FRANCE
O.N.E.R.A. (Direction)
29, Avenue de la Division Leclerc
92, Châtillon-sous-Bagneaux

GERMANY
Zentralstelle für Lüftfahrtdokumentation
und Information
Maria-Theresia Str. 21
8 München 27
Attn: Dr Ing. H.J.RAUTENBERG

GREECE
Hellenic Armed Forces Command
D Branch, Athens

ICELAND
Director of Aviation
c/o Flugrad
Reykjavik

ITALY
Aeronautica Militare
Ufficio del Delegato Nazionale all'AGARD
3, Piazzale Adenauer
Roma/EUR

LUXEMBOURG
Obtainable through BELGIUM

NETHERLANDS
Netherlands Delegation to AGARD
National Aerospace Laboratory, NLR
Attn: Mr A.H.GEUDEKER
P.O. Box 126
Delft

NORWAY
Norwegian Defense Research Establishment
Main Library, c/o Mr P.L.EKERN
P.O. Box 25
N-2007 Kjeller

PORTUGAL
Direccao do Servico de Material
da Forca Aerea
Rua de Escola Politecnica 42
Lisboa
Attn: Brig. General Jose de Sousa OLIVEIRA

TURKEY
Turkish General Staff (ARGE)
Ankara

UNITED KINGDOM
Ministry of Technology Reports Centre
Station Square House
St. Mary Cray
Orpington, Kent BR5 3RE

UNITED STATES
National Aeronautics and Space Administration (NASA)
Langley Field, Virginia 23365
Attn: Report Distribution and Storage Unit

* * *

If copies of the original publication are not available at these centres, the following may be purchased from:

Microfiche or Photocopy

National Technical
Information Service (NTIS)
5285 Port Royal Road
Springfield
Virginia 22151, USA

Microfiche

ESRO/ELDO Space
Documentation Service
European Space
Research Organization
114, Avenue de Neuilly
92, Neuilly-sur-Seine, France

Microfiche

Ministry of Technology
Reports Centre
Station Square House
St. Mary Cray
Orpington, Kent BR5 3RE
England

The request for microfiche or photocopy of an AGARD document should include the AGARD serial number, title, author or editor, and publication date. Requests to NTIS should include the NASA accession report number.

Full bibliographical references and abstracts of the newly issued AGARD publications are given in the following bi-monthly abstract journals with indexes:

Scientific and Technical Aerospace Reports (STAR)
published by NASA,
Scientific and Technical Information Facility,
P.O. Box 33, College Park,
Maryland 20740, USA

United States Government Research and Development Report Index (USGDRI), published by the Clearinghouse for Federal Scientific and Technical Information, Springfield, Virginia 22151, USA

Printed by Technical Editing and Reproduction Ltd
Harford House, 7-9 Charlotte St, London. W1P 1HD